The Abdus Salam
International Centre for Theoretical Physics

United Nations
Educational, Scientific and
Cultural Organization

IAEA
International Atomic Energy Agency

2145-37

Spring College on Computational Nanoscience

17 - 28 May 2010

Nanowires and Nanopatterned Graphene
Computational Methods and Physical Phenomena

Antti-Pekka JAUHO

Dept. of Micro and Nanotechnology
DTU, Denmark and Dept. of Applied Physics, Aalto University
Finland

Strada Costiera 11, 34151 Trieste, Italy - Tel.+39 040 2240 111; Fax +39 040 224 163 - sci_info@ictp.it

TKK

Technical University of Denmark DTU

Nanowires and nanopatterned graphene – computational methods and physical phenomena

Antti-Pekka Jauho

Dept. of Micro and Nanotechnology, DTU, Denmark

Dept. of Applied Physics, Aalto University, Finland

- Some comments on nonequilibrium Green's functions
- Nanowires (electric, thermal transport)
- Antidots on graphene; graphene edges and nanoribbons; carbon atomic chains and spintronics; chemical vs structural disorder

Technical University of Denmark DTU

Methods for ab initio calculations of transport in nanoscale systems

- Review of NEGF; the basic equations for transport properties, underlying assumptions and caveats
- Uses and misuses of the Meir-Wingreen formula
- An application: density functional method for nonequilibrium electron transport

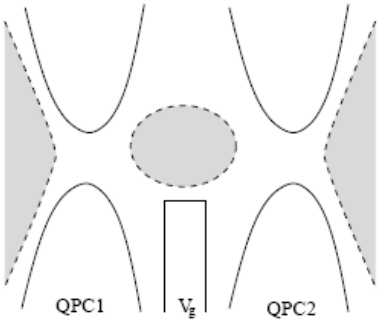

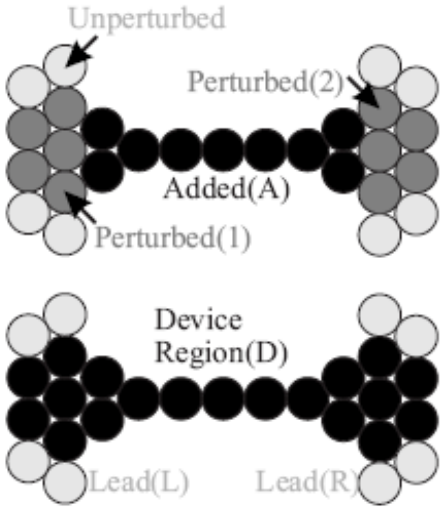

Technical University of Denmark DTU

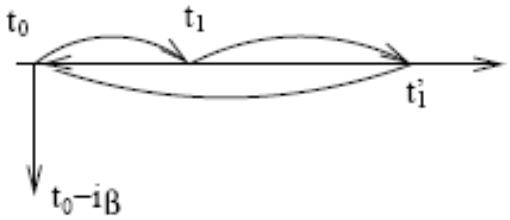

Philosophy:

- small system coupled to ideal, large contacts
- in infinite past, the subsystems are separated with respective chemical potentials (Caroli et al. 1970-72)
- the couplings between subsystmes are turned on adiabatically, and a nonequilibrium state in the central region is established
- Keldysh contour enters because final state is not known (S(-◎,◎) unknown)
- nonperturbative, self-consistent calculation of the system parameters may be necessary
- This is not unique – can think of other ways of approaching the problem

The basic equations (examples of Hamiltonians)

$$H = \sum_{k,\alpha\in L/R} \epsilon_{k,\alpha} c^{\dagger}_{k,\alpha} c_{k,\alpha} + \sum_{k,\alpha\in L/R;n} \left[V_{k\alpha;n} c^{\dagger}_{k,\alpha} d_n + \text{h.c.} \right] + H_{\text{cen}} \left[\{d_n\}, \{d^{\dagger}_n\} \right]$$

$$H_{\text{cen}} = \sum_n \epsilon_n d^{\dagger}_n d_n + H_{\text{int}}$$

$$H^{\text{el-ph}}_{\text{int}} = \sum_{m\sigma} d^{\dagger}_{m,\sigma} d_{m,\sigma} \sum_{\mathbf{q}} M_{m,\mathbf{q}} \left[a^{\dagger}_{\mathbf{q}} + a_{\mathbf{q}} \right]$$

$$H^{A}_{\text{int}} = U \sum_{m} d^{\dagger}_{m,\uparrow} d_{m,\uparrow} d^{\dagger}_{m,\downarrow} d_{m,\downarrow}$$

Calculation of the current

The current operator (just compute $[N_L, H]$):

$$I_L = -\frac{ie}{\hbar}\sum_{k,n}\left[-V_{kL;n}c^\dagger_{kL}d_n + V^*_{kL;n}d^\dagger_n c_{kL}\right]$$

Current leaving the left contact (requires **noninteracting** (mean-field – for example BCS would be OK) contacts):

$$\left[\Gamma^L(\varepsilon_k)\right]_{mn} = 2\pi\sum_{\alpha\in L}\varrho_\alpha(\varepsilon_k)V_{\alpha,n}(\varepsilon_k)V^*_{\alpha,m}(\varepsilon_k)$$

$$\langle I_L\rangle = J_L(t) = -\frac{2e}{\hbar}\int_{-\infty}^{t}dt_1\int\frac{d\epsilon}{2\pi}\mathrm{Im}\mathrm{Tr}\Big\{e^{-i\epsilon(t_1-t)}\mathbf{\Gamma}^L(\epsilon,t_1,t)\times\left[\mathbf{G}^<(t,t_1)+f^0_L(\epsilon)\mathbf{G}^r(t,t_1)\right]\Big\}.$$

WJM,JWM PRB 1993,1994

Static limit ❶ Meir-Wingreen formula

$$J = \frac{ie}{2\hbar}\int\frac{d\epsilon}{2\pi}\mathrm{Tr}\Big\{\left[\mathbf{\Gamma}^L(\epsilon)-\mathbf{\Gamma}^R(\epsilon)\right]\mathbf{G}^<(\epsilon) + \left[f^0_L(\epsilon)\mathbf{\Gamma}^L(\epsilon)-f^0_R(\epsilon)\mathbf{\Gamma}^R(\epsilon)\right]\left[\mathbf{G}^r(\epsilon)-\mathbf{G}^a(\epsilon)\right]\Big\}$$

The basic equations (comments)

- this is just a paradigm – one still needs to evaluate the fully interacting Green functions of the central region (in one way or another!):

$$G^{<}_{nm}(t,t_1) = i\langle d^{\dagger}_m(t_1) d_n(t)\rangle$$
$$G^{r}_{nm}(t,t_1) = -i\theta(t-t_1)\langle [d_n(t), d^{\dagger}_m(t_1)]\rangle$$

- displacement currents **not** included ➧ require separate treatment
- interpretation – write MW formula in an alternative form:

$$J_L = \frac{e}{h}\int d\epsilon \mathrm{Tr}\left\{\mathbf{\Sigma}^{L,<}(\epsilon)\mathbf{G}^{>}(\epsilon) - \mathbf{\Sigma}^{L,>}(\epsilon)\mathbf{G}^{<}(\epsilon)\right\}$$

- first term: current from left contact to central region
- second term: current from central region to left contact

The basic equations (comments cont'd

- In general, one needs to solve the coupled Keldysh-Dyson equations:

$$G^< = G^r \Sigma^< G^a,$$
$$G^r = G_0^r + G_0^r \Sigma^r G^r$$

$$\mathbf{\Sigma}_{\rm tot} = \mathbf{\Sigma}_{\rm int} + \mathbf{\Sigma}_L + \mathbf{\Sigma}_R$$

Limitations & things to worry about:

- physical criteria for selecting what is contact, and what is central region (i.e, where are the non-mean field interactions allowed to operate)?
- charge neutrality of the system?
- energy relaxation in the noninteracting leads (no such Hamiltonians present in the formulation)?
- adiabatic turning-on of the contacts – not necessarily realized in experiments! (e.g., alternative "non-partitioning" formulation due to Stefanucci et al., following early work of Cini)

Applications of the Meir-Wingreen formula

(i) For a mean-field theory (technically, self-energies in the interacting region are one-point functions – DFT belongs to this category!) a direct calculation gives:

$$J_L = \frac{e}{h} \int d\epsilon T_{\rm tot}(\epsilon)[f_L^0(\epsilon) - f_R^0(\epsilon)],$$

$$T_{\rm tot}(\epsilon) = {\rm Tr}\left\{\mathbf{\Gamma}^L(\epsilon)\mathbf{G}^r(\epsilon)\mathbf{\Gamma}^R(\epsilon)\mathbf{G}^a(\epsilon)\right\}$$

- an excellent formula (see, e.g., Datta's books, or Haug-Jauho 2nd edition) – but not the whole truth
- forms the basics for a huge number of calculations (for example, most results described in these lectures), even on commercial/industrial level
- emphatically not applicable for inelastic transport, or for GW, or etc.

2. Applications (cont'd)

(ii) Conservation rules: write

$$\mathbf{\Sigma}_{\rm tot} = \mathbf{\Sigma}_{\rm int} + \sum_{\alpha \in L/R} \mathbf{\Sigma}^{\alpha}$$

Then (using Keldysh equation)

$$\mathrm{Tr}\left\{\mathbf{\Sigma}^{<}_{\rm tot}\mathbf{G}^{>} - \mathbf{\Sigma}^{>}_{\rm tot}\mathbf{G}^{<}\right\} \equiv 0$$

and current conservation $\sum_{\alpha} J^{\alpha} = 0$ leads to

$$\int d\epsilon \mathrm{Tr}\left\{\mathbf{\Sigma}^{<}_{\rm int}(\epsilon)\mathbf{G}^{>}(\epsilon) - \mathbf{\Sigma}^{>}_{\rm int}(\epsilon)\mathbf{G}^{<}(\epsilon)\right\} = 0$$

which is a useful check on numerics, and for consistency of chosen approximations. (N.B. This formula is familiar for people working with kinetic theory (BE): integrated collision term must vanish!)

3. DFT for nonequilibrium electron transport

- Standard methods for electronic structure calculations assume a finite, or a periodic geometry
- Standard methods assume that the electronic system is in equilbrium
- Molecular electronics requires something entirely different:

  (a) small, translationally noninvariant subsystem

  (b) coupling to semi-infinite leads

  (c) nonequilibrium state in the subsystem

To use DFT in nonequilibrium, one must assume that the Kohn-Sham orbitals can be used to calculate the current. (Possible extensions: use TDDFT, or current-density-functional theory)

Given this **(unproven)** assumption, one can use NEGF to construct a nonequlibrium electron density, which can be fed back in the DFT loop. The price is an extra iterative subloop, but the convergence can be tested, and improved, by an appropriate choice of exchange-correlation functional, and/or basis set.

3. DFT for nonequilibrium electron transport (summary of TranSIESTA method)

$$n(x) = -iG^{<}(x = x', t = t') = \int \frac{d\epsilon}{2\pi i} G^{<}(x = x', \epsilon)$$

$$G^{<} = G^{r}\Sigma^{<}G^{a} \qquad \Sigma^{<} = i(\Gamma^{L} f_L + \Gamma^{R} f_R)$$

$$\mathbf{G}^{r}(E) = [E\mathbf{I} + i\eta - \mathbf{H}]^{-1} \qquad \mathbf{H} = \begin{pmatrix} \mathbf{H}_L + \mathbf{\Sigma}_L & \mathbf{V}_L & 0 \\ \mathbf{V}_L^{\dagger} & \mathbf{H}_C & \mathbf{V}_R \\ 0 & \mathbf{V}_R^{\dagger} & \mathbf{H}_R + \mathbf{\Sigma}_R \end{pmatrix}$$

$$\text{initial}\, n(x) \Rightarrow \text{SIESTA} \Rightarrow \psi_{\text{KS}}(x) \Rightarrow \text{NEGF} \Rightarrow \text{new}\, n(x)$$

This approach can be applied to many systems – bearing in mind its limitations.

TKK

Technical University of Denmark DTU

Part II Heat and electrical conductance in quantum structures

Electronic transport phenomena in nanostructures are important both for basic science as well as for applications. In recent years it has become clear that **thermal transport** also plays an important role in many nanoscale systems. In this part of my lectures I provide a background to these phenomena, and describe two different yet interrelated cases: (i) Modelling of thermoelectric effects in (realistic) **Silicon nanowires**, and (ii) Theory of **radiative heat** transport between **mesoscopic bodies**. Though operating at very different temperature and length scales, these two examples share certain common features, and can be analyzed with similar theoretical tools.

TKK

Technical University of Denmark DTU

Literature & Acknowledgements

[1] Scaling theory put into practice: First-principles modeling of transport in doped silicon nanowires, T. Markussen, R. Rurali, M. Brandbyge, and APJ, Phys. Rev. Lett. 99, 076803 (2007)

[2] Heat conductance is strongly anisotropic for pristine silicon nanowires, T. Markussen, APJ, and M. Brandbyge, Nano Letters 8, 3771-3775 (2008).

[3] Electron- and phonon transport in silicon nanowires: an atomistic approach to thermoelectric properties, T. Markussen, APJ, and M. Brandbyge, Phys. Rev. B 79, 035415 (2009); arXiv:0810.5462

[4] Surface decorated silicon nanowires: a route to high-ZT thermoelectrics, T. Markussen, M. Brandbyge, and APJ, Phys. Rev. Lett., 103, 055502 (2009)

[5] Mesoscopic photon heat transistor, T. Ojanen and APJ, Phys. Rev. Lett. 100; 155902 (2008); arXiv:0712.2767

[6] Thermal rectification in nonlinear quantum circuits, T. Ruokola, T. Ojanen, and APJ, Phys. Rev. B 79, 115420 (2009); arXiv:0812.3634

[7] Scattering cross section of metal catalyst atoms in silicon nanowires, T. Markussen, R. Rurali, X. Cartoixà, APJ, and M. Brandbyge, Phys. Rev. B 81, 125307 (2010)

TKK

Technical University of Denmark DTU

Why are nanowires interesting?

- They can be fabricated with a number of different methods
- They can be used for many things:

1. Interconnects in nanoelectronics
2. Ultrasensitive sensors (chemical, electronic, mechanical…)
3. Spintronic applications
4. Thermoelectric components
5. They have fascinating physical properties (mechanical, electrical, optical, thermal, and even "nonstandard properties")

What are nanowires?

Technical University of Denmark DTU

"Number of Atoms"

10^6

- Supra-molecular conductors
  (TB + Quantum diff./Kubo)

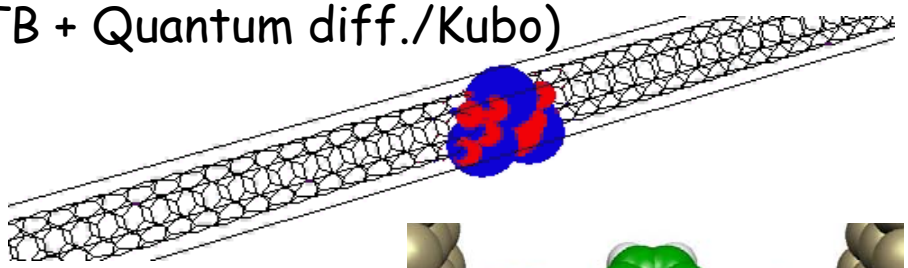

- Molecular conductors
  (DFT + NEGF + LOE)

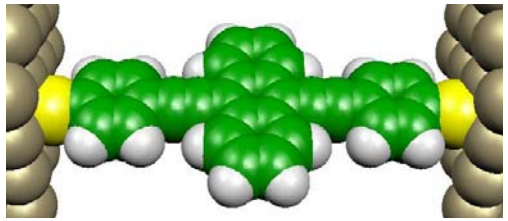

10^2

- Atomic metal wires/contacts
  (DFT + NEGF + SCBA)

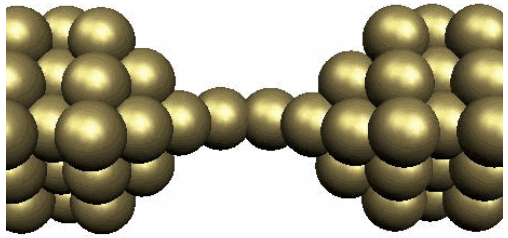

10^1

- Numerically exact solution (DMRG/noneqBA)

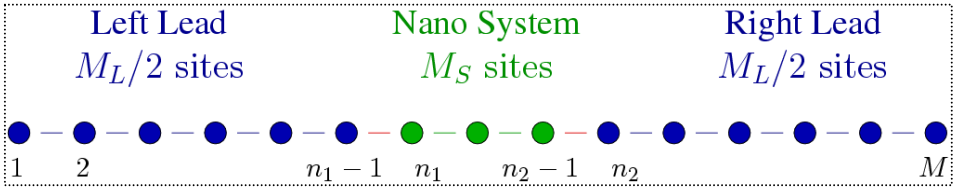

"Number of Approximations"

movie

TKK

Technical University of Denmark DTU

An example of inelastic transport: vibrations in an atomic gold wire (Agraït et al)

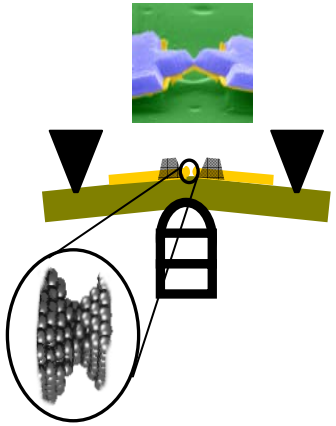

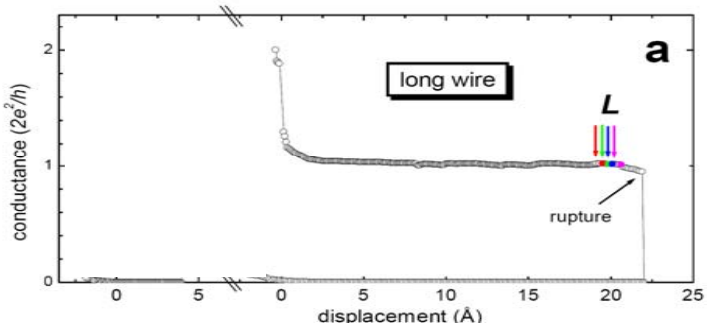

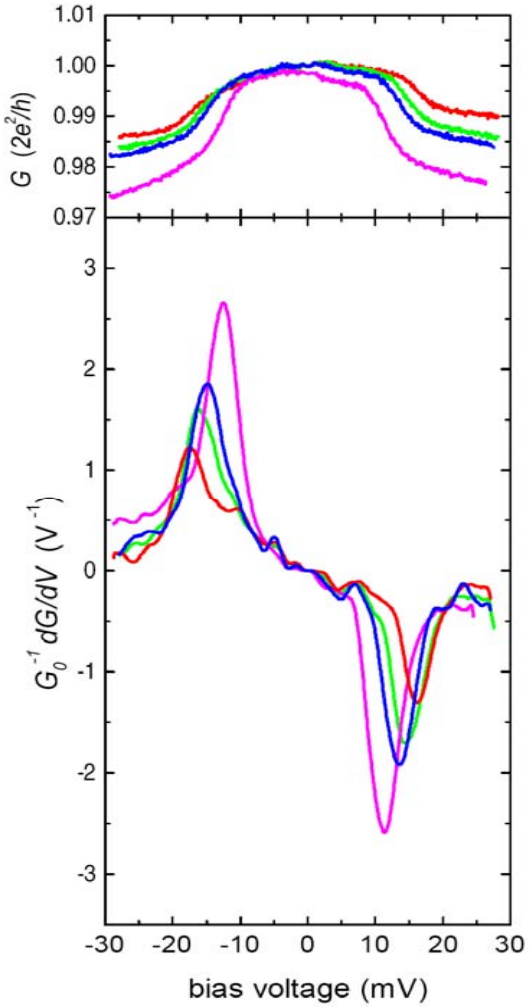

Frederiksen et al PRL 2004, PRB 2007: SCBA, 1st principles el-vib coupling, treat phonon heating with a rate-equation approach. State-of-art: see Engelund et al PRB 2009

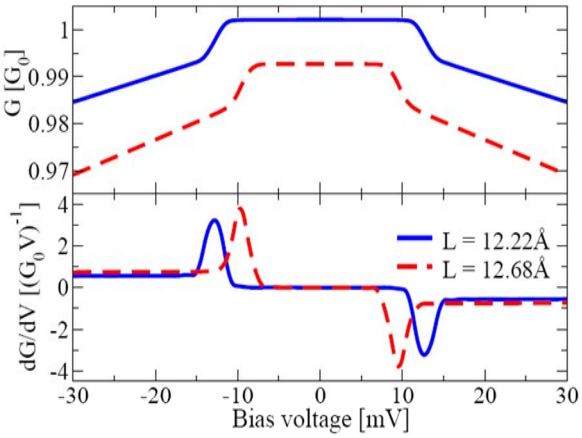

Transport in Disordered Si Nanowires

- A nanowire with 10 nm diameter and length in the micron scale has ~10^6-10^7 atoms
- Imperfect systems: impurities, defects etc.
- Fully first principles methods become very tedious due to $O(N^3)$ scaling
- Need for approximate methods:
  - Influence of impurities in bulk and on the surface; localization, impurity distribution?
  - Defects, roughness
  - Barcodes

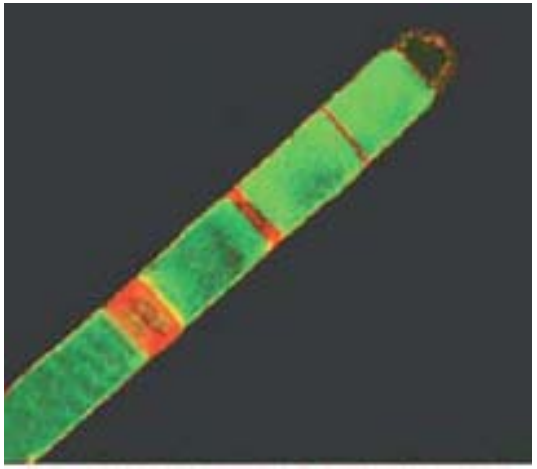

III-V steeple-chase NW from Lund University

TKK

Technical University of Denmark DTU

- Parameters for a tight-binding Hamiltonian are evaluated from first principles using the SIESTA code, and thus contain microscopic information on geometrical relaxation, defects, dopants, etc. and e-e interactions on DFT level.
- SIESTA solves the electronic scattering properties within a super-cell, and the sample is assembled from these building blocks
- The conductance of the sample (with given disorder) is evaluated with the (generalized) Landauer formula, where the transmission probability is obtained with a Green functions computed with a recursive technique

$$\hat{H} = \sum_i \left[\epsilon_i \, | \, i \, \rangle \langle \, i \, | + \sum_{j=n.n.} \left(t_{ij} \, | \, j \, \rangle \langle \, i \, | + t_{ij}^* \, | \, i \, \rangle \langle \, j \, | \right) \right]$$

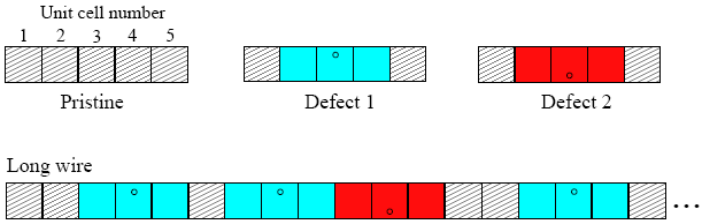

$$T(\epsilon) = \mathrm{Tr}[\Gamma_L(\epsilon)\mathbf{G}^a(\epsilon)\Gamma_R(\epsilon)\mathbf{G}^r(\epsilon)]$$

Construction of a disordered nanowire

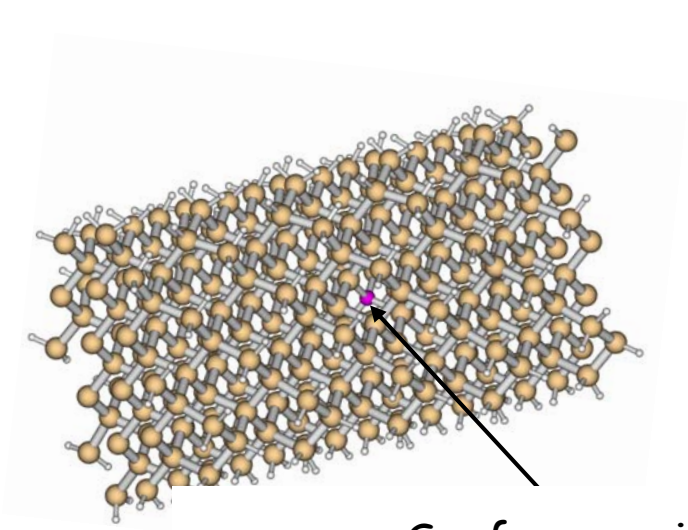

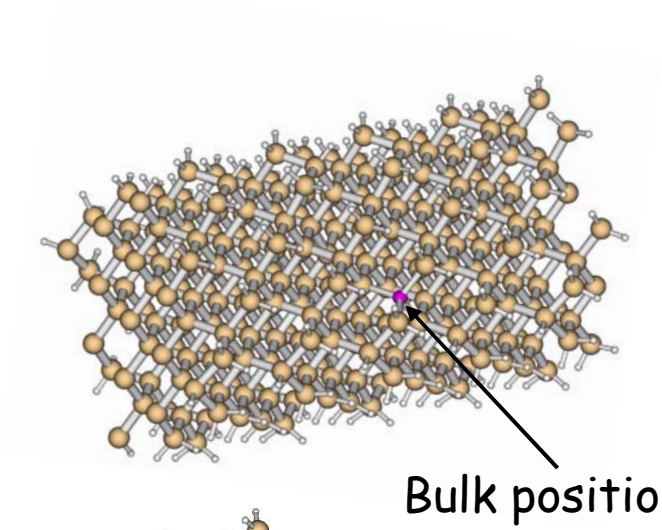

Surface position

Bulk position

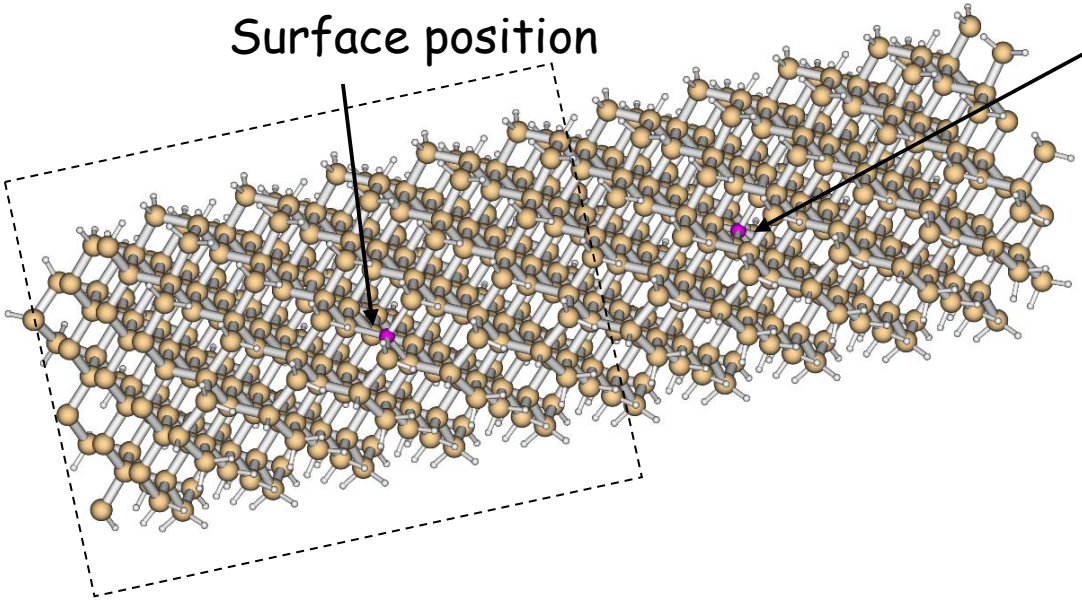

Supercell data: typically nine wire unit cells, i.e., 837 atoms; length 50.4 Å

Some calcs with 11 wire cells.

Each element is treated "exactly" within DFT, i.e., atomistic positions within central unit cell + 2 neighbors **fully relaxed**. No dopant-dopant interactions (upper limit for doping density)

Electronic transport in a Si-nanowire with H-adatoms

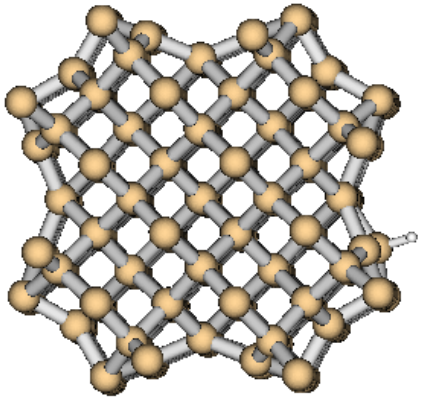

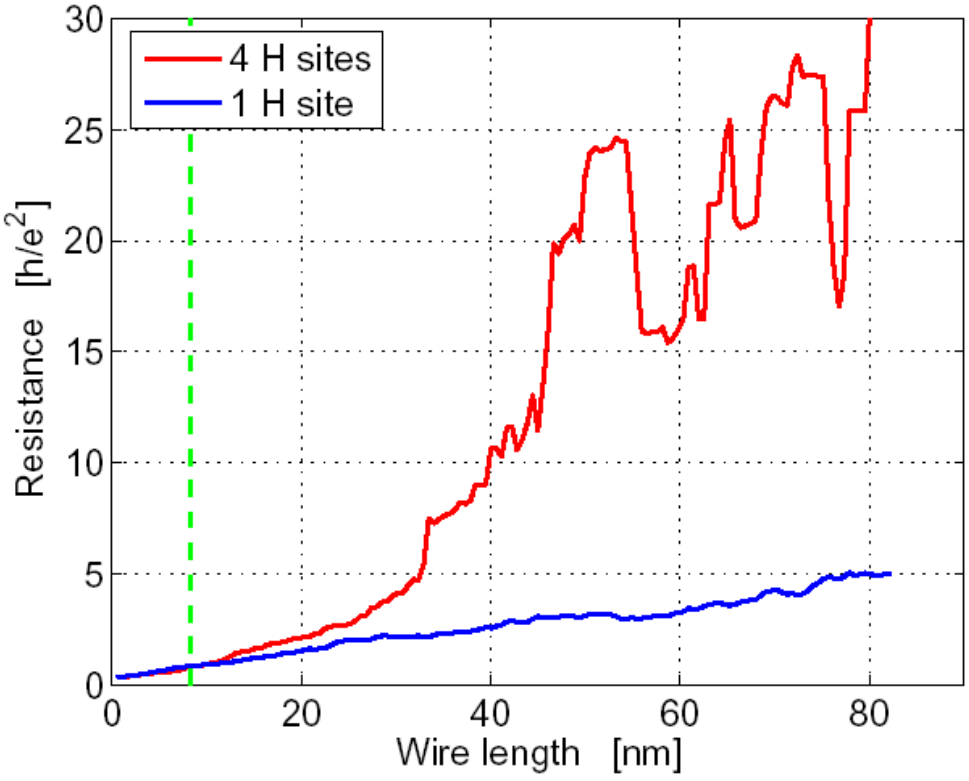

Blue curve: Ohmic behavior

Red curve: Indication of localization (a long story….)

TKK

Technical University of Denmark DTU

Results: Si-nanowire with H-vacancies

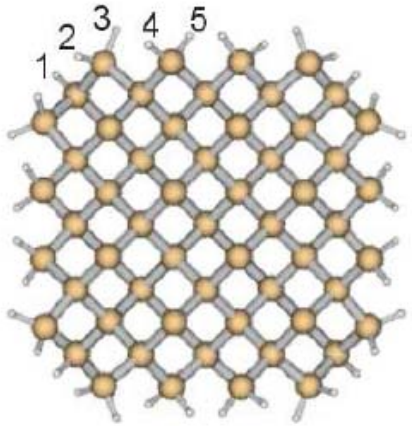

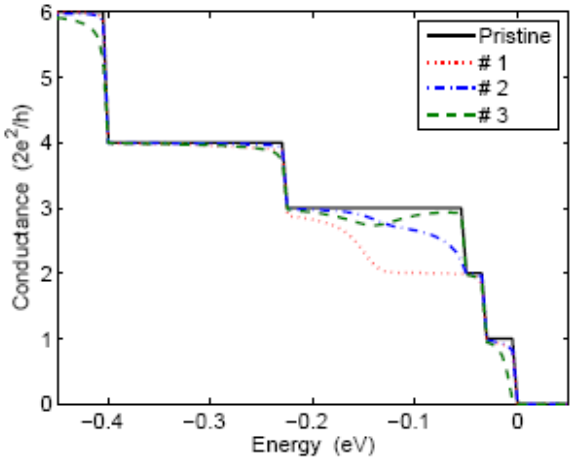

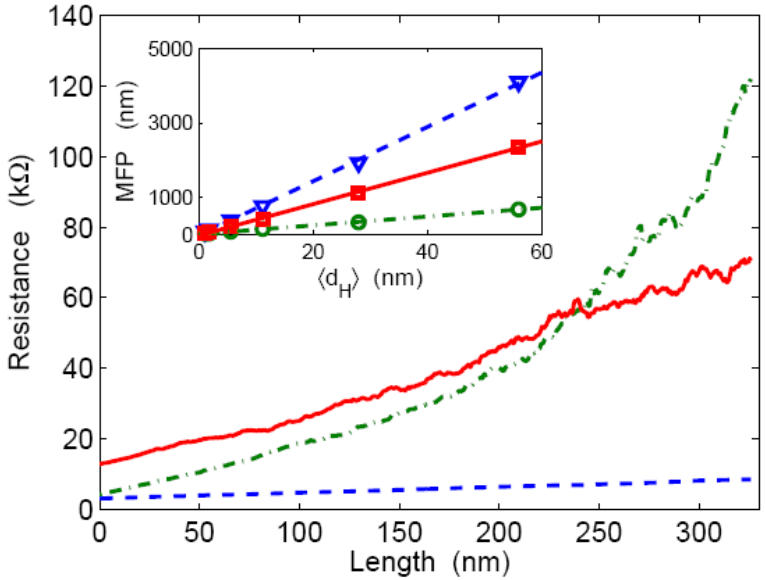

Blue: E=-0.3 eV
Green: E=-0.15 eV
Red: E=-0.03 eV
$\langle d_H \rangle$=2.8nm

Thermal conductance of SiNW

Thermal conductance is important:

- Nano-electronic devices: Need high κ
- Thermo-electric applications: Need low κ

(Thermoelectric figure of merit $ZT=S^2T\sigma/\kappa$. Challenge: maximize ZT.)

TKK

Nature, 10 January 2008, News and views:

Technical University of Denmark DTU

MATERIALS SCIENCE

Desperately seeking silicon

Cronin B. Vining

Using silicon as a 'thermoelectric' material to convert heat into electricity would be a technological leap forward. But silicon conducts heat so well that nobody thought that could work — until now.

Enhanced thermoelectric performance of rough silicon nanowires

Allon I. Hochbaum[1]*, Renkun Chen[2]*, Raul Diaz Delgado[1], Wenjie Liang[1], Erik C. Garnett[1], Mark Najarian[3], Arun Majumdar[2,3,4] & Peidong Yang[1,3,4]

Nature, **451**, 163, (2008)

Silicon nanowires as efficient thermoelectric materials

Akram I. Boukai[1]†, Yuri Bunimovich[1]†, Jamil Tahir-Kheli[1], Jen-Kan Yu[1], William A. Goddard III[1] & James R. Heath[1]

Nature, **451**, 169, (2008)

Examples of SNW's:

Silicon nanowires orientations:

- VLS growth
- Lithographic/Etch process
- <100>, <110>, <111>, <112>

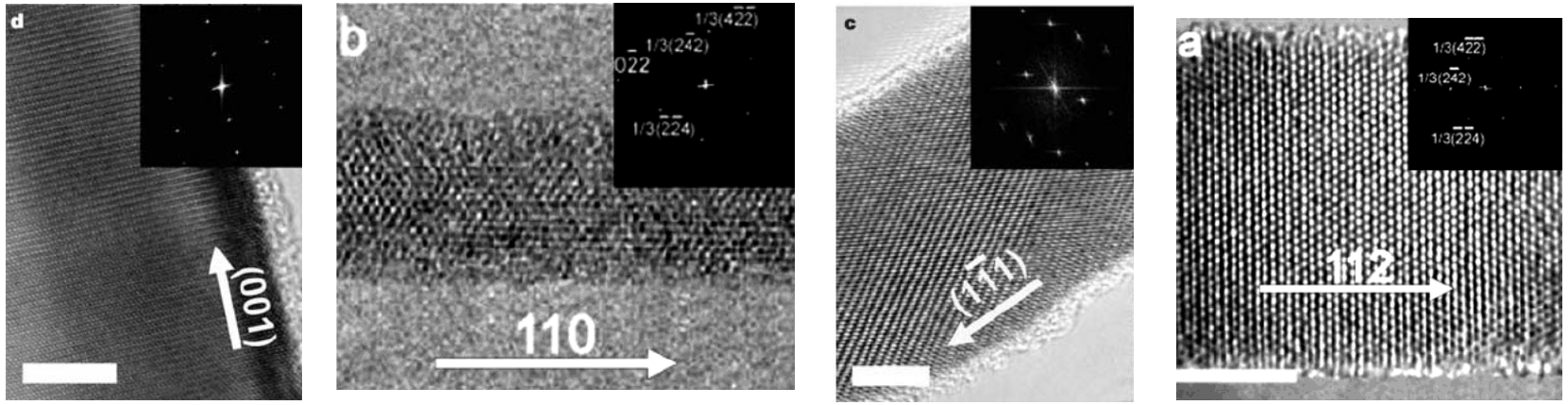

Y. Wu, Y. Cui, L. Huynh, C. Barrelet, D. Bell, C. Lieber, Nano Lett. 4, 433 (2004).
Y. Wu, J. Xiang, C. Yang, W. Lu, C. M. Lieber, Nature, 430, 61, (2004)

Theory on anisotropic transport – state of the art:

- Electronic properties vs. orientation
- Several theoretical studies (Tight-binding, DFT, GW)
- Band structure, band gap, effective masses [1-4]
- Transport [5]

[1] X.Zhao, C. M. Wei, L. Yang, M.Y. Chou, Phys. Rev. Lett., 92, 236805, (2004)
[2] Y. M. Niquet, A. Lherbier, N. H. Quang, M. V. Fernández-Serra, X. Blase, and C. Delerue, Phys. Rev. B 73, 165319 (2005).
[3] R. Rurali, B. Aradi, T. Frauenheim, and A. Gali, Phys. Rev. B 76, 113303 (2007).
[4] T. Vo, J. Williamson, and G. Galli, Phys. Rev. B 74, 045116 (2006).
[5] A. Svizhenko, P. Leu, and K. Cho, Phys. Rev. B 76, 125417 (2007).

Phonon transport vs. orientation has received less attention

TKK

Technical University of Denmark DTU

This work:

- Heat conductance in small nanowires (with and w/o defects)
- Diameters 1-5 nm.
- Orientations <100>, <110>, <111>
- Harmonic approximation: only linear forces, $F_{ij} = -kx_{ij}$
- Dynamical matrix:

$$K_{I\mu,J\nu} = \frac{\partial^2 E}{\partial R_{I\mu} \partial R_{J\nu}}$$

  - "Spring constants" between atom *I* and *J* in directions m and n
  - DFT. *Time consuming. Only very small wires, D~1 nm!*
  - Empirical potentials: *Fast!*

Phonon band structures

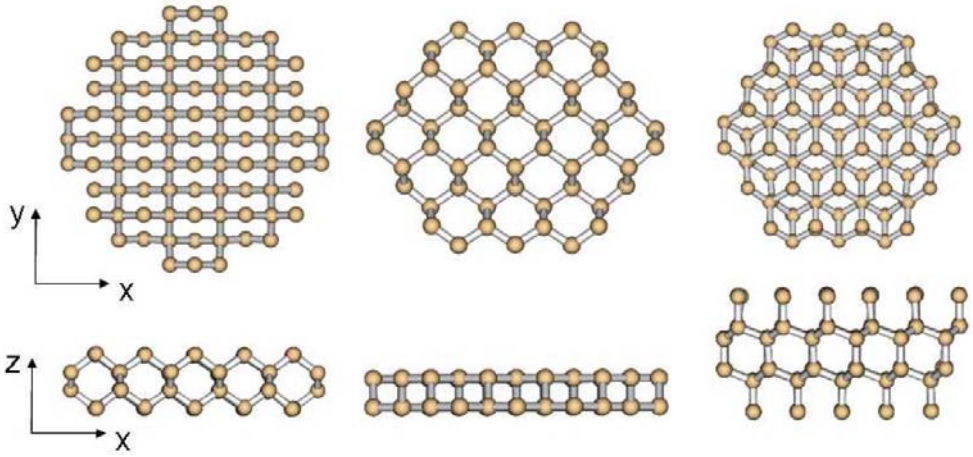

Cross section

Side view of unit cell
(transport along z-axis)

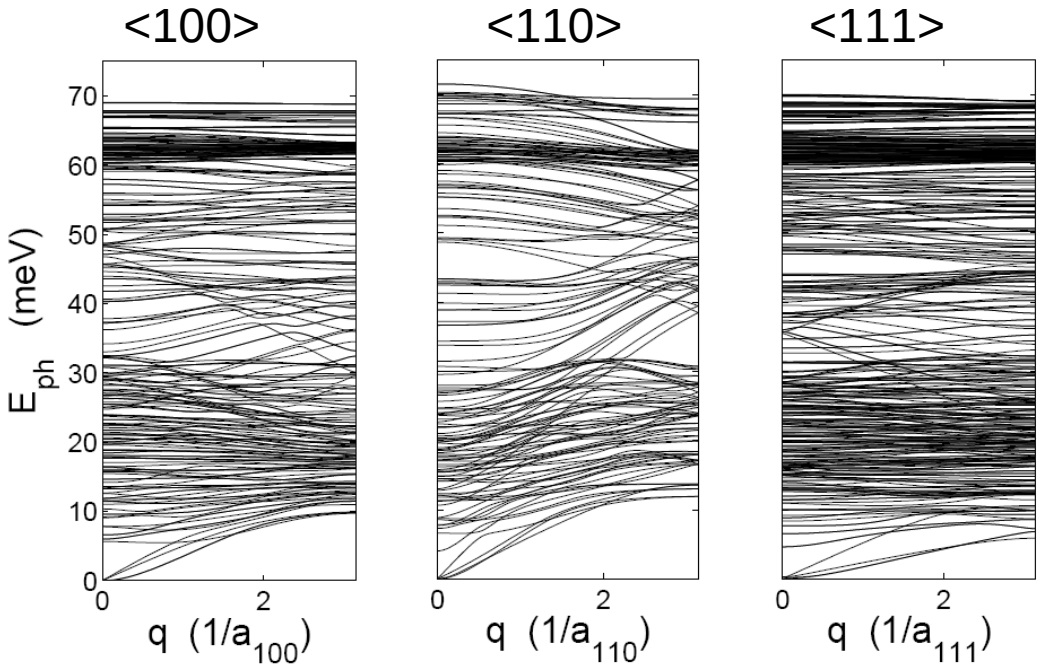

← Bulk optical band

Four acoustic modes:

- Mode 1,2: Flexural, $w \sim q^2$
- Mode 3: Torsional, $w \sim q$
- Mode 4: Dilatational, $w \sim q$

Thermal conductance from Landauer formula

Thermal current

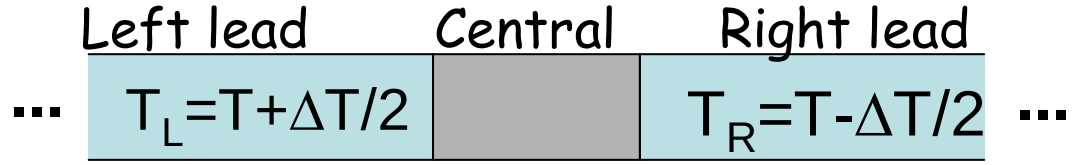

$$J_{th}(T) = \frac{\hbar}{2\pi}\int_0^\infty \mathrm{d}\omega\,\omega\,\mathcal{T}(\omega)\,[n_B(T_L) - n_B(T_R)]$$

Thermal conductance dJ/d(ΔT)

$$G(T) = \frac{\hbar^2}{2\pi k_B T^2}\int_0^\infty \mathrm{d}\omega\,\omega^2\,\mathcal{T}(\omega)\,\frac{e^{\hbar\omega/k_BT}}{(e^{\hbar\omega/k_BT}-1)^2}$$

Transmission function

$$\mathcal{T}(\omega) = \mathrm{Tr}[\,\mathbf{\Gamma}_L(\omega)\,\mathbf{G}_C^r(\omega)\,\mathbf{\Gamma}_R(\omega)\,\mathbf{G}_C^a(\omega)]$$

Retarded Green's function (harmonic approximation)

$$\mathbf{G}_C^r(\omega) = [\,\omega^2\,\mathbf{M} - \mathbf{K}_C - \mathbf{\Sigma}_L^r(\omega) - \mathbf{\Sigma}_R^r(\omega)]^{-1}$$

- Thermal conductance

$$G(T) = \frac{\hbar^2}{2\pi k_B T^2} \int_0^\infty \mathrm{d}\omega\, \omega^2\, \mathcal{T}(\omega)\, \frac{e^{\hbar\omega/k_B T}}{(e^{\hbar\omega/k_B T} - 1)^2}$$

- Transmission function in *ideal ballistic* limit: $\mathcal{T}(\omega) = N_b(\omega)$

$N_b(\omega)$: Number of bands at $\hbar\omega$

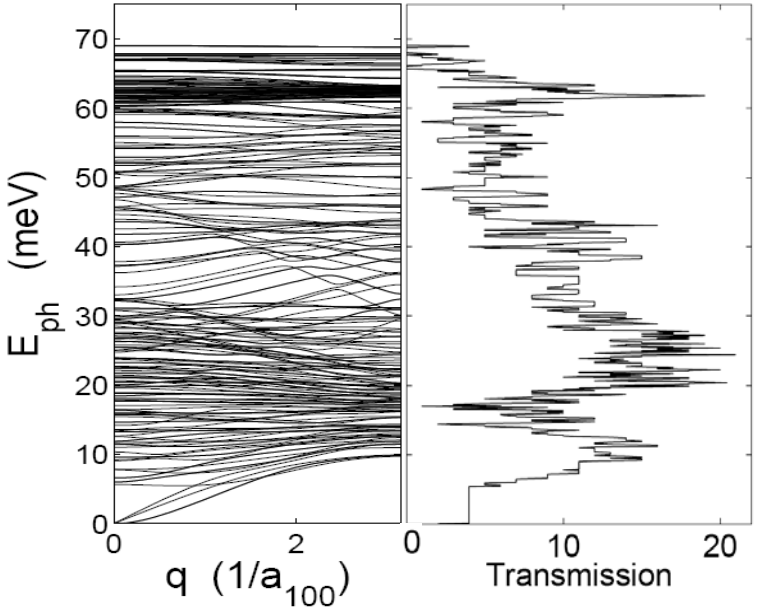

Transmission function

- Areas (diam~4 nm):
  $A_{\langle 100\rangle} = 8.9\ \mathrm{nm}^2$
  $A_{\langle 110\rangle} = 11.2\ \mathrm{nm}^2$
  $A_{\langle 111\rangle} = 9.0\ \mathrm{nm}^2$.

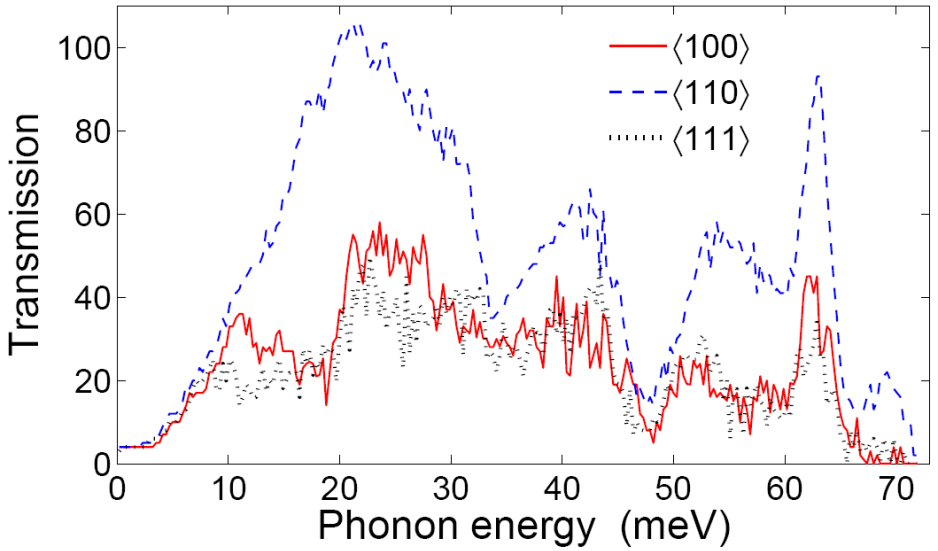

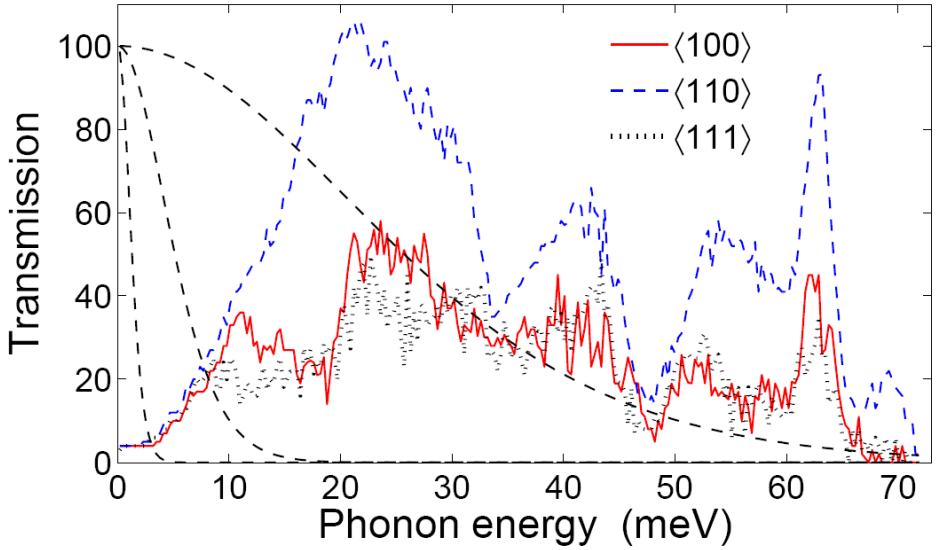

- Dashed lines: $\omega^2 \frac{e^{\hbar\omega/k_BT}}{(e^{\hbar\omega/k_BT}-1)^2}$ T=5, 20, 100 K

$$G(T) = \frac{\hbar^2}{2\pi k_B T^2}\int_0^\infty \mathrm{d}\omega\,\omega^2\,\mathcal{T}(\omega)\,\frac{e^{\hbar\omega/k_BT}}{(e^{\hbar\omega/k_BT}-1)^2} \qquad \text{T<5 K} \quad = 4(\pi^2 k_B^2 T/3h)$$

Conductivity vs. area

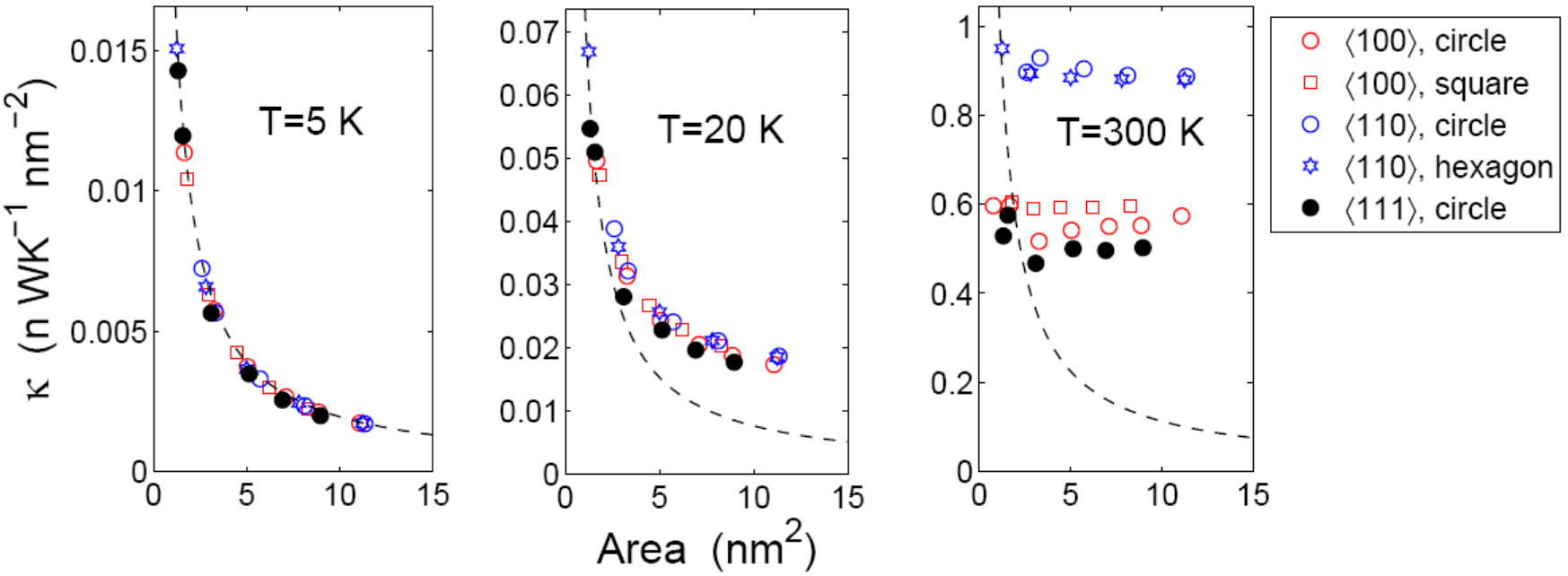

- Conductivity: $\kappa(T) = \frac{G(T)}{A}$
- Dashed lines: $\frac{G_Q(T)}{A} = \frac{1}{A}\frac{4\pi^2 k_B^2 T}{3h}$

At T=300 K, <110> wires have 50-75% larger k than <100> and <111> wires!

T. Markussen *et al.* Nano Letters 8, 3771-3775 (2008).

Role of vacancies

- Here we present some recent results for both surface and bulk vacancies (PRB 79, 035415 (2009))
- The improved thermoelectric properties in the two experiments was attributed to phonon scattering against vacancies

Example of a surface vacancy

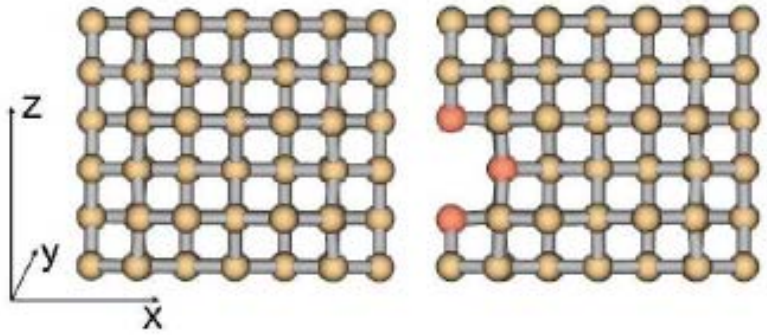

FIG. 5: (color online). Relaxed structure of a 1.2 nm diameter ⟨110⟩ wire (3 unit cells seen from the ⟨100⟩ direction) with (right) and without (left) a vacancy. The vacancy primarily affects the three nearest neighbors indicated with a red tone in the right plot. The wire is oriented along the $z-$direction in the inserted coordinate system.

Results – benchmarking phenomenology

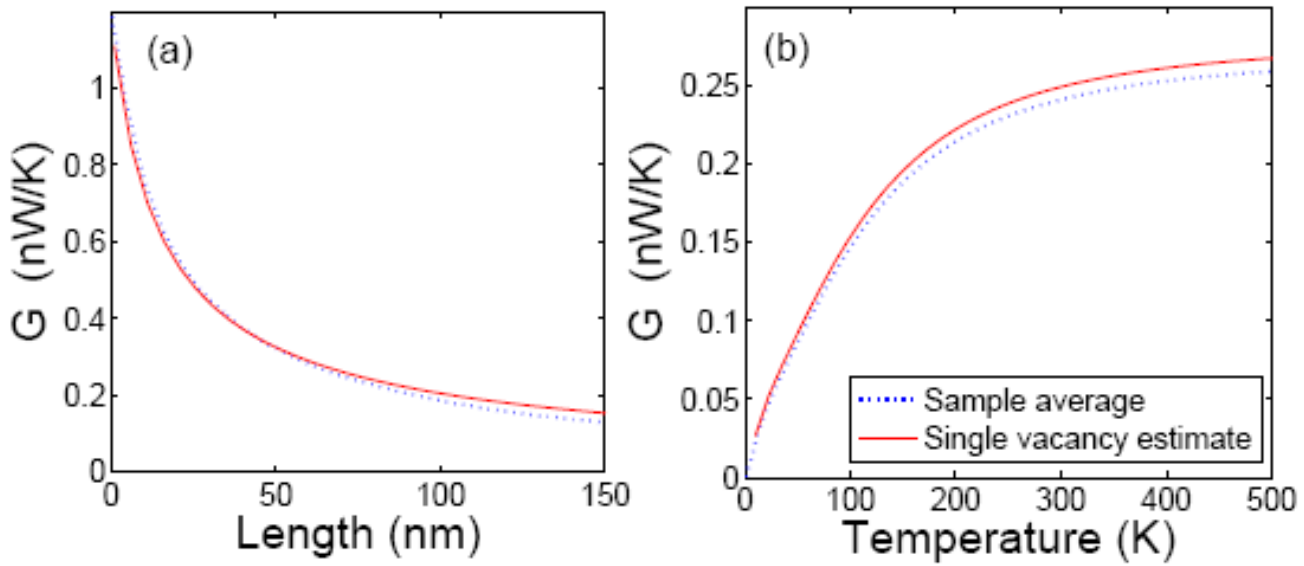

FIG. 6: (color online). Thermal conductance vs. length (a), at $T = 300\,\mathrm{K}$ and vs. temperature (b) at $L = 75\,\mathrm{nm}$. Solid line is obtained from long wire calculations and sample averaging, while the squares are obtained using (6).

Results – bulk vs surface

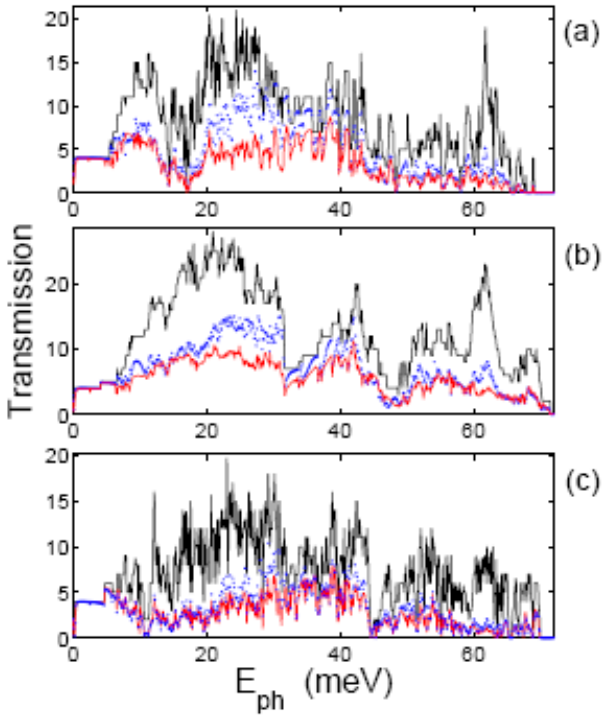

FIG. 8: (color online). Transmission function vs. phonon energy for wires with different orientations containing a total number of five vacancies. The upper solid curve shows the ballistic transmission (through a wire with zero vacancies) while the lower solid curve correspond to a wire with only bulk vacancies. The dots are obtained for wire containing only surface vacancies.

Trend: surface vacancies scatter *less* efficiently than bulk vacancies!

Thus, experimentalists: find a fabrication method with lots of bulk vacancies!

Idea: stop phonons but let electrons flow!

How to realize in practice: fine-tune dos!

Technical University of Denmark DTU

$ZT=S^2T\sigma/\kappa$

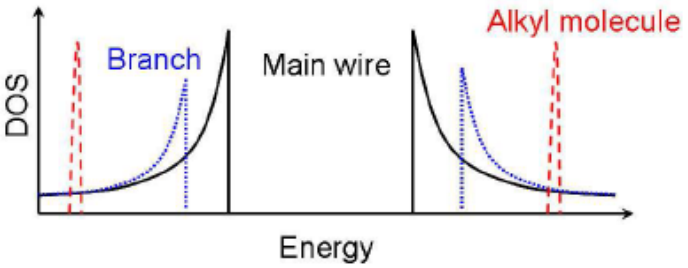

Arrange so that extra dos due to scatterers is away from band-edges.

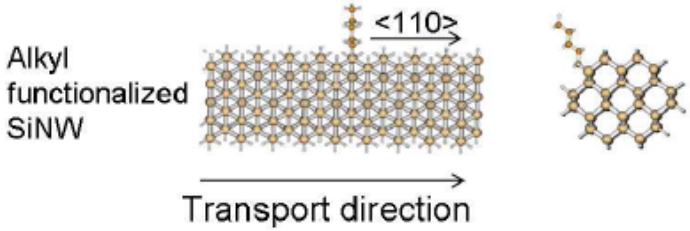

Both of these structures exist!

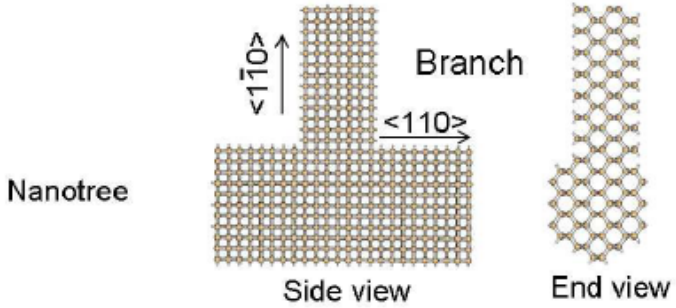

Charge transmission

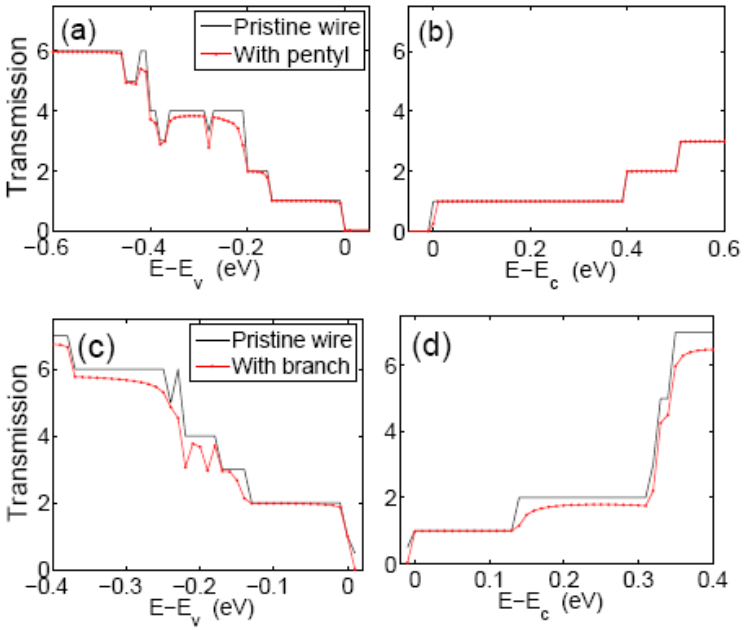

Phonon transmission

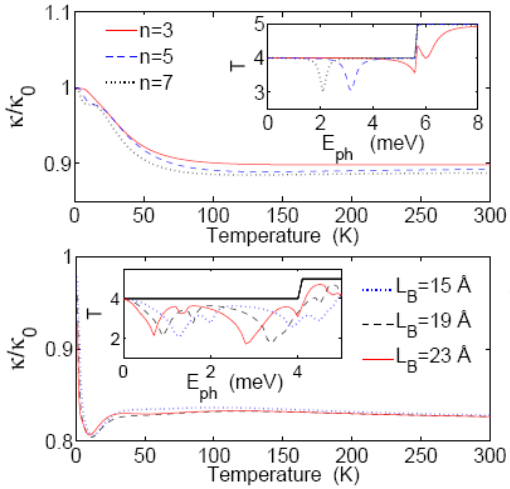

alkyls

nanotrees

Figure of merit as a function of coverage

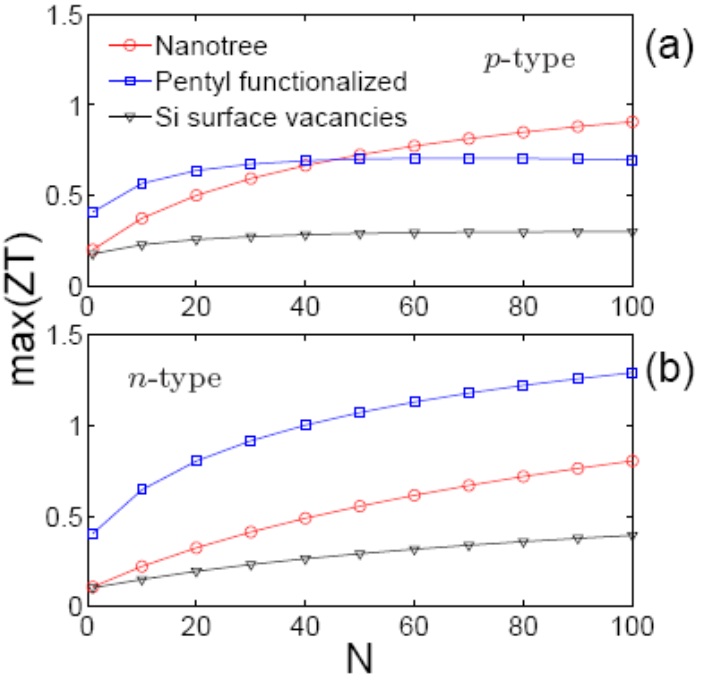

Summary – Part I

• DEFT/NEGF formalism can be used to study transport properties of **real** nanowires

•The heavy computational load can be diminished by using phenomenological models to scale single-impurity calculations to long-wire calculations

•The method has predictive power and is useful in designing experiments and fabrication technologies

• An example of a physical results: crystalline orientation for <110> has 50-75% larger κ than <100> and <111>. The result is expected to hold for other materials than just Si.

• An example of a suggestion for further enhancment of ZT: use "nanodecoration"

•The method can be used together with "fancier" theoretical concepts to study basic physics phenomena

Part 2 – smaller and colder…

TKK

Technical University of Denmark DTU

Measurement of the quantum of thermal conductance

NATURE | VOL 404 | 27 APRIL 2000 |

K. Schwab*, E. A. Henriksen*, J. M. Worlock*† & M. L. Roukes*

$$G_{\mathrm{th}} = \frac{J_{\mathrm{th}}}{\Delta T} = \frac{k_{\mathrm{B}}^2}{h} \sum_m \int_{x_m}^{\infty} \mathrm{d}x \frac{x^2 e^x}{(e^x - 1)^2} T_m(x k_{\mathrm{B}} T/\hbar)$$

Heat conductance quantum per ballistic mode

$$G_{\mathrm{th}} = g_0 = \pi^2 k_{\mathrm{B}}^2 T/(3h)$$

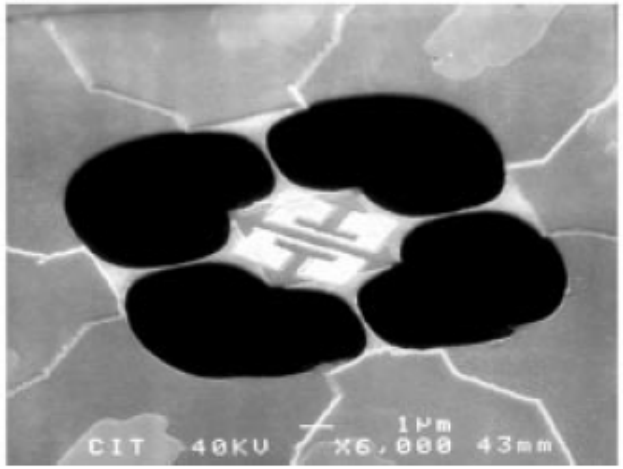

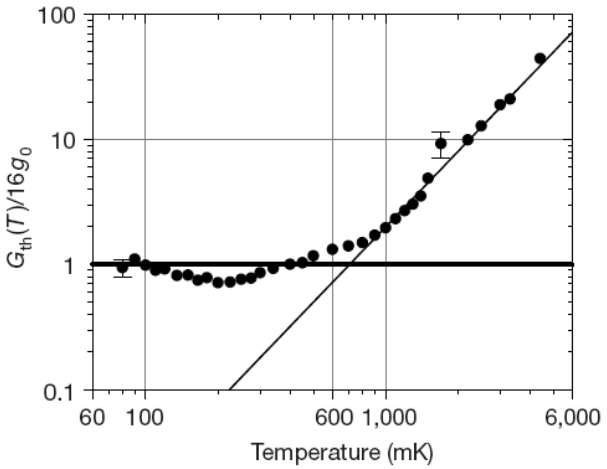

Why 16 quanta? (1 dilatational+1 torsional+2 flexural)·(4 arms) = 16

Schmidt et al (PRL, 2004): At very low temperatures one must also take into account the **photon thermal conductance**, which may become the dominant mechanism for small samples. The photon heat conductance is $G_\gamma = r\pi^2 k_B T/3h$, where r is a "matching factor".

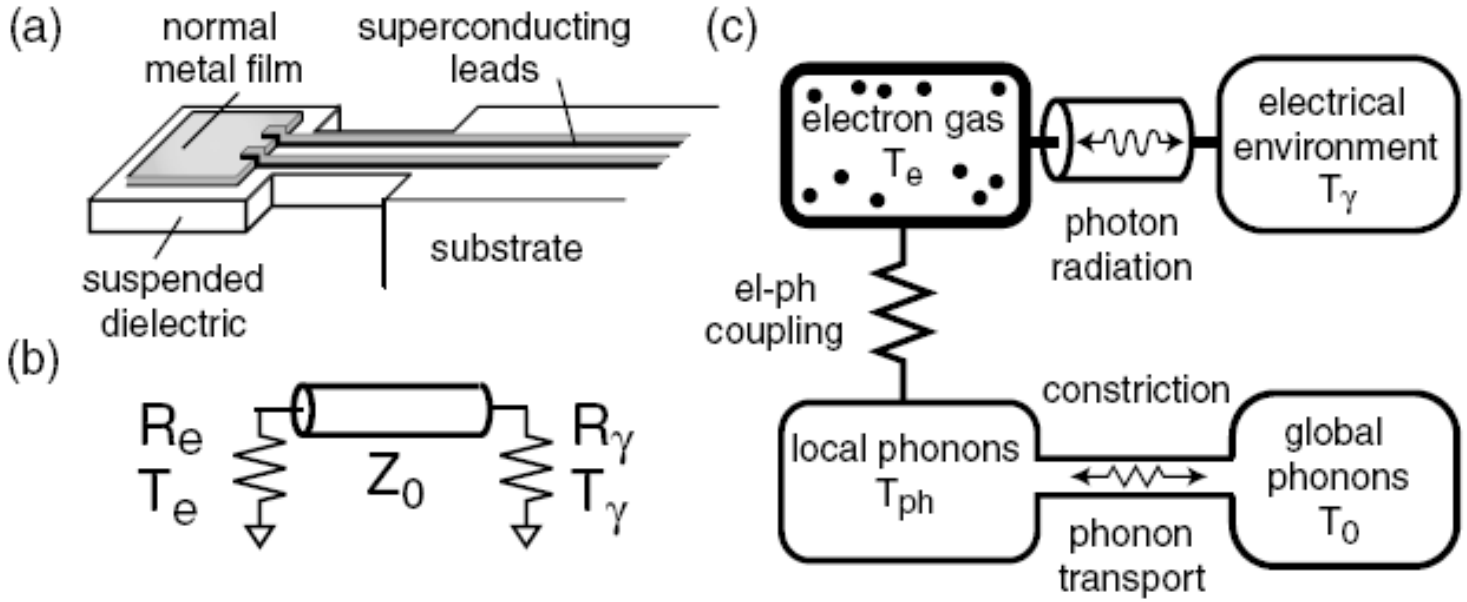

At low temperatures there is a crossover:

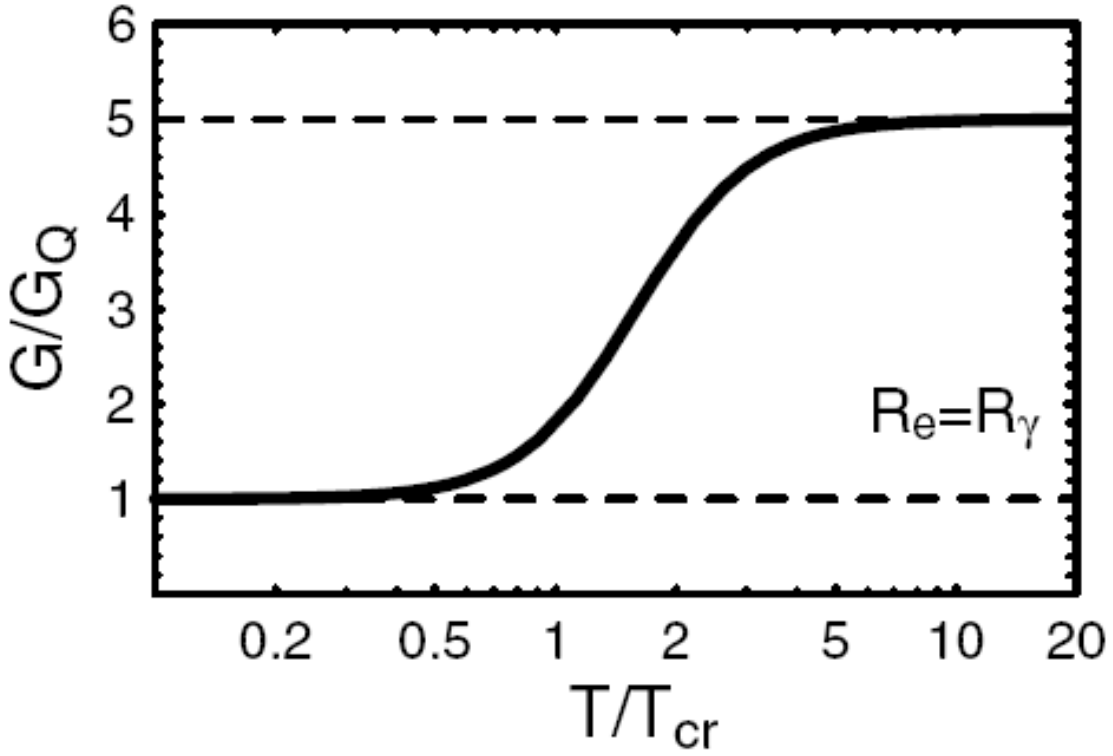

Estimate cross-over by equating photon and phonon contributions: $T_{cr} \approx 50$ mK/(V/μm^3)$^{1/3}$

Generalize to two resistors, mutually coupled via superconducting links, interrupted by SQUIDS (thus no conventional heat conduction), and individually coupled to heat a sink at T_0 via electron-phonon interaction.

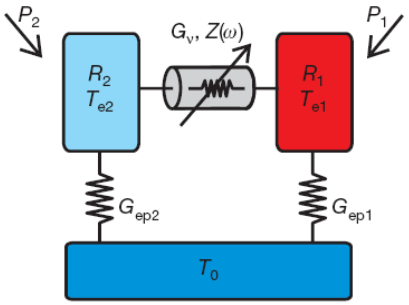

Photon heat flux (Pendry 1983):

$$P_v = \int_0^\infty \frac{d\omega}{2\pi} \frac{4R_1 R_2}{|Z_t(\omega)|^2} \hbar\omega [n_1(\omega) - n_2(\omega)]$$

$$Z_t(\omega) \equiv R_1 + R_2 + Z(\omega)$$

Tunable impedance (via dc SQUID)

Matched circuit (max value):

$$P_v^{Z=0} = r_0 \frac{\pi k_B^2}{12\hbar} \left(T_{e1}^2 - T_{e2}^2\right)$$

Heat flux due to electron-phonon coupling:

$$P_{ep} \approx \Sigma\Omega (T_{ei}^5 - T_0^5)$$

TKK

Technical University of Denmark DTU

Vol 444|9 November 2006|doi:10.1038/nature05276

Single-mode heat conduction by photons

Matthias Meschke[1], Wiebke Guichard[1,2] & Jukka P. Pekola[1]

Ext. heat leak $P_i = \pm \frac{\pi k_B^2}{12\hbar}\left(r_1 T_{e1}^2 - r_2 T_{e2}^2\right) + \Sigma\Omega_i\left(T_{ei}^5 - T_0^5\right), i = 1,2$

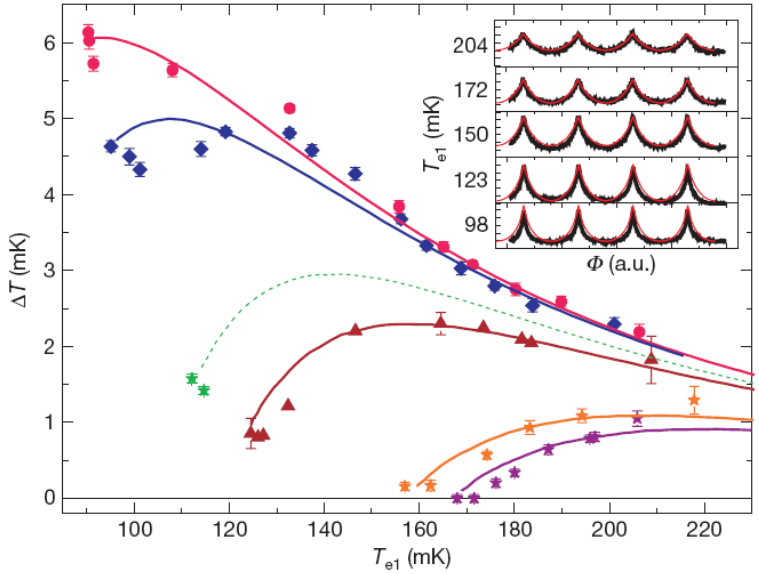

Inset: primary data for T0=75mK, at different power levels

T_o=60, 75, 105, 157, 167 mK. Solid line: theory fit.

TKK

Technical University of Denmark DTU

We pose the question:

Can one build thermal quantum circuits that perform some advanced functions, such as transistor action, or rectification, based on photonic heat conduction?

We study the following generic circuit:

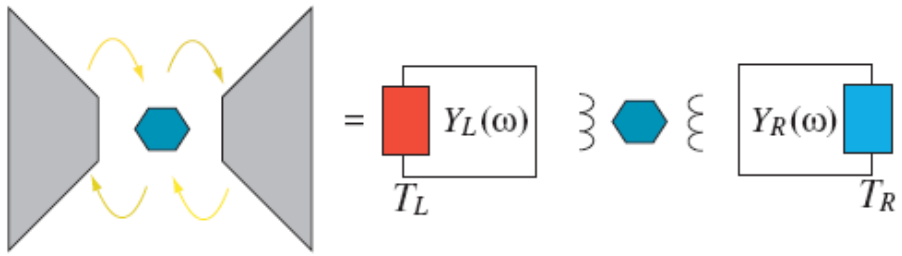

The left and right reservoirs are assumed to behave as linear dissipative elements, and they couple only through the middle element.

This setup bears a close analogy with the approach by Caroli et al (or the modern version due to Meir and Wingreen): noninteracting elementary excitations couple via tunneling barriers to an interacting central region.

Meir-Wingreen formula (PRL 1992) gives the tunneling current through an interacting mesoscopic region (here, for proportionate coupling):

$$J = \frac{ie}{\hbar}\int \frac{d\varepsilon}{2\pi}\,\mathrm{Tr}\left\{\frac{\mathbf{\Gamma}^L(\varepsilon)\mathbf{\Gamma}^R(\varepsilon)}{\mathbf{\Gamma}^L(\varepsilon)+\mathbf{\Gamma}^R(\varepsilon)}\left[\mathbf{G}^r(\varepsilon)-\mathbf{G}^a(\varepsilon)\right]\right\}\left[f_L(\varepsilon)-f_R(\varepsilon)\right]$$

Teemu Ojanen & APJ (PRL 100, 155902 (2008)) show that the photonic heat current is given by (here, proportionate admittances)

$$J = M^2\int_0^\infty \frac{d\omega\,\omega^2}{2\pi}\,\frac{2\mathrm{Re}[Y_L(\omega)]\mathrm{Re}[Y_R(\omega)]}{\mathrm{Re}[Y_L(\omega)]+\mathrm{Re}[Y_R(\omega)]}\left[S_I(\omega)-S_I(-\omega)\right]\left[n_L(\omega)-n_R(\omega)\right]$$

Electronic transport	Photonic transport
$\Gamma(\omega)$, coupling to leads, proportional to density-of-states in leads	$Y(\omega)$, reservoir admittance, prop. to mode density in reservoir
$-i(G_r-G_a)$ = spectral function of the central region=dos in central region	$S_I(\omega)- S_I(-\omega)$ = noise power density for central region connected to reservoirs
$f_L(\omega)- f_R(\omega)$ = voltage window	$n_L(\omega)- n_R(\omega)$ = thermal window

Final result for a single LC-resonator, valid for arbitrary reservoir admittances:

$$J = \int_0^\infty \frac{d\omega}{2\pi} \frac{4\hbar\omega^5 M^4 \mathrm{Re}[Y_L(\omega)]\mathrm{Re}[Y_R(\omega)]}{|\omega F(\omega) - M^2\omega^2[Y_L(\omega) + Y_R(\omega)]|^2} [n_L(\omega) - n_R(\omega)]$$

$$F(\omega) \equiv (i\hbar/I_0^2)(\omega^2 - \omega_0^2)/(2\omega_0)$$

It can be shown that the upper limit for conductance is $G_Q = \pi^2 k_B^2 T/3h$

Use a dc SQUID to tune the properties of the central region. This will modify the heat current through the system.

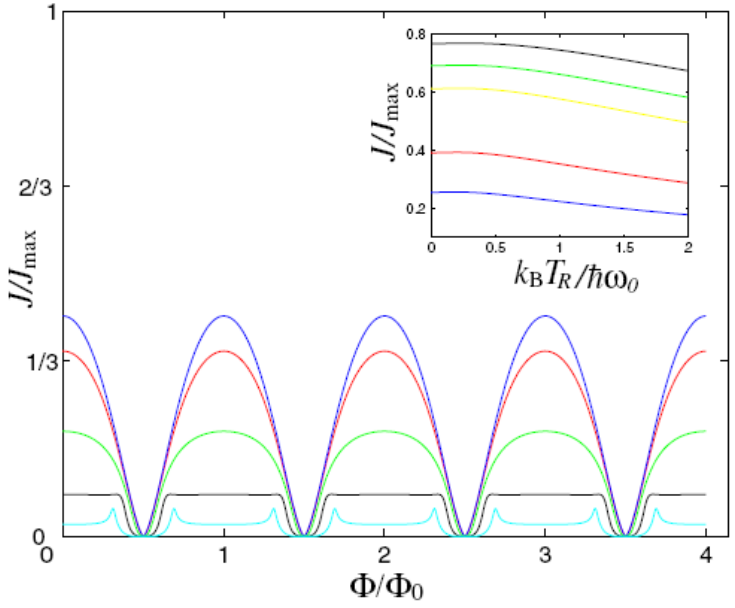

$$L(\Phi) \approx L/|\cos(\pi\Phi/\Phi_0)|$$

$$\Phi_0 = h/2e$$

Photon heat transistor!

TKK

Technical University of Denmark DTU

Application 2: Rectification in a nonlinear quantum circuit (arXiv:0812.3634)

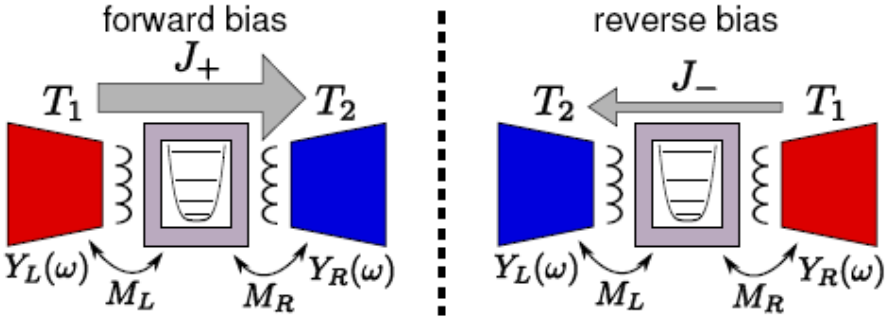

Rectification:

$$\mathcal{R} = (J_+ - J_-)/\max\{J_+, J_-\}$$

Previous studies of thermal rectification:

(i) Classical/quantum nonlinear chain is coupled asymmetrically to linear reservoirs (Terraneo et al PRL 88, 094302 (2002), Li et al PRL 98, 18401 (2004), Hu et al PRL 97, 124302 (2006), Zeng et al PRB 78, 024305 (2006))

(ii) Nonlinear reservoirs are coupled through a harmonic oscillator (Segal, PRL 100, 105901 (2008))

Here, we demonstrate photonic thermal rectification in a fully quantum mechanical and **experimentally realizable** system. (Rectification 7 % has been observed for phonons in nanotubes, Chang et al, Science 314, 1121 (2006))

TKK Consider the model (come back to physical realization later)

$$H_M = \hbar\omega_0(\hat{b}^\dagger\hat{b} + \frac{1}{2}) + \frac{\hbar\epsilon}{2}(\hat{b} + \hat{b}^\dagger)^4$$

Use again (now need to keep the asymmetry)

$$J = \int_0^\infty \frac{d\omega\omega^2 M_L^2}{2\pi}\left\{2\left[S_I(-\omega) - S_I(\omega)\right]\mathrm{Re}[Y_L(\omega)]n_L(\omega) + S_I(-\omega)2\mathrm{Re}[Y_L(\omega)]\right\}$$

We work in a mean-field approximation (NB – this needs to be examined):

$$H_M \approx \hbar\omega_0(\hat{b}^\dagger\hat{b} + \frac{1}{2}) + \hbar\epsilon\Phi(\hat{b}^\dagger + \hat{b})^2 \qquad \text{where} \qquad \Phi = \langle(\hat{b}^\dagger + \hat{b})^2\rangle$$

This leads to a renormalized noninteracting problem,

$$H_M = \hbar\tilde{\omega}_0(\tilde{b}^\dagger\tilde{b} + \frac{1}{2}), \qquad \hat{I} = \tilde{I}_0(\tilde{b} + \tilde{b}^\dagger)$$

$$\tilde{\omega}_0 = \omega_0\sqrt{1 + \tfrac{4\epsilon\Phi}{\omega_0}} \text{ and } \tilde{I}_0 = \sqrt{\tfrac{\omega_0}{\tilde{\omega}_0}}I_0$$

TKK

Technical University of Denmark DTU

The self-consistent equations are

Dyson: $$\langle \hat{I}\hat{I}\rangle^r(\omega) = \frac{1}{\left(\langle \hat{I}\hat{I}\rangle_0^r(\omega)\right)^{-1} - \tilde{I}_0^{-2}\Sigma^r(\omega)}$$

Keldysh: $$\langle \hat{I}\hat{I}\rangle^<(\omega) = \tilde{I}_0^{-2}|\langle \hat{I}\hat{I}\rangle^r(\omega)|^2\Sigma^<(\omega)$$

$$\langle \hat{I}\hat{I}\rangle_0^r(\omega) = 2\tilde{I}_0^2\tilde{\omega}_0/(\omega^2 - \tilde{\omega}_0^2)$$

$$\Sigma^r(\omega) = -\frac{i\tilde{I}_0^2\omega}{\hbar}\left[M_L^2 Y_L(\omega) + M_R^2 Y_R(\omega)\right]$$

$$\Sigma^<(\omega) = -\frac{i\tilde{I}_0^2\omega}{\hbar}\left[M_L^2 \mathrm{Re}(Y_L(\omega))n_L(\omega) + M_R^2 \mathrm{Re}(Y_R(\omega))n_R(\omega)\right]$$

$$\Phi = \langle(\hat{b}^\dagger + \hat{b})^2\rangle = -I_0^{-2}\int_{-\infty}^{\infty}\frac{d\omega}{2\pi i}\langle \hat{I}\hat{I}\rangle^<(\omega)$$

The numerical solution poses no fundamental difficulty. 9 parameters:

$$\epsilon/\omega_0,\ k_B T_{1/2}/\hbar\omega_0,\ M_{L/R}^2 I_0^2/\hbar R_{L/R},\ Q_{L/R},\ \text{and}\ \omega_{L/R}/\omega_0$$

Model: resistor, capacitance, inductor in series

$$Y_{L/R}(\omega) = R_{L/R}^{-1}[1 - iQ_{L/R}(\frac{\omega}{\omega_{L/R}} - \frac{\omega_{L/R}}{\omega})]^{-1}$$

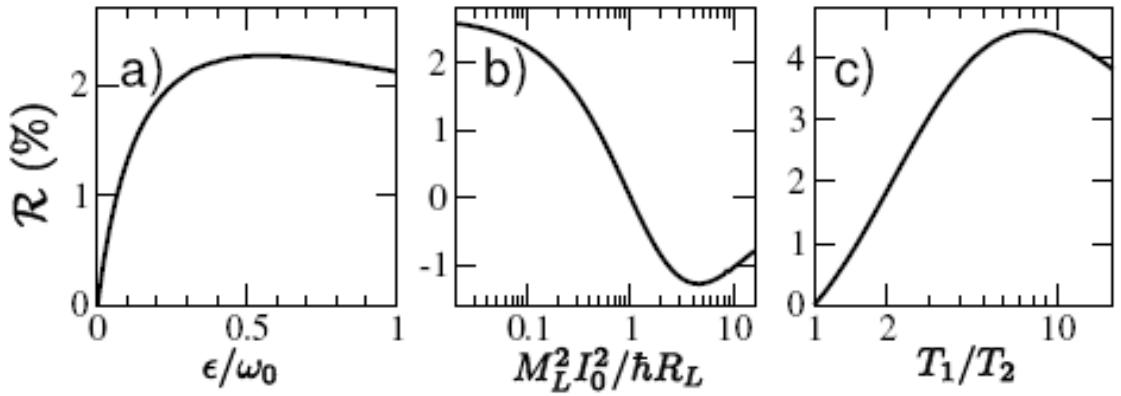

FIG. 2: Rectification with purely resistive reservoirs, $Q_L = Q_R = 0$, as a function of (a) nonlinearity ϵ, (b) coupling M_L, and (c) temperature ratio T_1/T_2. In all panels we have $\epsilon/\omega_0 = 0.2$, $k_B T_1/\hbar\omega_0 = 0.2$, $k_B T_2/\hbar\omega_0 = 0.1$, $M_L^2 I_0^2/\hbar R_L = 0.2$, and $M_R^2 I_0^2/\hbar R_R = 1$, except for the variable on the horizontal axis. In panel (c) T_1 is varied.

TKK

Technical University of Denmark DTU

$$J_{\max} = \frac{\pi k_B^2}{3\hbar}(T_1^2 - T_2^2)$$

Note competition: large rectification requires high temperatures, however this leads to small overall current.

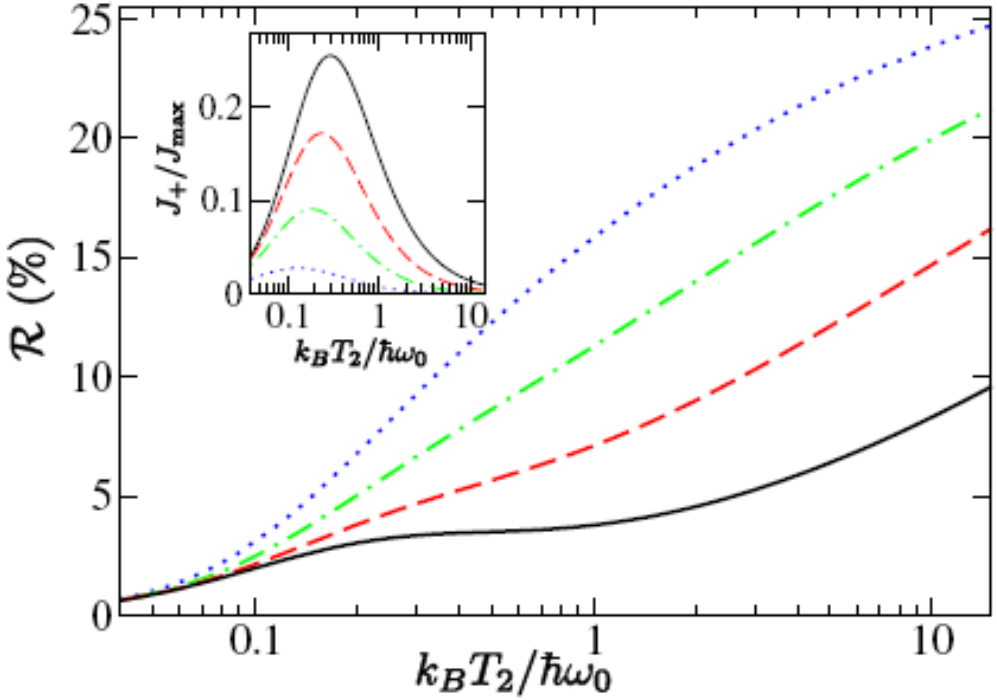

FIG. 3: Rectification with one reactive reservoir ($Q_L = 0.1$). Here $T_1/T_2 = 2$ and the different curves correspond to $\omega_L/\omega_0 = 0.2$ (solid), 0.1 (dashed), 0.05 (dash-dotted), 0.02 (dotted). Other parameters as in Fig. 2.

For large ω_L the rectification may change sign as a function of temperature!

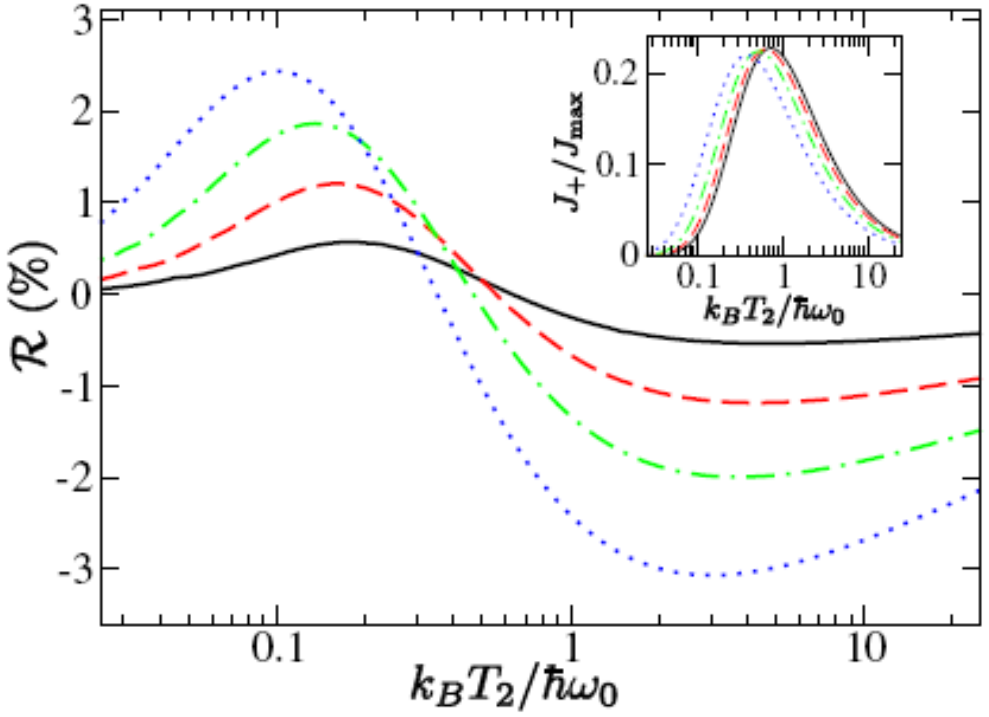

FIG. 4: Rectification as a function of temperature. Here $Q_L = 0.1$, $\omega_L = 10\,\omega_0$ and the curves correspond to $T_1/T_2 =$ 1.2 (solid), 1.5 (dashed), 2 (dash-dotted), 3 (dotted). Other parameters as in Fig. 2.

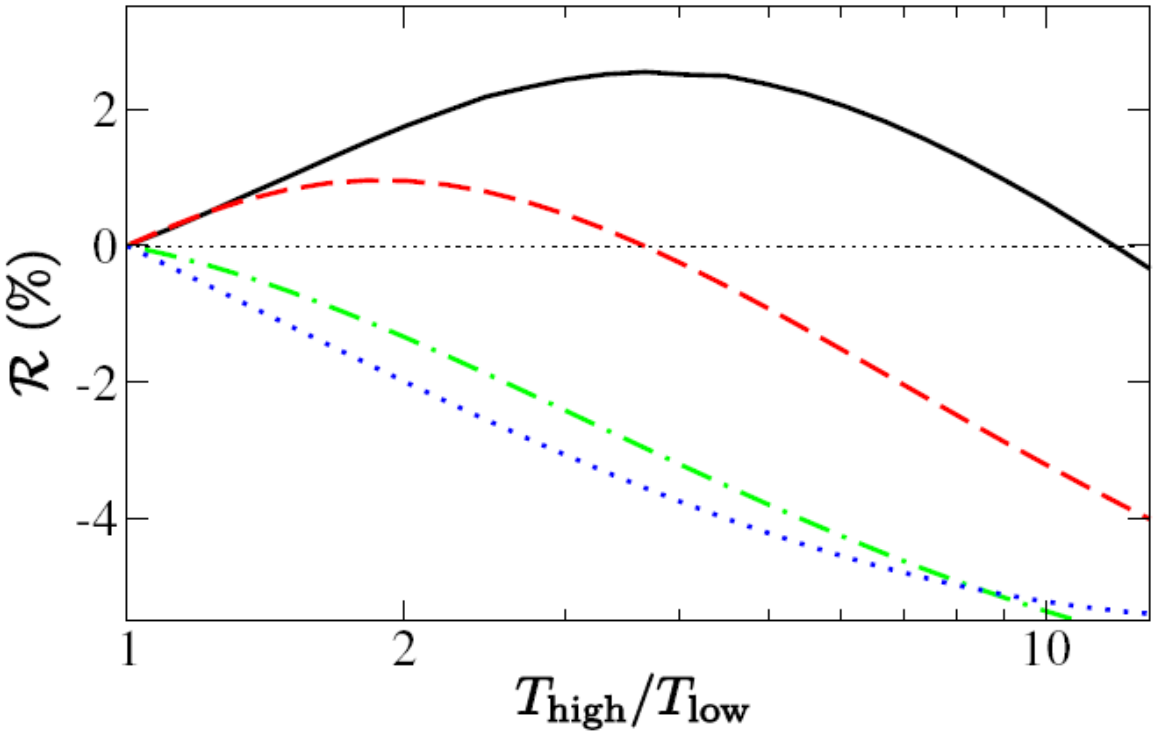

FIG. 4: Change of rectification sign as a function of operating temperature. Here the lower temperature is kept fixed, with values $k_B T_{\mathrm{low}}/\hbar\omega_0 = 0.1$ (solid), 0.3 (dashed), 1 (dash-dotted), 3 (dotted), and the higher temperature is varied. The left reservoir is reactive with $Q_L = 0.1$ and $\omega_L = 10\,\omega_0$, and other parameters are as in Fig. 2.

TKK

Technical University of Denmark DTU

Physical realization: superconducting loop (L) with a Josephson junction (E_J, C):

$$H_M = E_C\hat{q}^2 + E_L(\hat{\phi} - \phi_x)^2 - E_J\cos\hat{\phi}$$ $E_C=e^2/2C$ $E_L=(\hbar/2e)^2/2L$

Approximate this with

$$H_M = E_C\hat{q}^2 + (E_L + \frac{1}{2}E_J\cos\phi_0)\hat{\phi}^2 - \frac{1}{24}E_J\cos\phi_0\,\hat{\phi}^4 \equiv E_C\hat{q}^2 + E_2\hat{\phi}^2 + E_4\hat{\phi}^4$$

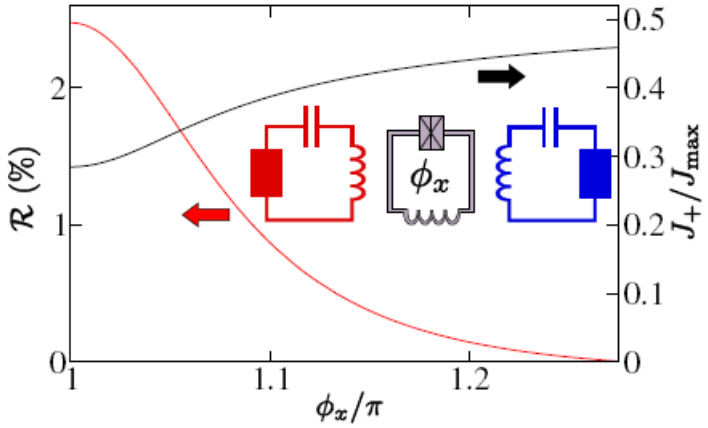

FIG. 5: Rectification and heat current through the SQUID system as a function of the control flux ϕ_x. Parameter values at $\phi_x = \pi$ as in Fig. 2, except $T_1 = 2T_2 = 0.4\hbar\omega_0/k_B$. Inset: Schematic of the SQUID setup with two linear reservoir circuits inductively coupled to a superconducting loop containing one Josephson junction.

TKK

Technical University of Denmark DTU

Conclusions:

- A conductance formula is proposed for radiative heat transfer between mesoscopic bodies
- Tunable middle circuit allows a transistor action
- A nonlinear middle circuit (e.g., superconducting loop with a Josephson junction) leads to rectification, and potentially a sign change for it
- The hard part of the calculation is the evaluation of noise spectrum in the presence of the coupling to em-environment

$$J = M^2 \int_0^\infty \frac{d\omega\omega^2}{2\pi} \frac{2\mathrm{Re}[Y_L(\omega)]\mathrm{Re}[Y_R(\omega)]}{\mathrm{Re}[Y_L(\omega)] + \mathrm{Re}[Y_R(\omega)]} [S_I(\omega) - S_I(-\omega)][n_L(\omega) - n_R(\omega)]$$

There are many potential applications for different central region: squeezed states, entangled states, cavities, multiple modes, capacitive coupling etc…

End of Part II.

TKK

Technical University of Denmark DTU

Antidot lattices in graphene – physics, models, devices

Antidot lattices, defined on a two-dimensional electron gas at a semiconductor heterostructure, are a well-studied class of man-made structures with intriguing physical properties. We point out that a closely related system, graphene sheets with regularly spaced holes (“antidots”), should display similar phenomenology, but within a much more favorable energy scale, a consequence of the Dirac fermion nature of the states around the Fermi level. Further, by leaving out some of the holes one can create defect states, or pairs of coupled defect states, which can function as hosts for electron spin qubits. We present a detailed study of the energetics of periodic graphene antidot lattices, analyze the level structure of a single defect, calculate the exchange coupling between a pair of spin qubits, and identify possible avenues for further developments.

PRL 100, 136804 (2008), see also Nature Research Highlights, April 17, 2008; review in NJP (2009) (special issue on graphene) arXiv:0907.0122

Work done in collaboration with T.G. Pedersen, M. Brandbyge, J. Fürst, J. Pedersen, T. Markussen, N. A. Mortensen, and K. Pedersen

Some acid rain remarks by A. K. Geim, Science **324**, 1530 (2009): (the skpeticism of an experimentalist against fancy theory)

…. as for the experiment, only Klein tunneling has been verified in sufficient detail….

…. transport properties have turned out to be much more complicated than theoretical quantum electrodynamics…

…. no consensus about the scattering mechanism that currently limits the mobility…

…. little understanding about the transport properties near the charge neutrality point…

…. no evidence about many of the predicted interaction effects…

TKK

Technical University of Denmark DTU

Throughout in this work we use simple models (tight-binding, finite elements, density-functional theory).

The complications arise because we attempt to model systems with nanopatterned extra features of experimentally achievable sizes, for which even DFT calculations are getting computationally very expensive (unit cells with rather low symmetry contain thousands of atoms).

In a sense, all our conclusions are "trivial" – what is important is that the parameters are "hard", and conclusions can be directly compared to experiment.

Also: this is a win-win situation: if single-particle (or DFT) theories fail, then the real fun starts with many-body physics.

TKK

Technical University of Denmark DTU

A short back-up on antidot physics (a very popular system in 80-90's, e.g., Weiss oscillations):

Antidot lattices on 2DEG (Nano Lett 5, 2515 (2005); Phys. Rev. B 77, 045325 (2008))

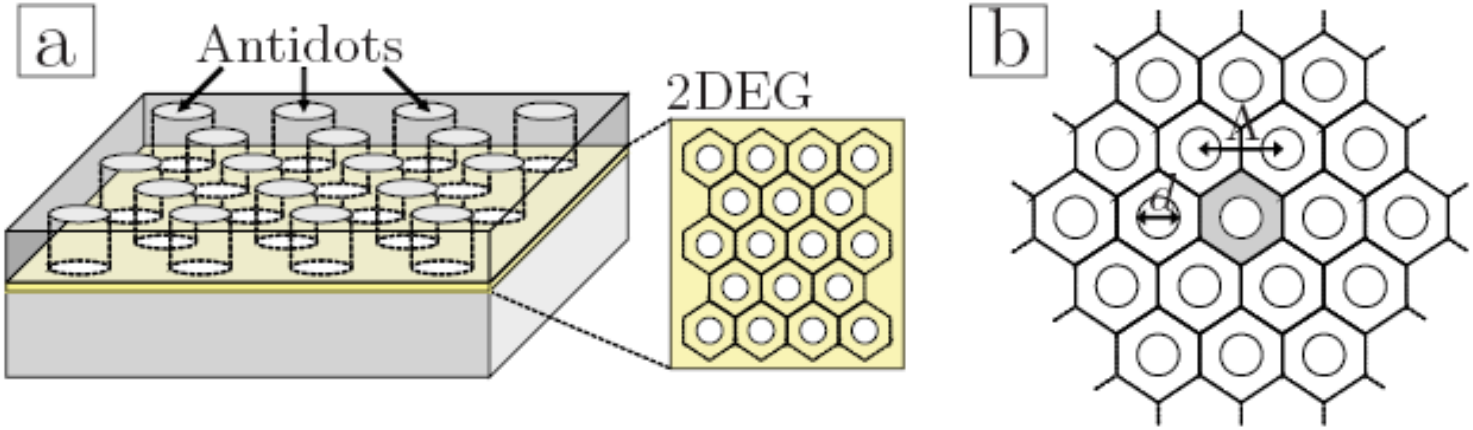

Our suggestion: use a designed defect leads to a state with a spin S

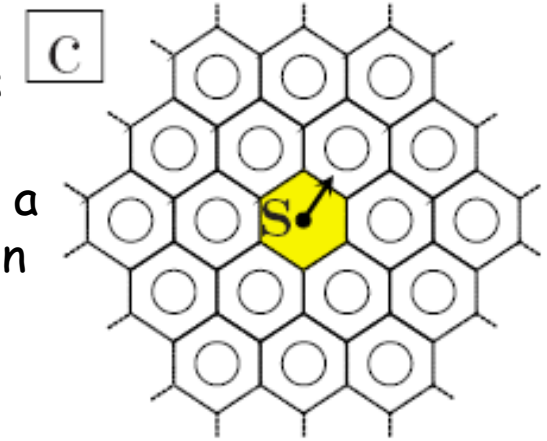

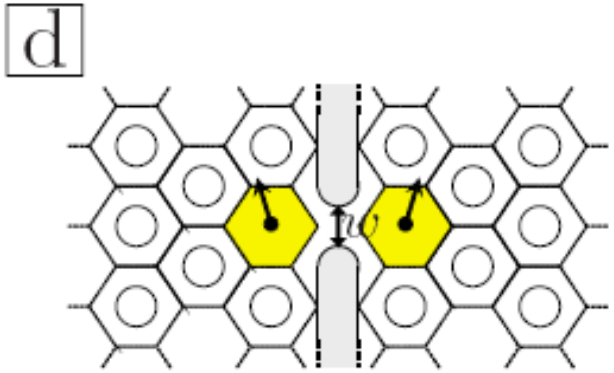

Coupling can be controlled by gate

Solid-state, scalable qubit?

$\epsilon_n \equiv E_n \Lambda^2 2m^*/\hbar^2$. For GaAs $\hbar^2/2m^* \simeq 0.6$ eV nm^2

Energetics for GaAs structures

$d/\Lambda = 0.5$

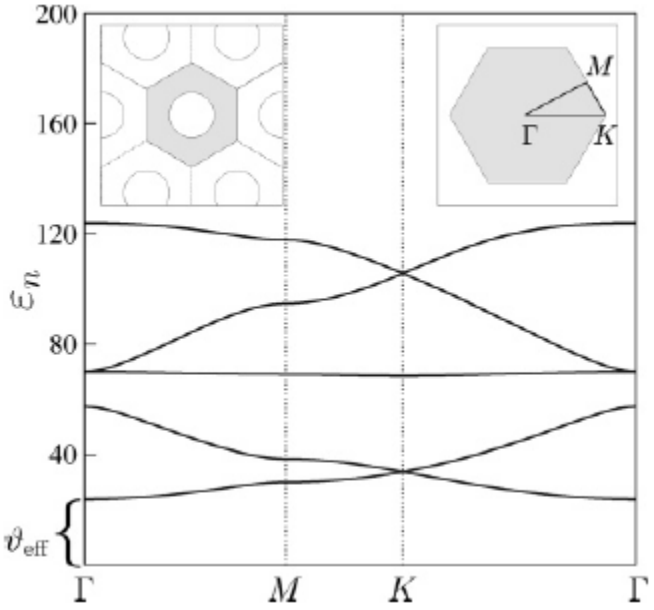

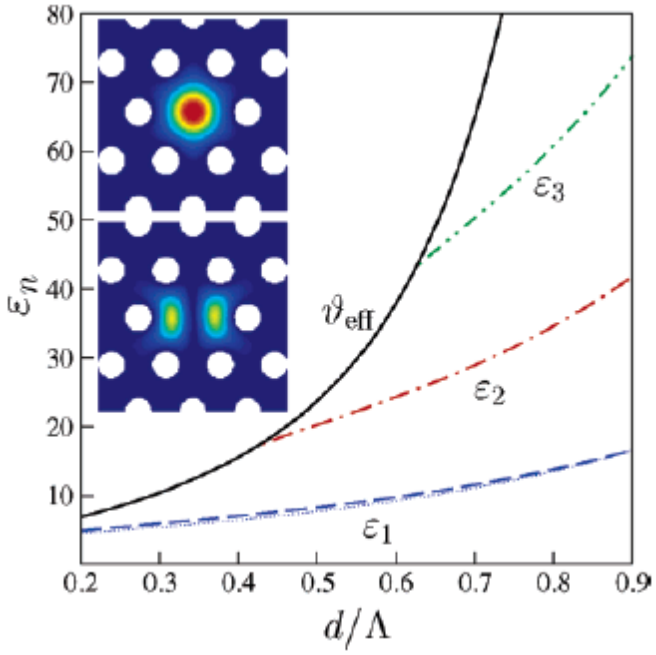

d: antidot size

☹: antidot lattice period

Perfect antidot lattice – notice the gap ❑$_{\text{eff}}$. For ☹=75nm, the gap is approx. 3 meV.

A missing antidot generates states in the gap (Inset: |✡|^2 for ground and 1st excited state)

TKK

Technical University of Denmark DTU

Tunneling matrix t element as a function of the width of the opening w, for three antidot lattices. $t = (E_+ - E_-)/2$

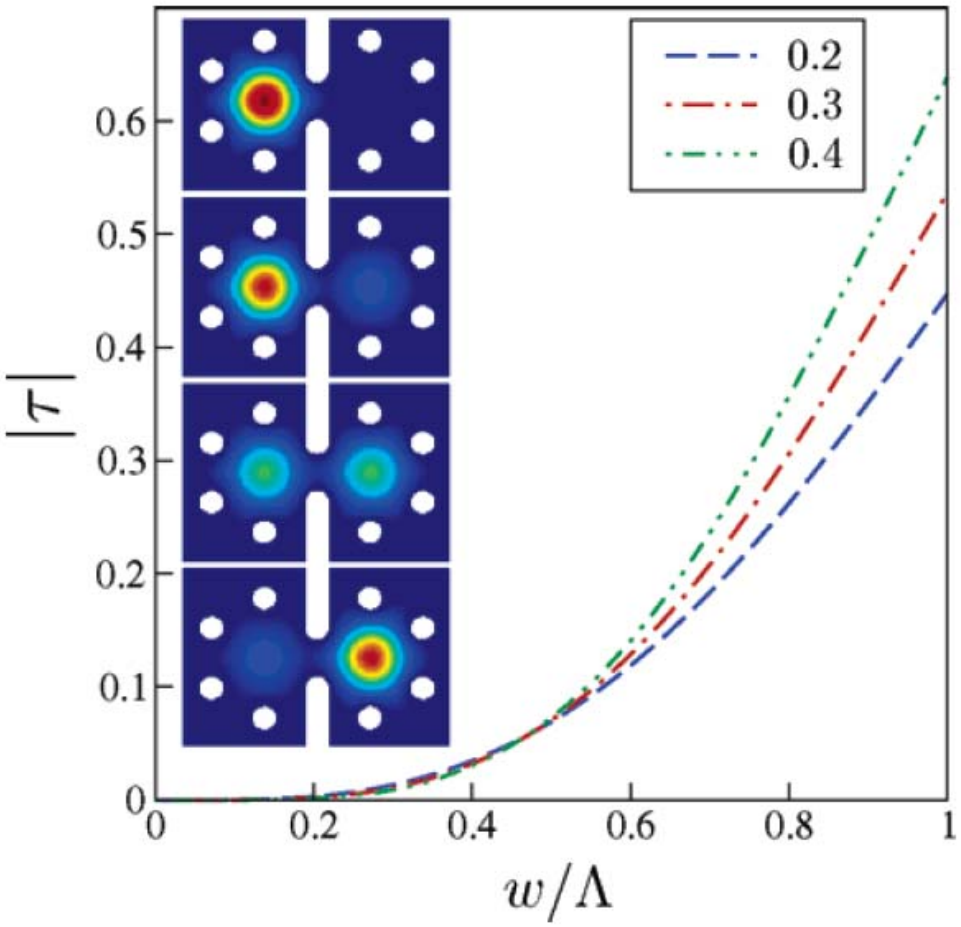

Two adjacent "missing antidots" can be used to construct a gate-controlled qubit.

This is technologically very demanding (requires antidot lattice spacing of a few nanometers (best realized structures as of date have spacing in hundreds of nm's) – therefore – enter:

GRAPHENE!

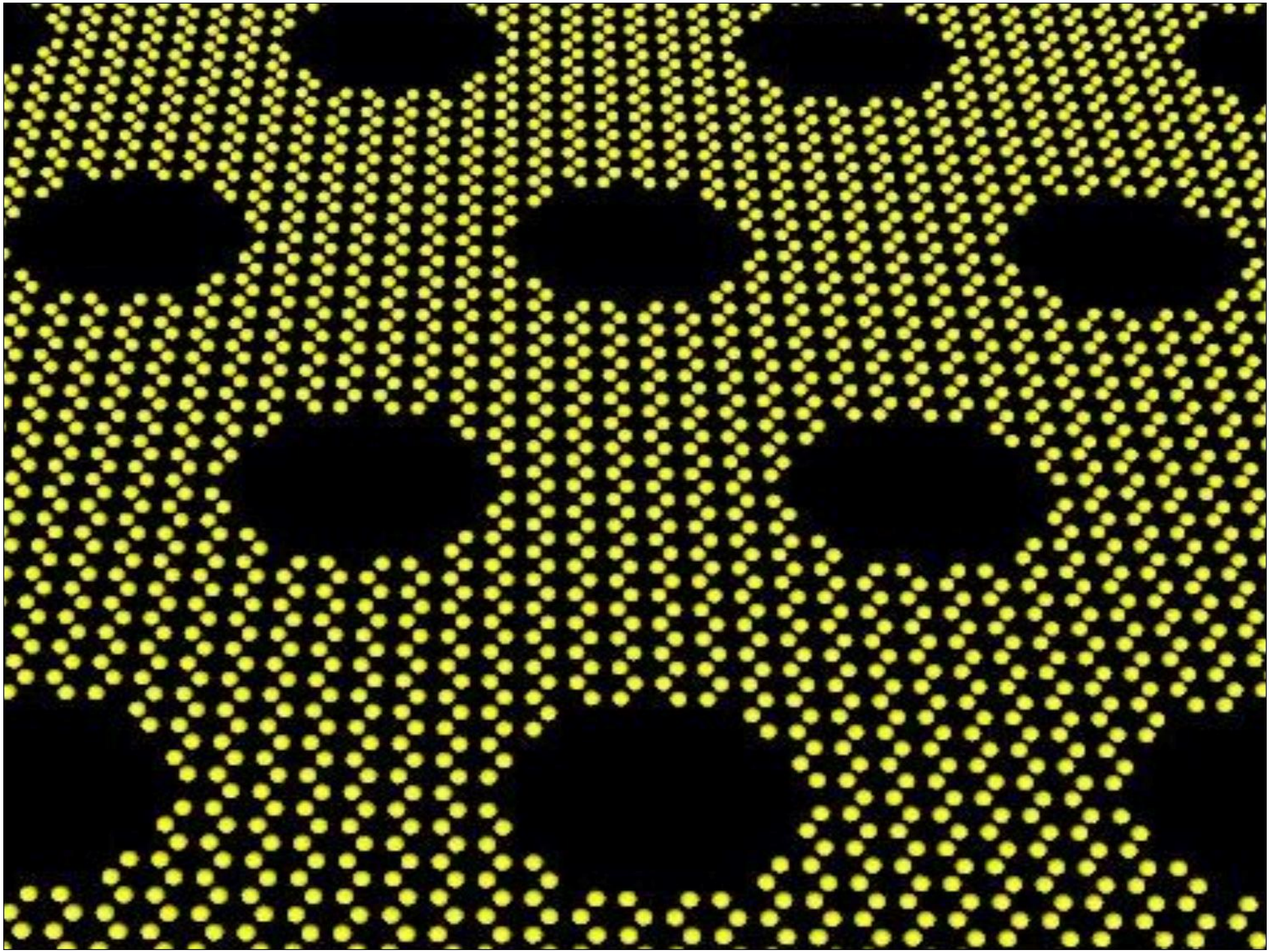

TKK

Technical University of Denmark DTU

Our proposal: construct a regularly perforated graphene sheet (PRL 100, 136804 (2008)):

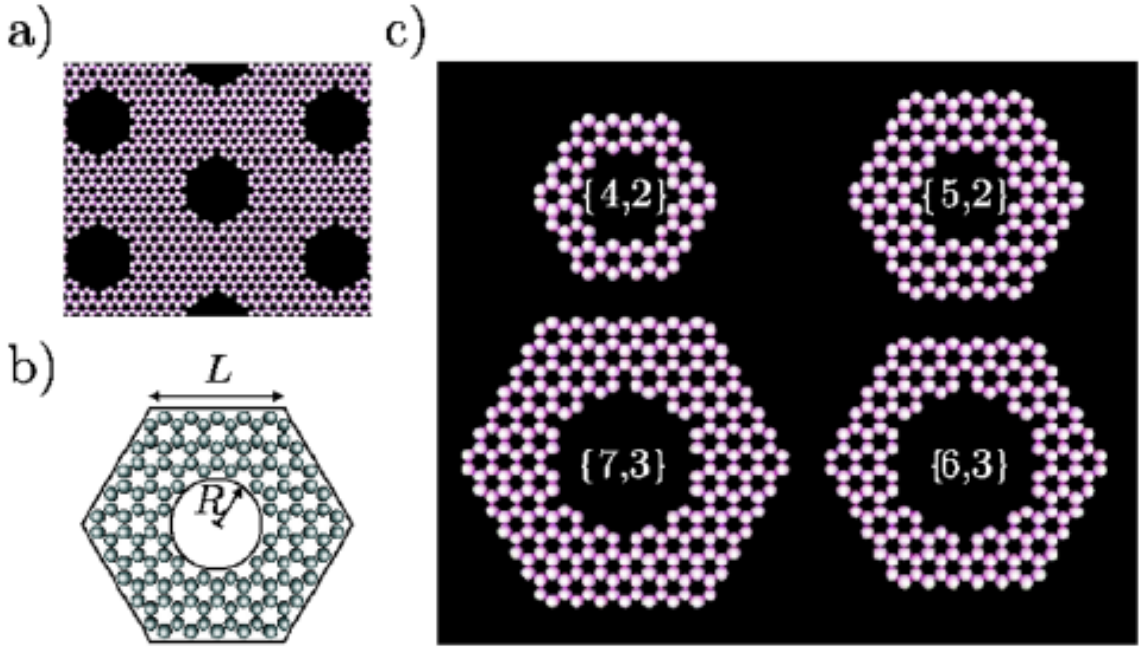

TKK

Technical University of Denmark DTU

Band structure and density-of-states

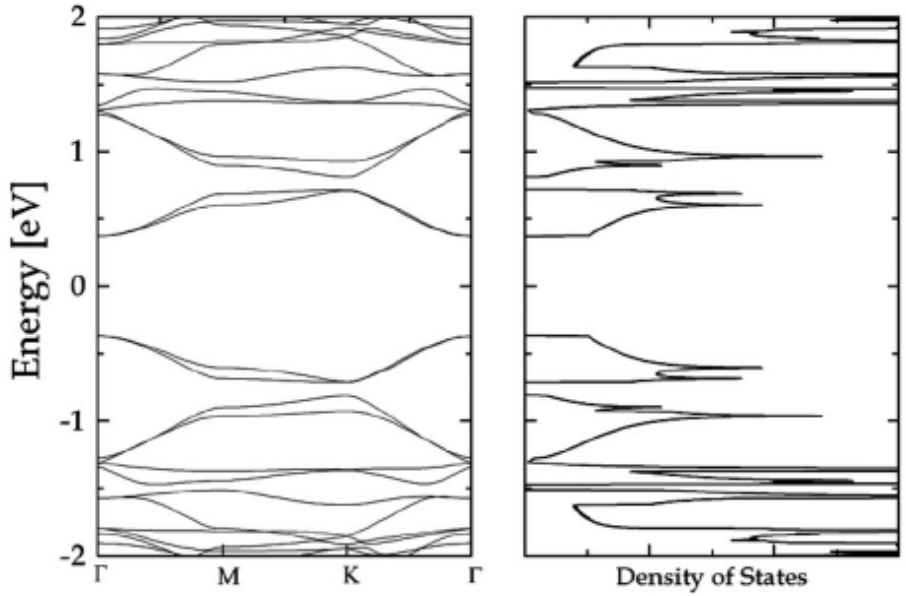

FIG. 2. Energy band structure and associated density of states for a $\{7, 3\}$ antidot lattice. The notation Γ, M, and K refers to high symmetry points of the Brillouin zone.

Tight-binding description, allowing for a modified hopping integral at edges (obtained from DFT), according to Son et al., PRL 97, 216803 (2006)

For a {7,3} structure one finds a band gap of 0.73 eV

Extrapolate to realistic lattice spacings:

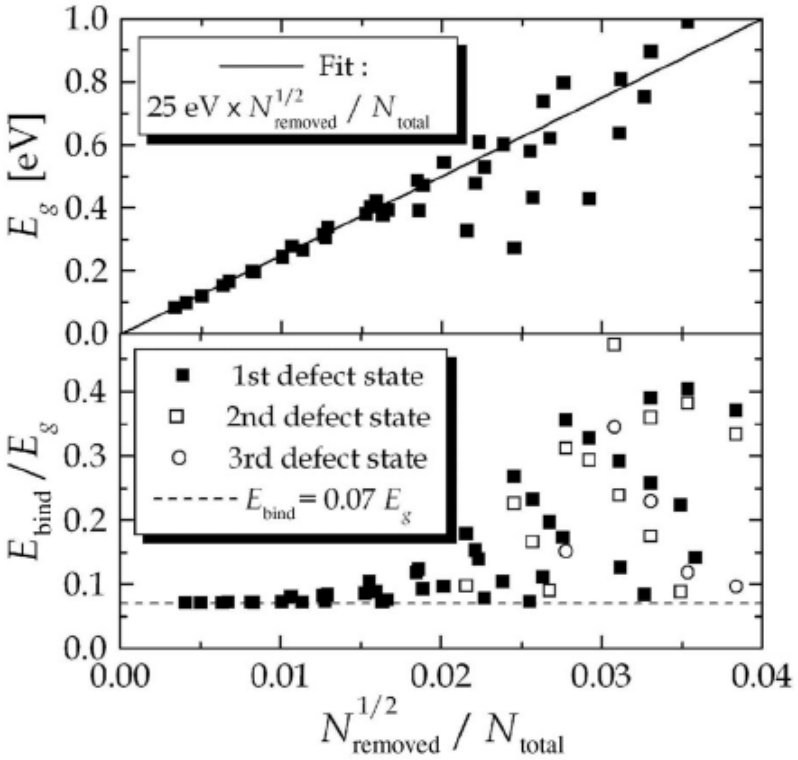

Realistic structures have a small ratio

With V(x,y) being the antidot potential, one needs to solve

$$H = \begin{pmatrix} V(x,y) & v_F(p_x - ip_y) \\ v_F(p_x + ip_y) & V(x,y) \end{pmatrix}$$

Example: 10 nm lattice spacing, $N_{removed}=N_{total}/4$ gives E_{gap}= 0.23 eV

TKK

Technical University of Denmark DTU

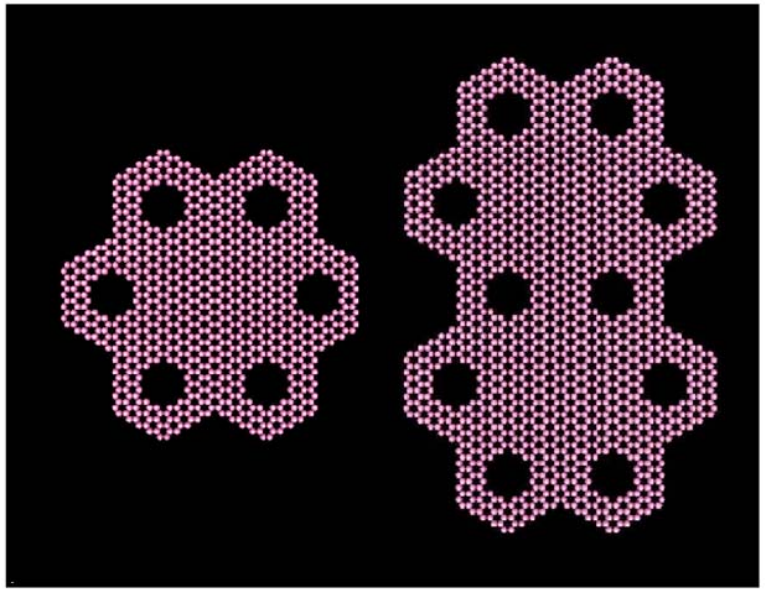

Consider now defect states:

Computational unit cells

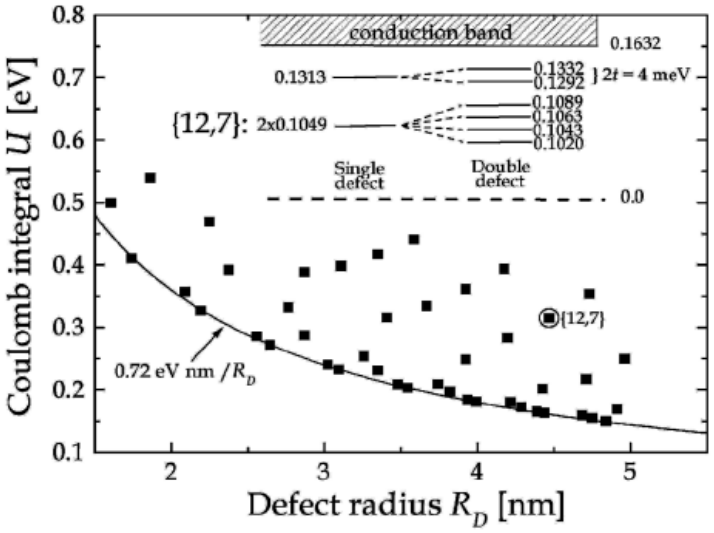

Single defect Double defect

Exchange coupling can be computed from: $J = 4t^2/\tilde{U}$

For example, {12,7} structure has J≈ 50 μeV

TKK

Technical University of Denmark DTU

Experimental status I

Single hole in graphene: Girit et al. Science 323, 1705 (2009) (March 27th)

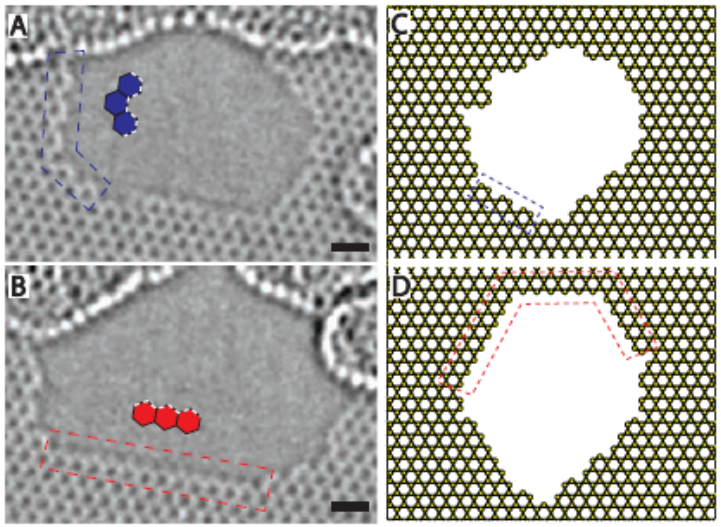

Fig. 2. Edge configurations. Aberration-corrected TEM image of (**A**) an armchair (frame 24) and (**B**) zigzag (frame 55) configuration of carbon atoms at the edge of a hole in graphene. The inset diagrams exemplify an armchair (upper panel) and zigzag (lower panel) arrangement. The armchair edge, roughly 12 hexagons long, makes a 60° turn at the lower left-hand corner. The zigzag edge is a continuous segment 12 hexagons long. Examples of the emergence of long-range order in the simulation of hole growth are (**C**), frame 113, with a 7-hexagon armchair segment at the edge of the simulated hole and (**D**), frame 223, an extremely long (19 hexagon) zigzag edge interrupted by two 60° turns.

These detailed images allow meaningful modeling!

Let us see film provided by Girit et al.

Sidetrack 1: Can one improve the quality of the edge? – Perhaps: Jia et al Science 323, 1701 (2009)

- Current makes the edges change shape

- Change depends on direction of current

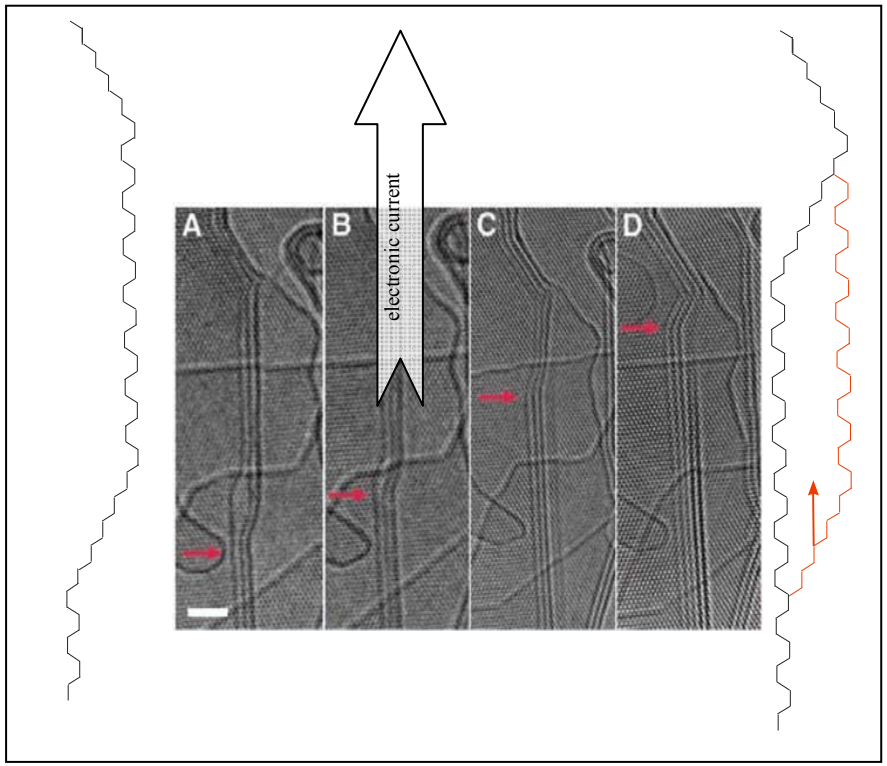

Why is that? – localized vibrational modes!

Localized modes exist along the finite armchair edges in graphene systems with mixed edges

The dynamical matrix is calculated by finite-difference SIESTA(DFT)*

*Soler et al., J. of Phys.-Cond. Mat., 2002, 14, 2745

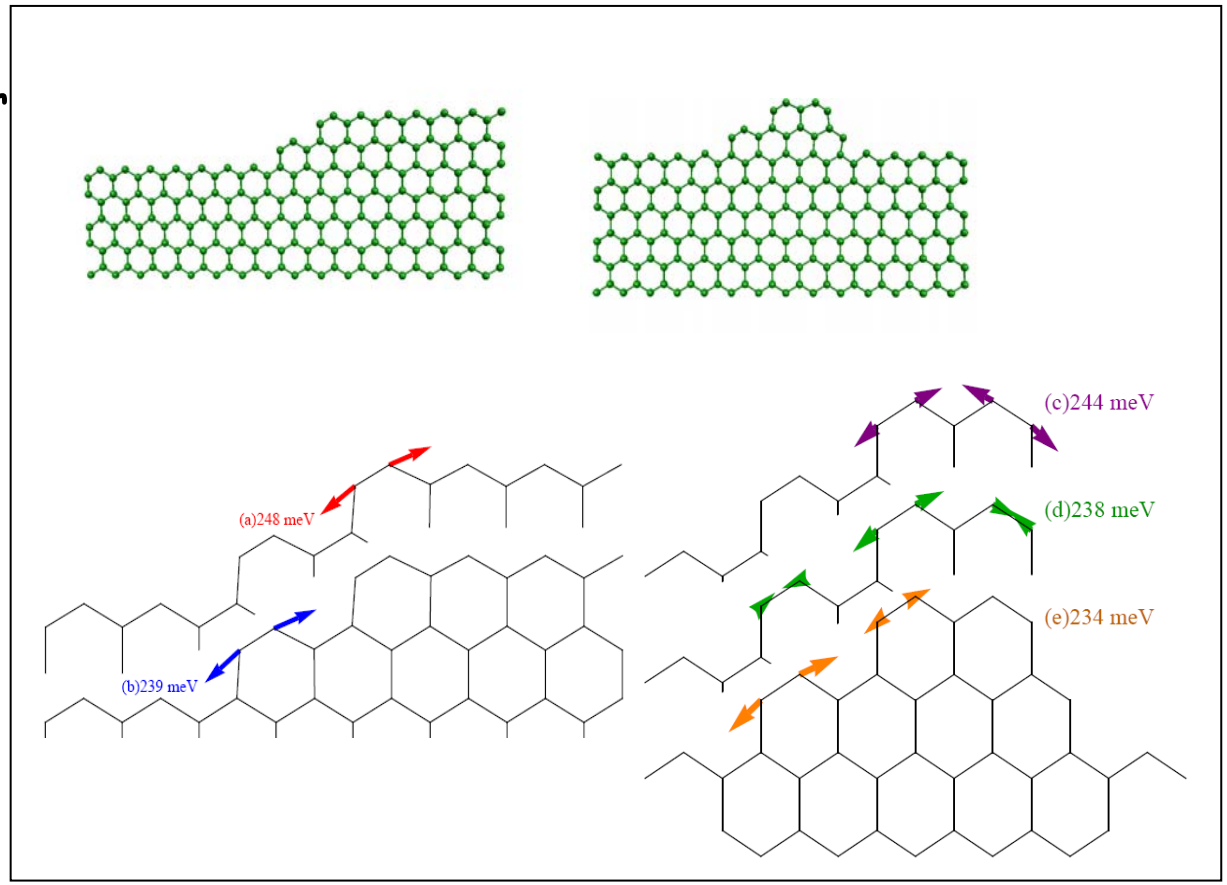

What are these localized modes? – armchair edge modes

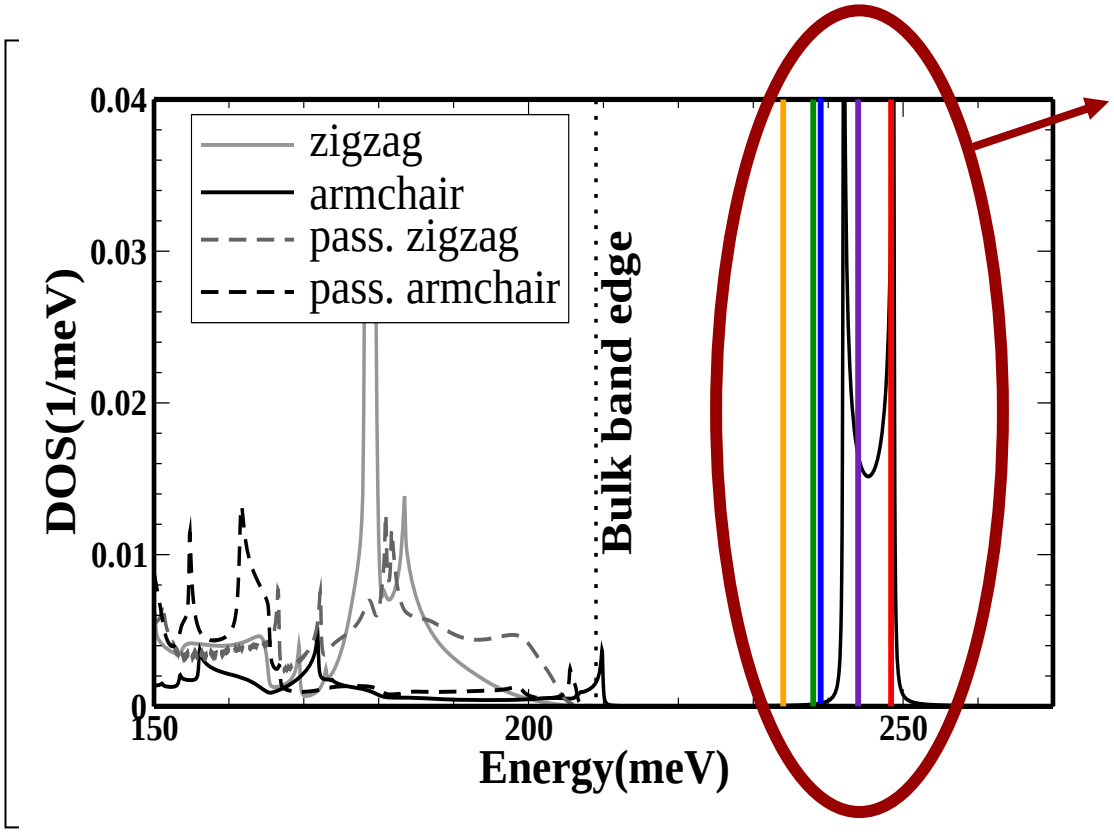

The modes are similar in energy (and mode vector) to an armchair edge mode outside the bulk band

The vibrational DOS is calculated by finite-difference calculations combined with recursion*

*Engelund et al., Phys. Rev. B, 2009. 80, 045427

Effective temperature as a function of voltage

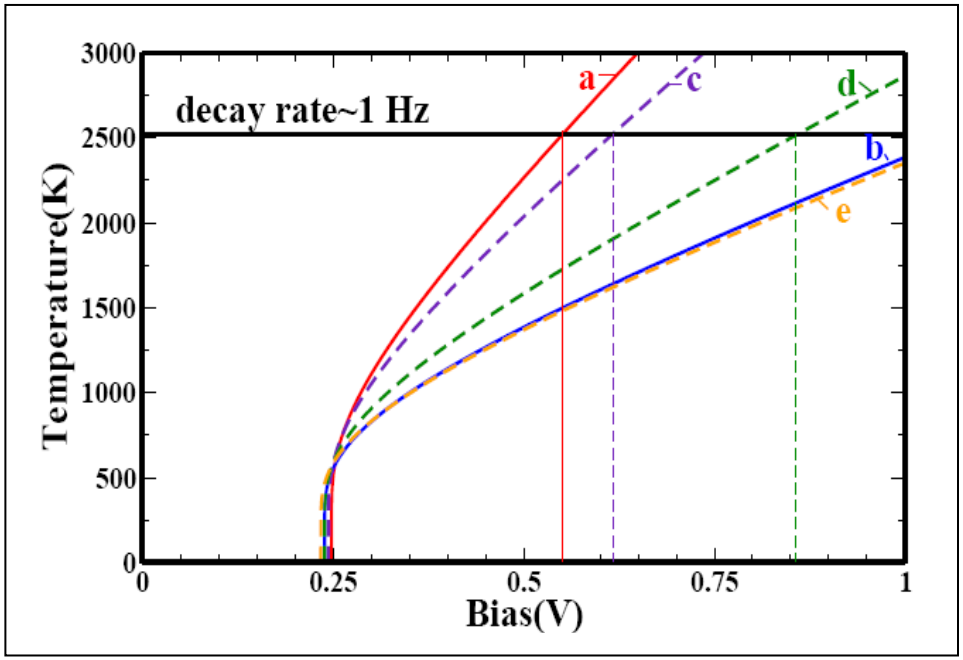

The localized modes can reach destabilising temperatures at low bias.

The mode temperature is estimated by a simple model combined with Transiesta(NEGF-DFT) parameters*,**

*Frederiksen et al., Phys Rev. B, 2007, 75, 205413

**Brandbyge et al., Phys Rev. B, 2002, 65, 165401

Localized modes exist along armchair edges which accumulate energy when a current flows.

This allows the weakly bound C-C dimers to evaporate. Further, we can make predictions of which edge geometries are likely to evaporate first.

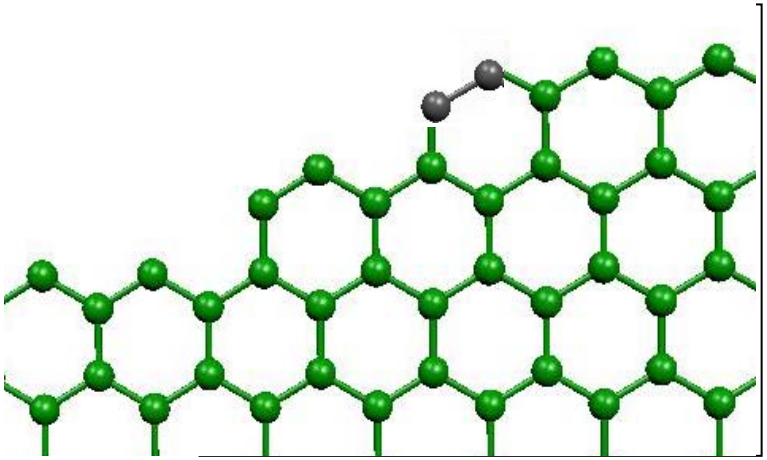

Engelund et al PRL 104, 036807 (2010)

movie

TKK

Technical University of Denmark DTU

Sidetrack 2: formation of carbon chains in TEM

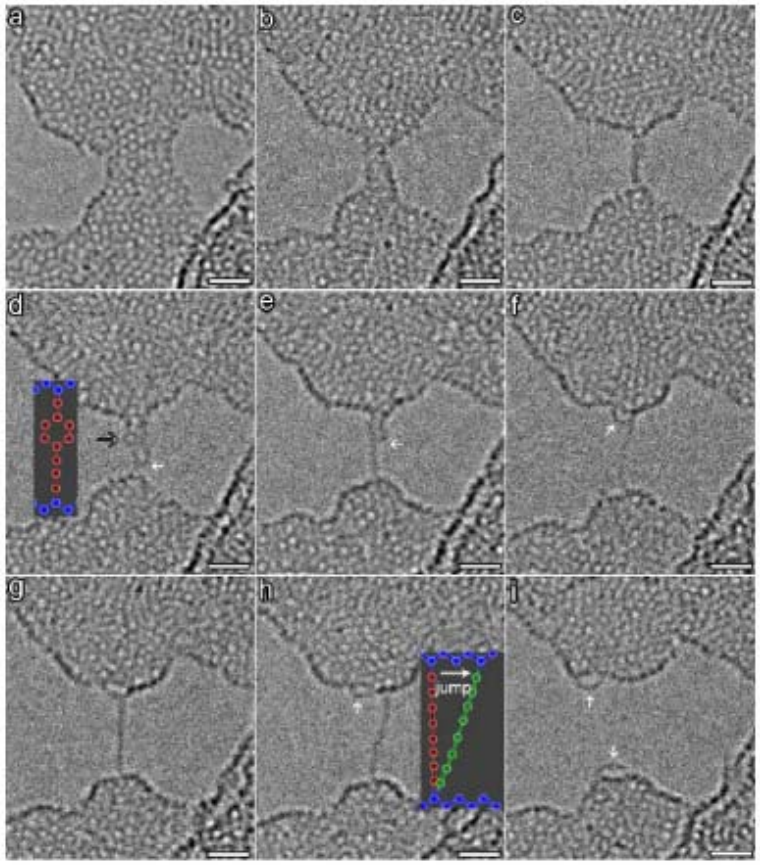

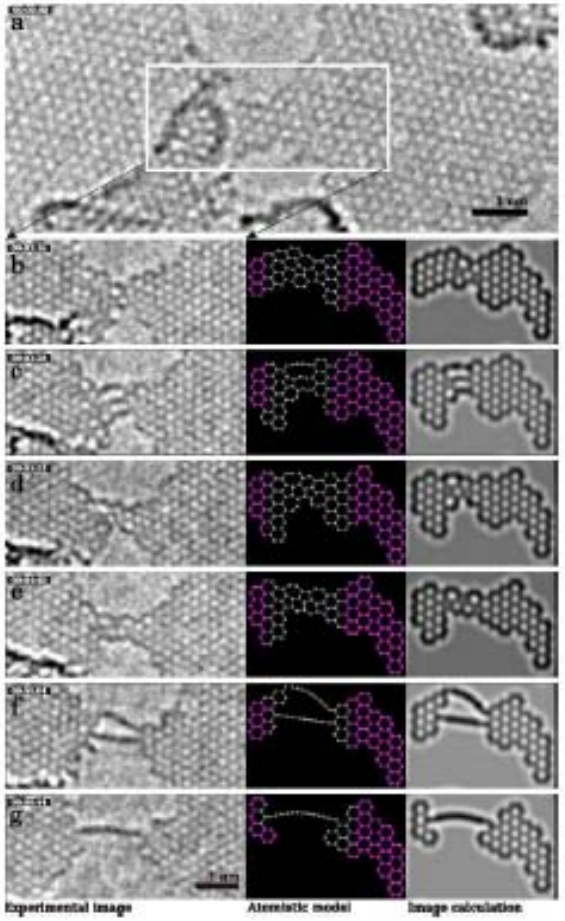

Jin et al. PRL 102, 205501 (2009) Chuvilin et al NJP 11, 083019 (2009)

carbon devices, and it would be very intriguing to explore the electrical transport properties on such a system: *sp*-hybridized carbon atomic chains as the conducing

TKK

Technical University of Denmark DTU

Atomic carbon chains can be spin-filters!

Fürst et al arXiv:0909.1756

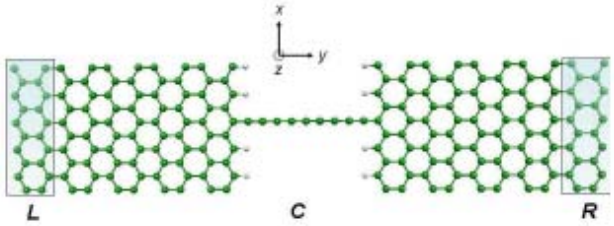

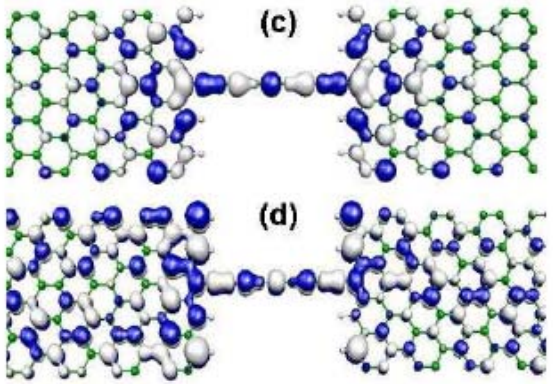

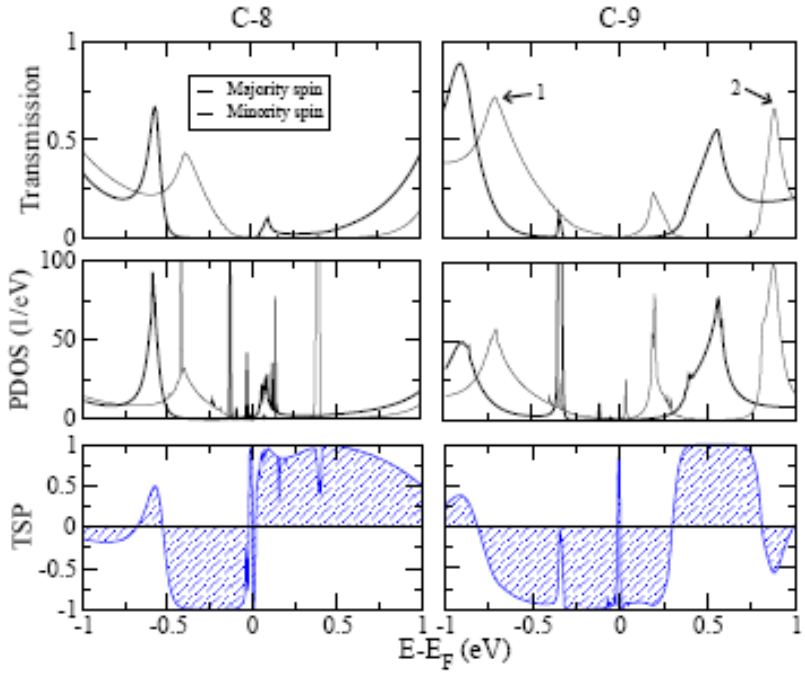

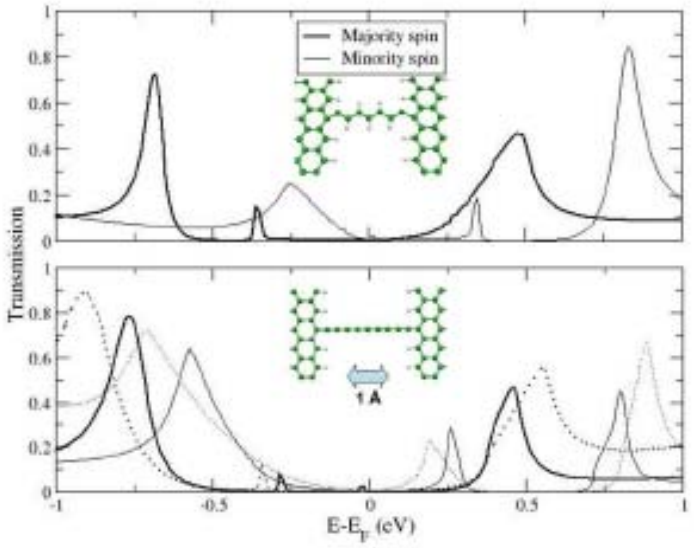

TKK

Technical University of Denmark DTU

Sidetrack 3: GNR's sensitivity to structural vs. chemical disorder (Saloriutta et al.)

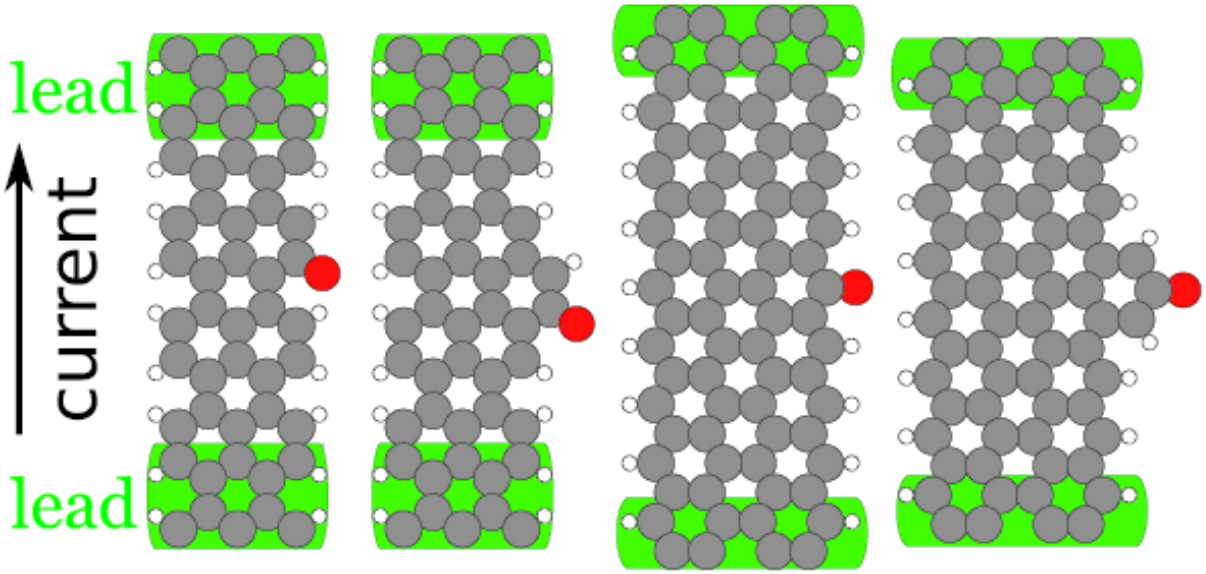

Figure 1: A schematic of the two-probe transport systems under study. From left to right: an ideal 5-AGNR, a 5-AGNR with armchair protrusion, an ideal 4-ZGNR and a 4-ZGNR with a zigzag protrusion. The green outline shows the first principal layer of the semi-infinite leads. Red and white circles indicate oxygen and hydrogen atoms, respectively.

TKK

Blue: without O; Red: with O

Technical University of Denmark DTU

ZGNR

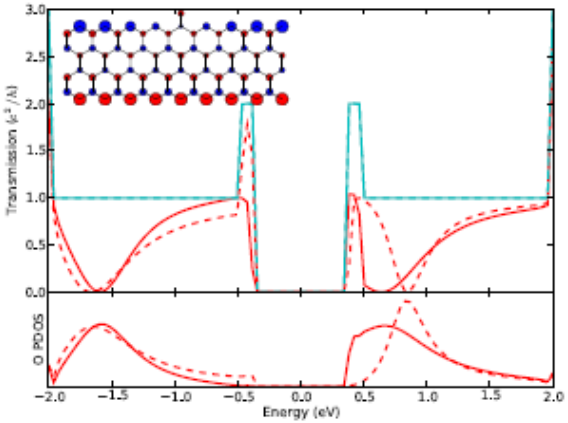

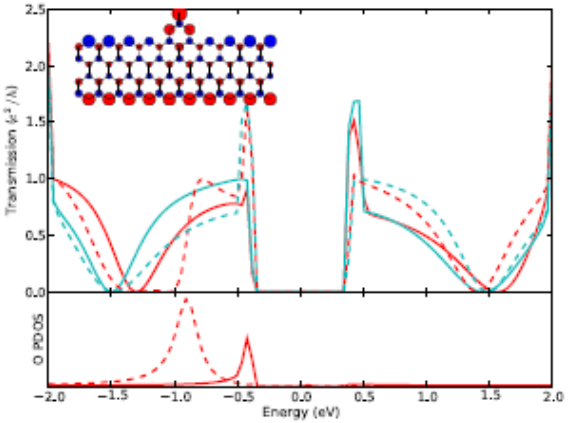

AGNR

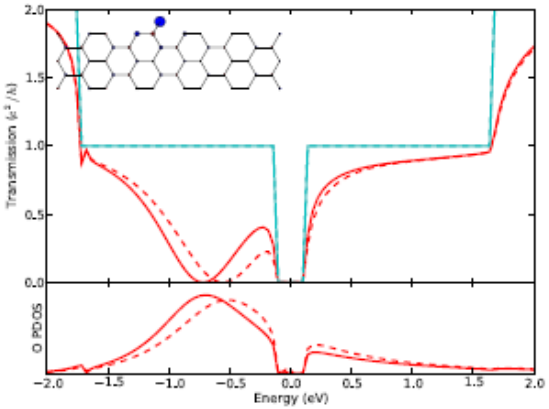

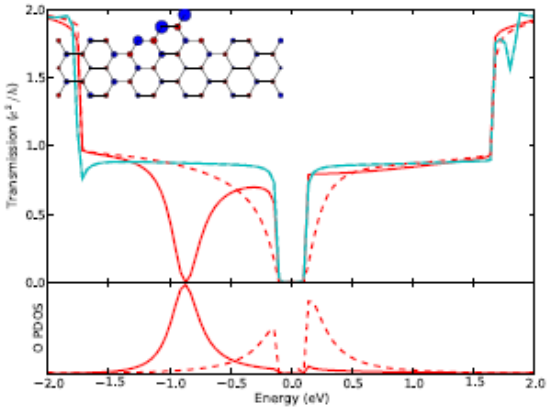

Conclusion: ZGNR appear less suited for chemical sensors.

ZGNR: structural disorder dominant (edge channels disturbed)

AGNR: chemical disorder dominant

TKK

Technical University of Denmark DTU

Antidot lattices on graphene: Where are we experimentally?

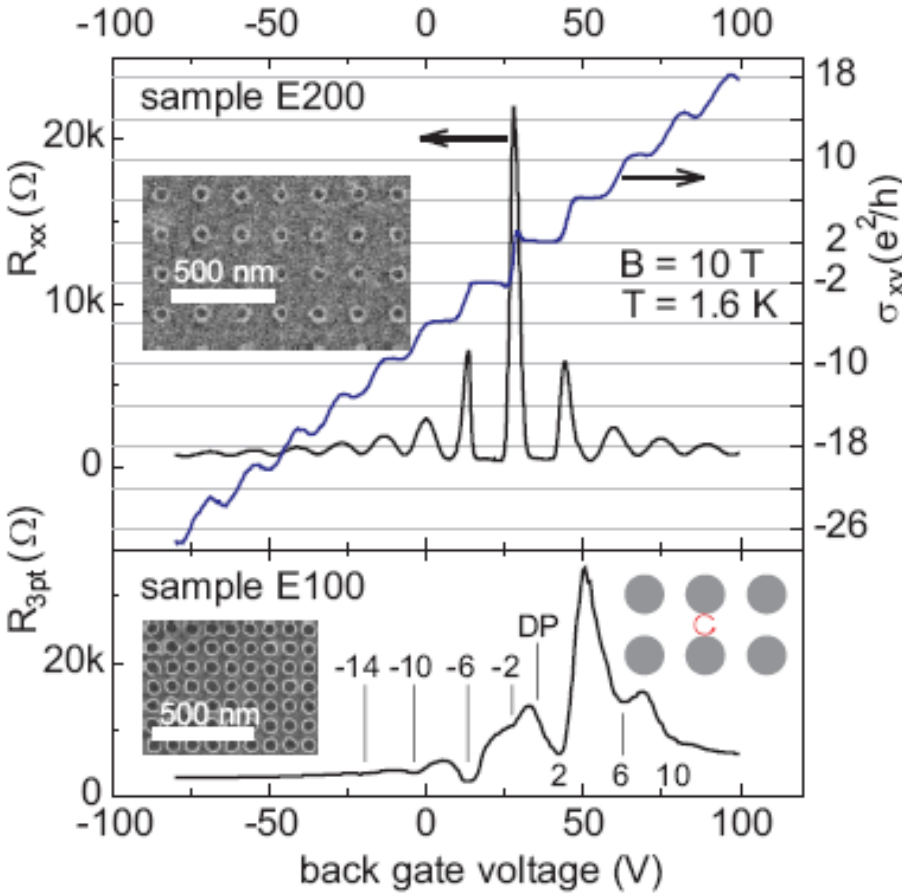

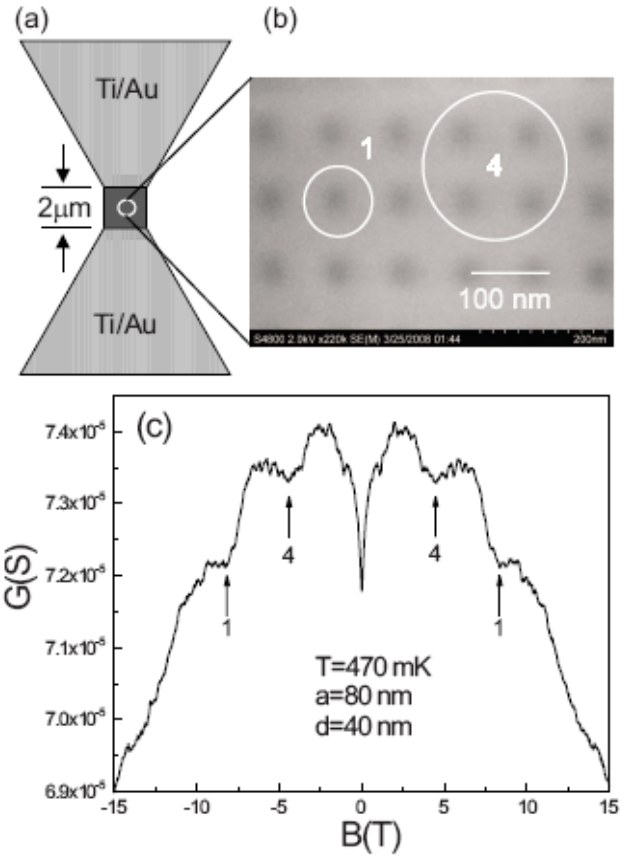

Eroms et al. arXiv.0109.840 (graphene on oxidized Si; low mobility)

Shen et al. APL 93, 122102 (2008) (graphene on SiC; no density meas.)

TKK

Technical University of Denmark DTU

ChemComm

Chemical Communications

www.rsc.org/chemcomm

Number 45 | 7 December 2009 | Pages 6865–7052

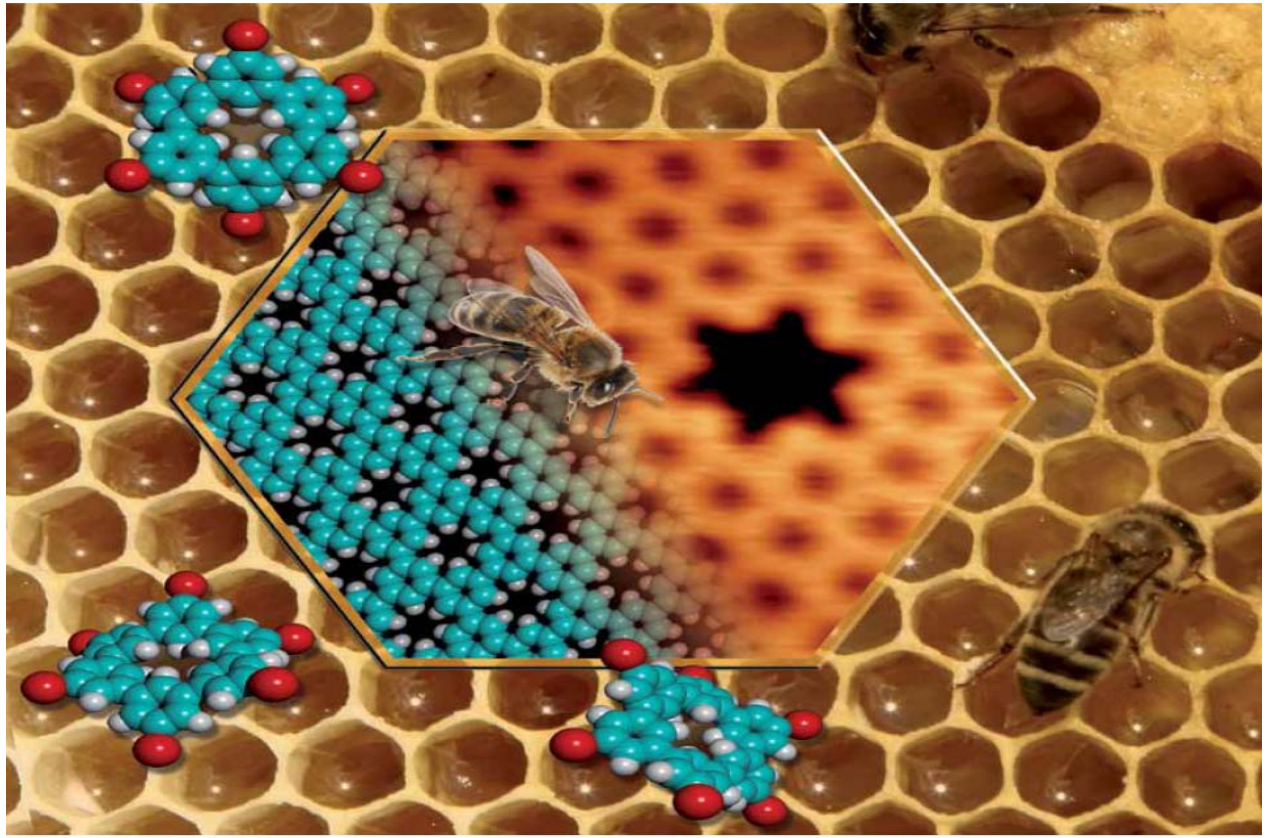

ISSN 1359-7345

RSC Publishing

COMMUNICATION
Roman Fasel, Marco Bieri *et al.*
Porous graphenes: two-dimensional polymer synthesis with atomic precision

TKK

Technical University of Denmark DTU

NANO LETTERS

pubs.acs.org/NanoLett

Fabrication and Characterization of Large-Area, Semiconducting Nanoperforated Graphene Materials

Myungwoong Kim,† Nathaniel S. Safron,† Eungnak Han, Michael S. Arnold,* and Padma Gopalan*

Department of Materials Science and Engineering, University of Wisconsin—Madison, Madison, Wisconsin 53706

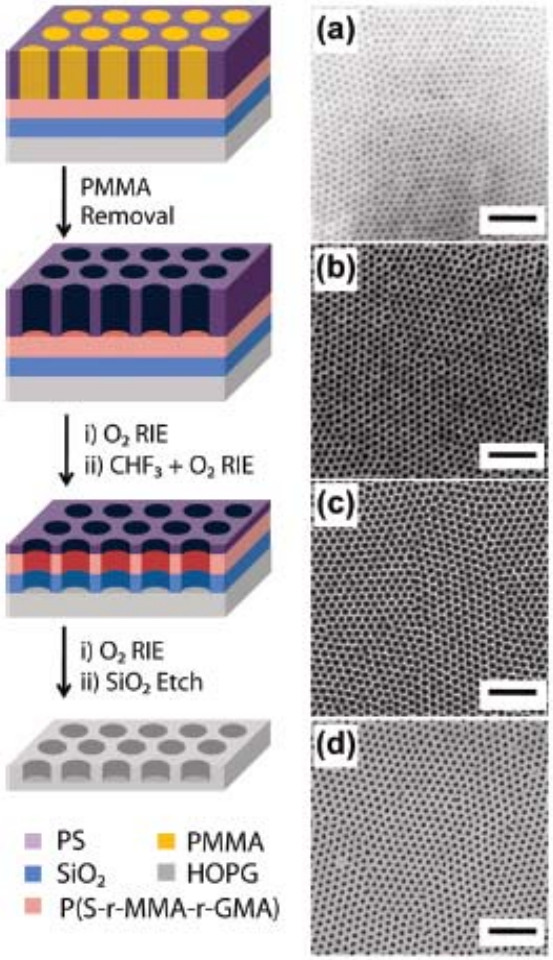

FIGURE 1. Schematic depicting the fabrication of nanoperforated HOPG using block copolymer lithography and the corresponding top-down SEM images of (a) vertically oriented PMMA cylinders in a block copolymer thin film obtained by thermal annealing, (b) residual PS honeycomb template obtained after selective PMMA removal with UV irradiation, (c) etched structures after O_2 followed by CHF_3 + O_2 plasma RIE resulting in the etching of the random copolymer mat and the oxide buffer layer, respectively, and (d) nanoperforated HOPG resulting from the final O_2 plasma RIE and the removal of the oxide buffer by HF solution. Scale bars = 200 nm.

TKK

Technical University of Denmark DTU

LETTERS
PUBLISHED ONLINE: 14 FEBRUARY 2010 | DOI: 10.1038/NNANO.2010.8
nature nanotechnology

Graphene nanomesh

Jingwei Bai[1], Xing Zhong[2], Shan Jiang[2], Yu Huang[1,3]* and Xiangfeng Duan[2,3]*

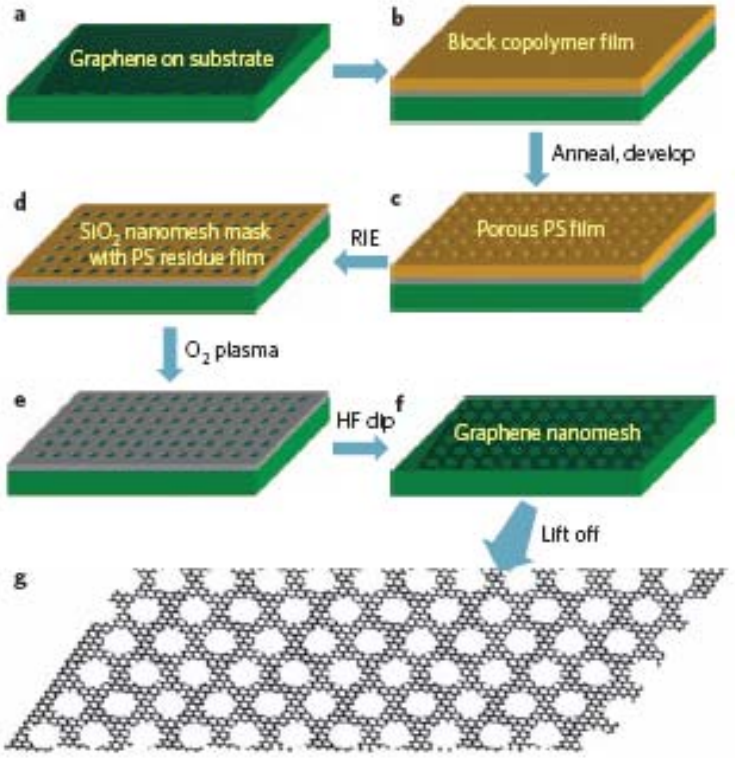

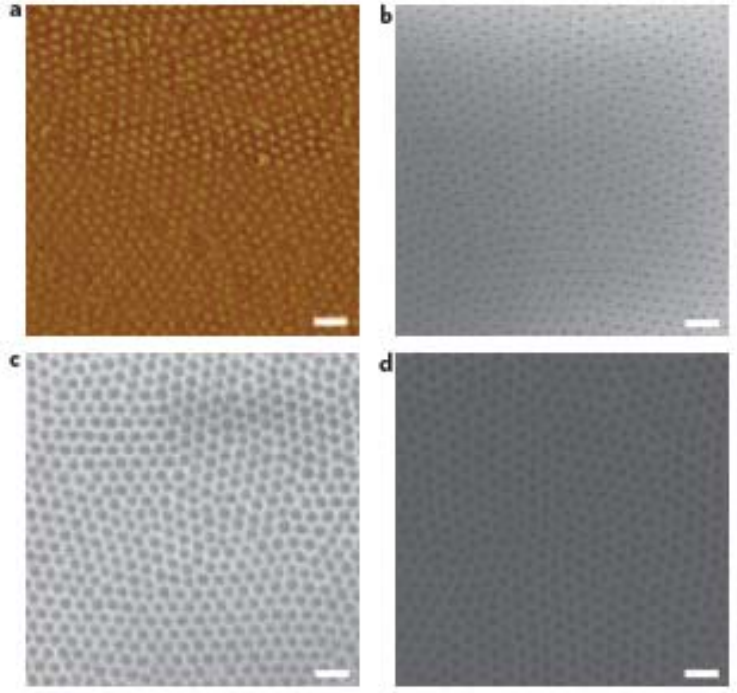

Scale bar: 100 nm

TKK

Technical University of Denmark DTU

nature materials

LETTERS

PUBLISHED ONLINE: 14 MARCH 2010 | DOI: 10.1038/NMAT2710

Bandgap opening in graphene induced by patterned hydrogen adsorption

Richard Balog[1], Bjarke Jørgensen[1], Louis Nilsson[1], Mie Andersen[1], Emile Rienks[2], Marco Bianchi[3], Mattia Fanetti[4], Erik Lægsgaard[1], Alessandro Baraldi[3,4], Silvano Lizzit[5], Zeljko Sljivancanin[6], Flemming Besenbacher[1], Bjørk Hammer[1], Thomas G. Pedersen[7], Philip Hofmann[2] and Liv Hornekær[1]*

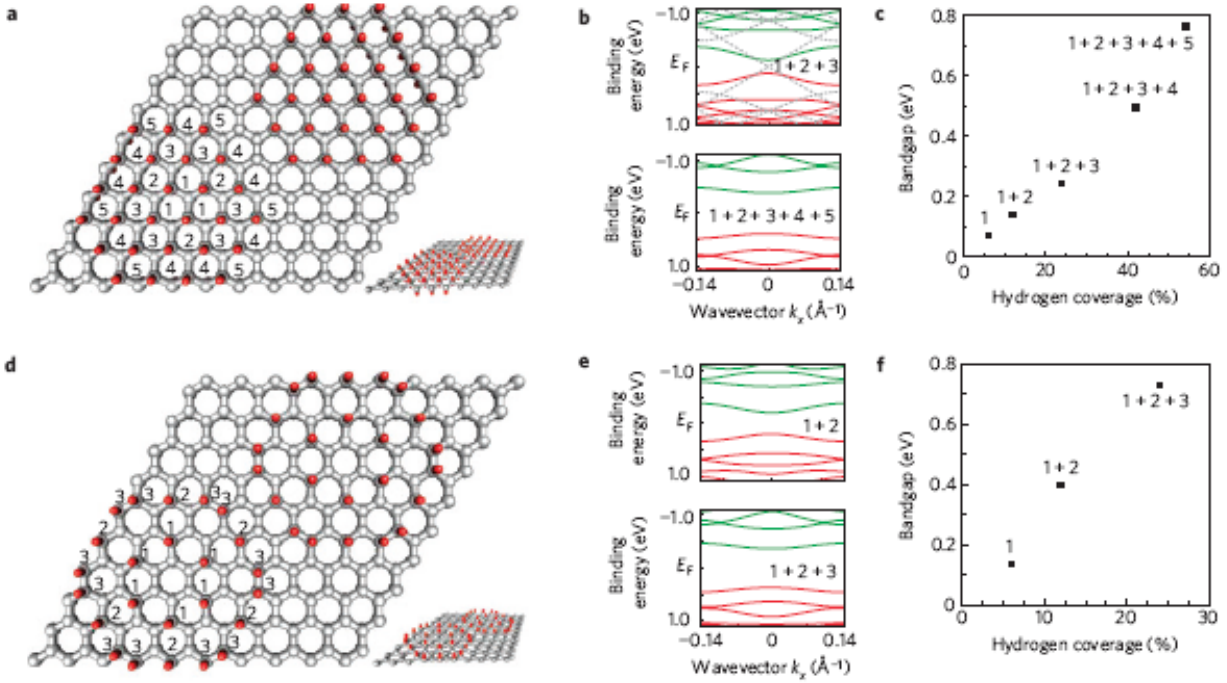

TKK

Technical University of Denmark DTU

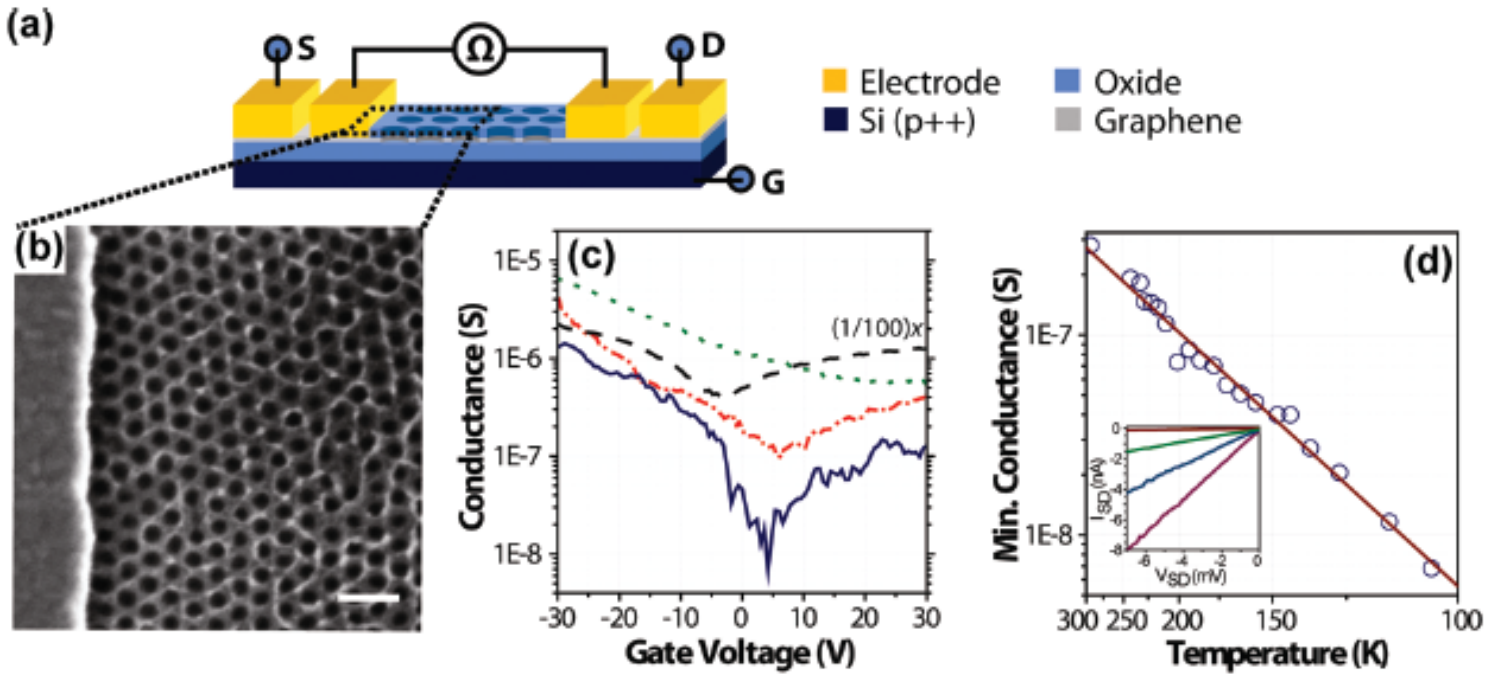

Further calculations: Optical properties (PRB 77, 24531 (2008))

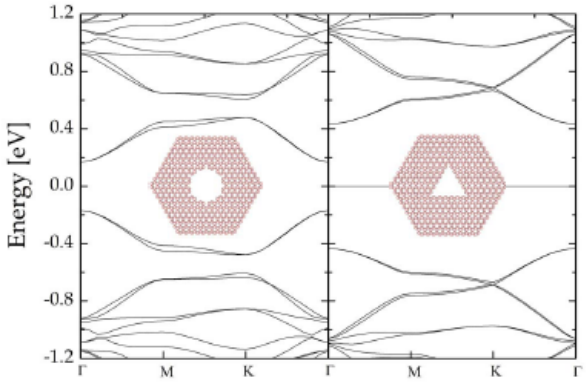

!!

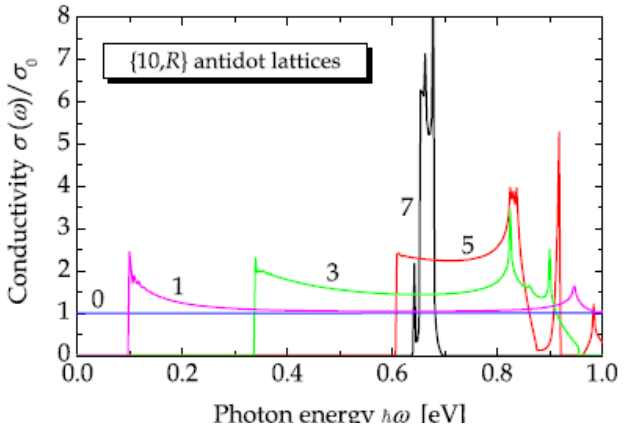

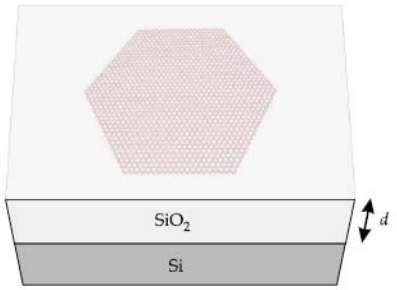

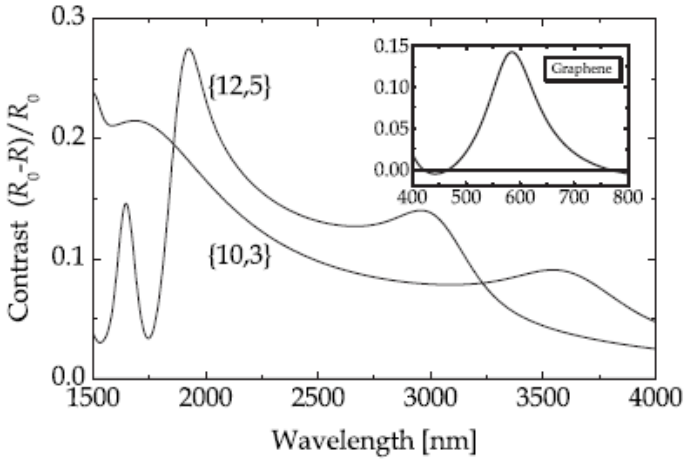

FIG. 7. Infrared reflectance contrast for {10,3} and {12,5} lattices. Inset: contrast for regular graphene in the visible.

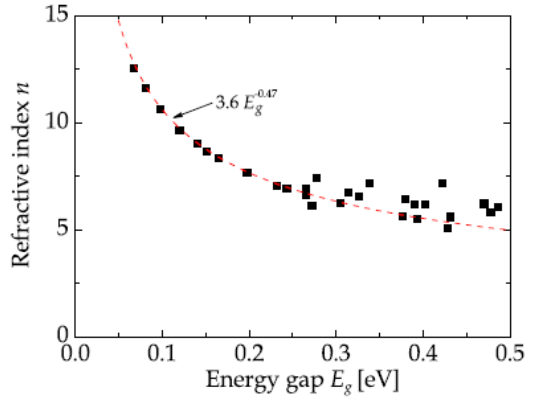

$$R = \left| \frac{e^{2idn_1\omega/c}(1+n_1-\bar{\sigma})(n_1-n_2)+(1-n_1-\bar{\sigma})(n_1+n_2)}{e^{2idn_1\omega/c}(1-n_1+\bar{\sigma})(n_1-n_2)+(1+n_1+\bar{\sigma})(n_1+n_2)} \right|^2$$

Excitons for *gapped* graphene (PRB 79, 113406 (2009))
(the gap could be due to "anything")

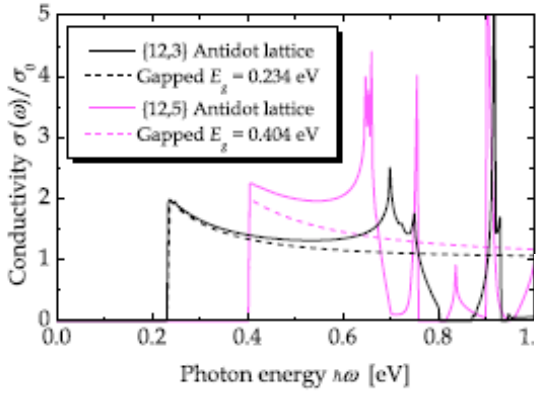

Effective hamiltonian:

$$H = \begin{pmatrix} \alpha & -\gamma f^*(\vec{k}) \\ -\gamma f(\vec{k}) & -\alpha \end{pmatrix}$$

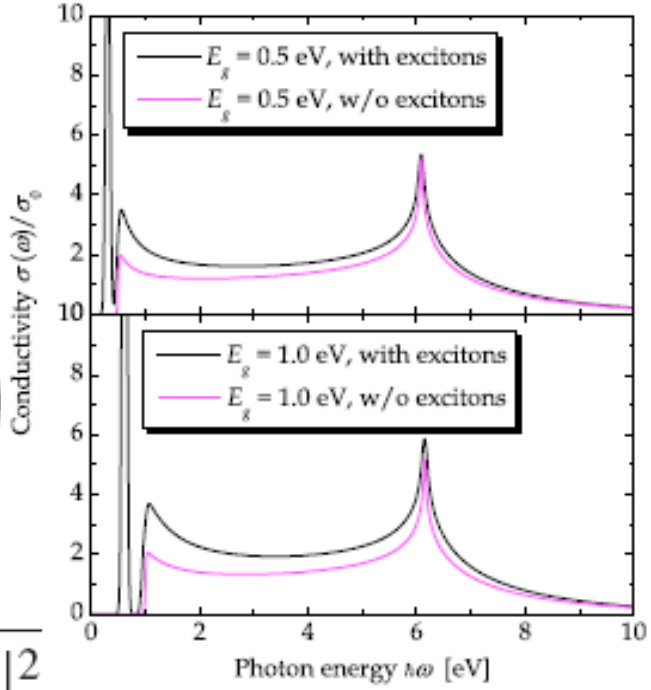

$$f(\vec{k}) = e^{ik_x a/\sqrt{3}} + 2e^{-ik_x a/2\sqrt{3}}\cos(k_y a/2)$$

$$E = \pm\sqrt{\alpha^2 + \gamma^2 |f(\vec{k})|^2}$$

Elliot formula:

$$\sigma_{FC}(\omega) = e^2\mu|p_{vc}|^2\,\breve{\jmath}/(\hbar^2 m^2\omega)$$

$$\sigma_X(\omega) = \sigma_{FC}(\omega)\left\{\sum_{n=0}^{\infty}\frac{4\delta\left(\Delta + \left(n+\frac{1}{2}\right)^{-2}\right.}{\left(n+\frac{1}{2}\right)^3} + \frac{2\theta(\Delta)}{1+\exp(-2\pi/\sqrt{\Delta})}\right\}$$

$$\Delta = (\hbar\omega - E_g)/\mathrm{Ry}^*$$

TKK

Technical University of Denmark DTU

Recent DFT studies: geometry relaxation and spin effects (arXiv:0904.1396; PRB 80, 115117 (2009))

Green: C
White: H

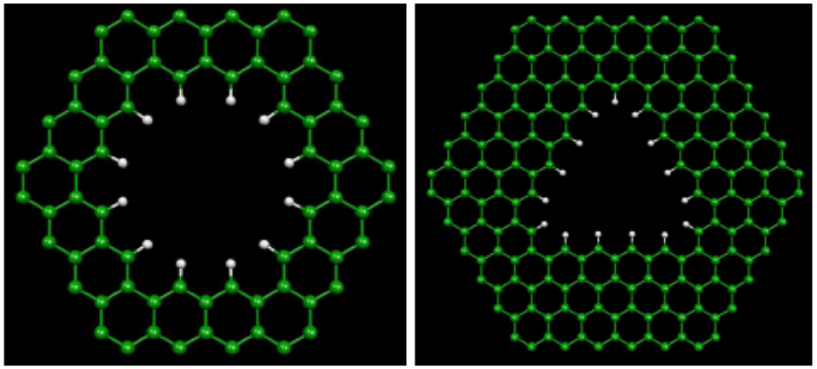

$\{4,2\}_O$ $\{6,5\}_\Delta$

Main challenge: DFT is getting expensive – thousands of atoms in unit cell. Therefore, use a cheaper DFTB!

	DFT			Non-spin DFT	DFTB	
Relaxation	None	DFT	DFTB	DFTB	None	DFTB
$\{4,2\}_\bigcirc$	0.93	1.01	0.97	0.97	0.99	1.05
$\{5,2.8\}_\bigcirc$	0.72	0.84	0.79	0.79	0.88	0.98
$\{5,3.5\}_\bigcirc$	1.27	1.51	1.35	1.35	1.72	1.74
$\{6,3.6\}_\bigcirc$	0.39	0.52	0.46	0.46	0.65	0.75
$\{6,5\}_\triangle$	0.24	0.22	0.22	0.00	0.00	0.00

Calculated band gaps

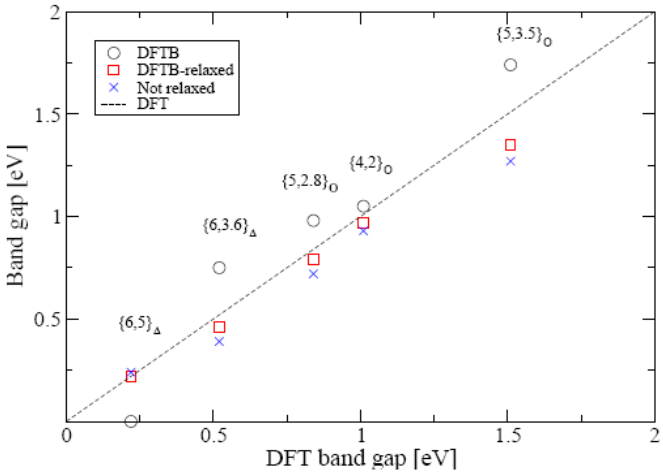

Trend: relaxation increases gap

TKK

Technical University of Denmark DTU

DFT studies II: geometry relaxation and spin effects

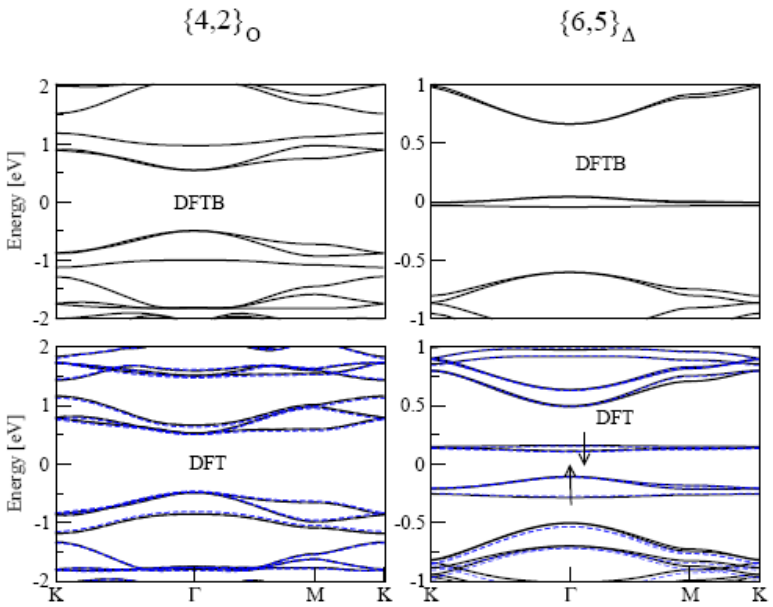

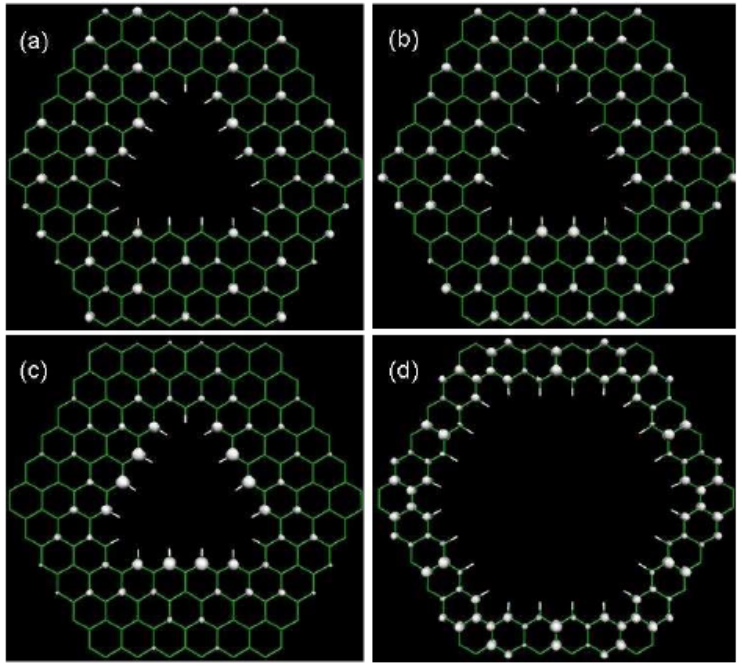

Dots: DFT on DFTB relaxation

a,b: degenerate midgap states; c: nondegenerate midgap state of {6,5}

d: highest filled band of {6,3.6} (All states at Γ-point)

TKK

Technical University of Denmark DTU

Magnetization of perforations

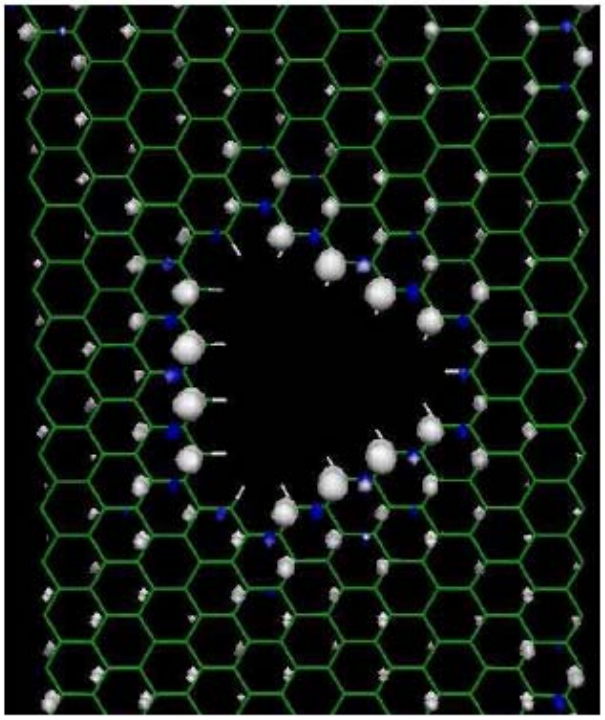

Blue: surplus of majority spin

White: surplus of minority spin

Lieb's Theorem: total magnetic moment is $M=N_A-N_B$ for bipartite lattice with *A* and *B* atoms.

Zigzag: for angle 0 or 60 all atoms at edge belong to same sublattice, while for angle 120 or 180 they belong to different sublattices. Thus: **hexagonal** hole is **nonmagnetic** whicle **triangular** hole is **magnetic**. A lot more to say about this!!

PRL **102,** 157201 (2009) PHYSICAL REVIEW LETTERS week ending 17 APRIL 2009

Topological Frustration in Graphene Nanoflakes: Magnetic Order and Spin Logic Devices

Wei L. Wang,[1] Oleg V. Yazyev,[2,3] Sheng Meng,[1] and Efthimios Kaxiras[1]

TKK

Technical University of Denmark DTU

Device proposals (unpublished work by J. Fürst):
transport through an array of triagonal perforations

x

y

Computational super-cell
(repeated in y-direction)

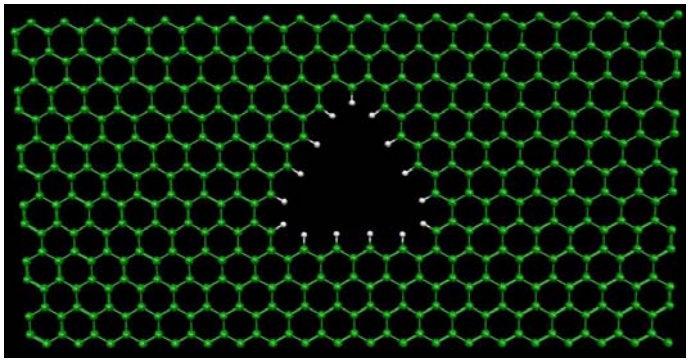

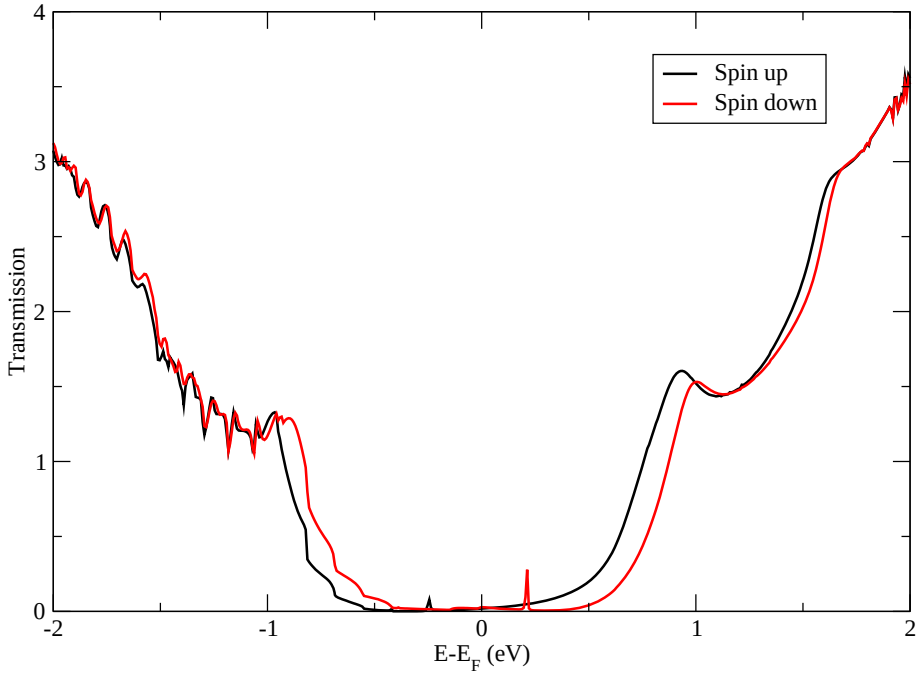

Clearly a bandgap,and a splitting of spin transmission. A spin-filter?

Technical University of Denmark DTU

Graphene Anti-Dots: Good Electron Transistor? (GADGET)

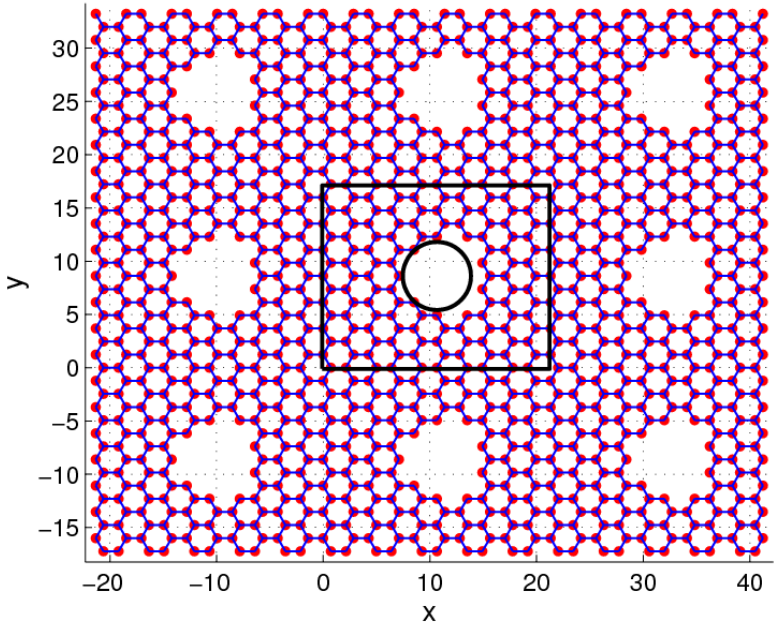

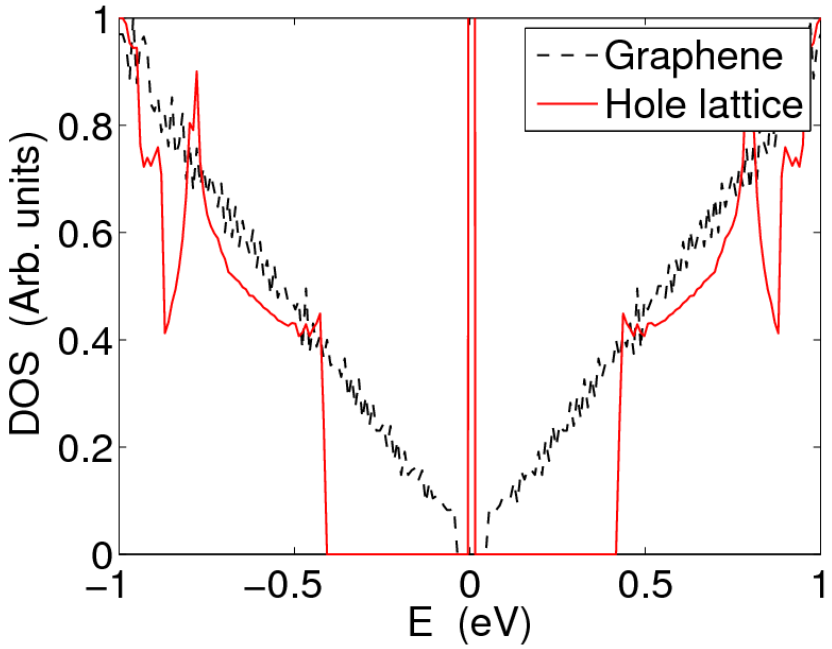

Transistor setup

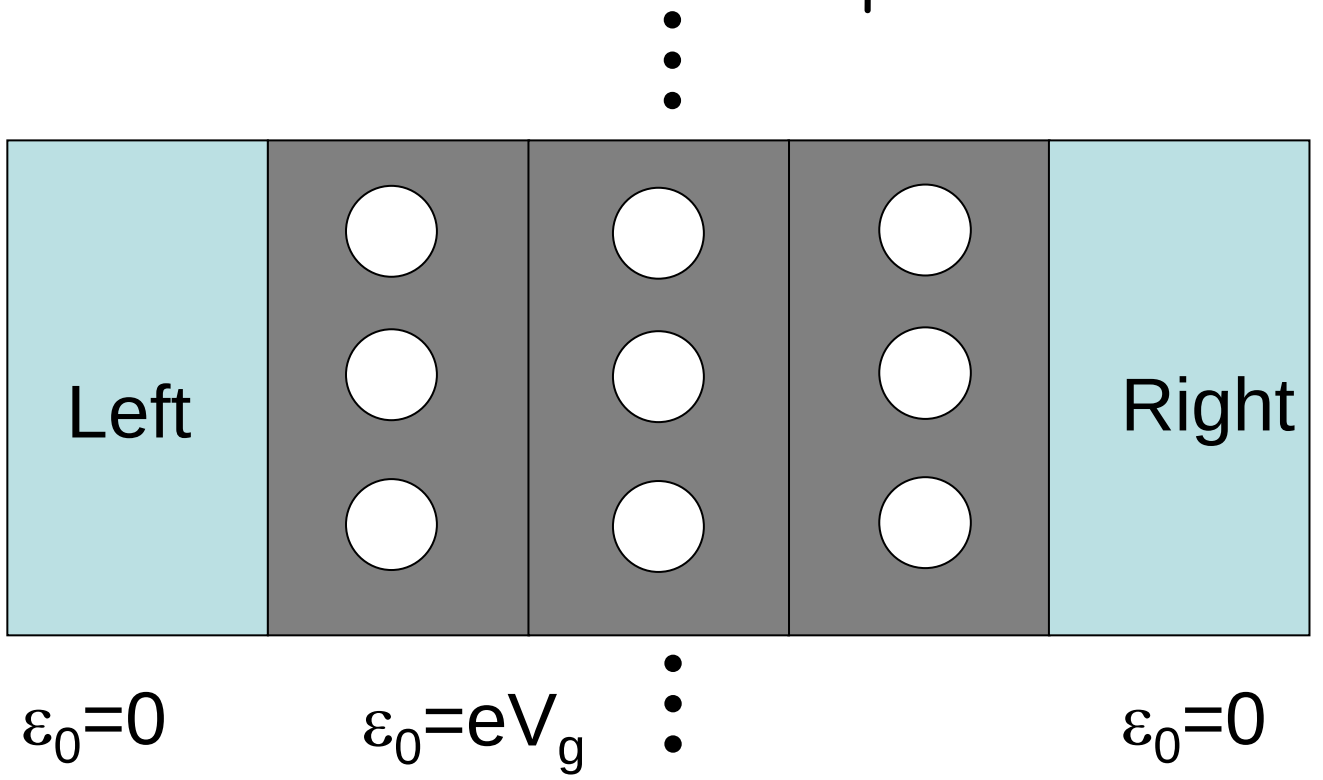

- Hole-hole distance: 30 Å
- Hole radius ~ 13 Å

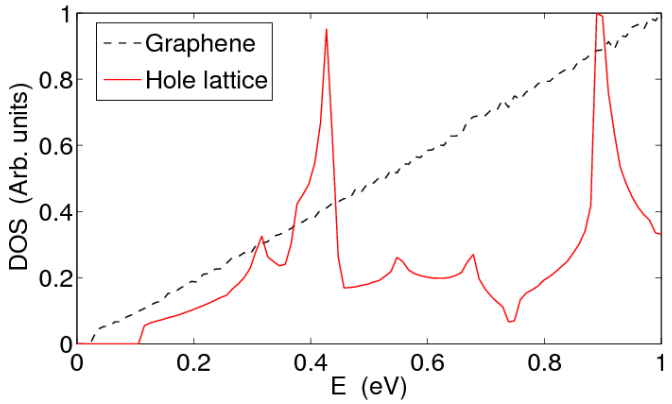

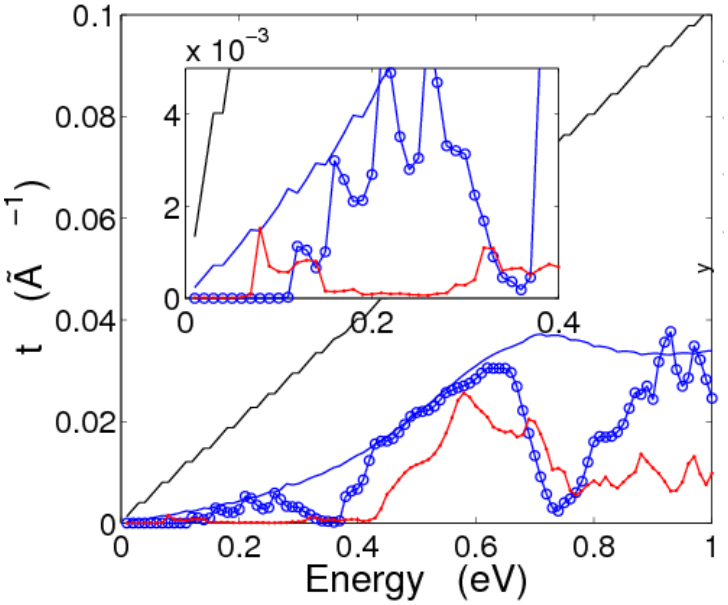

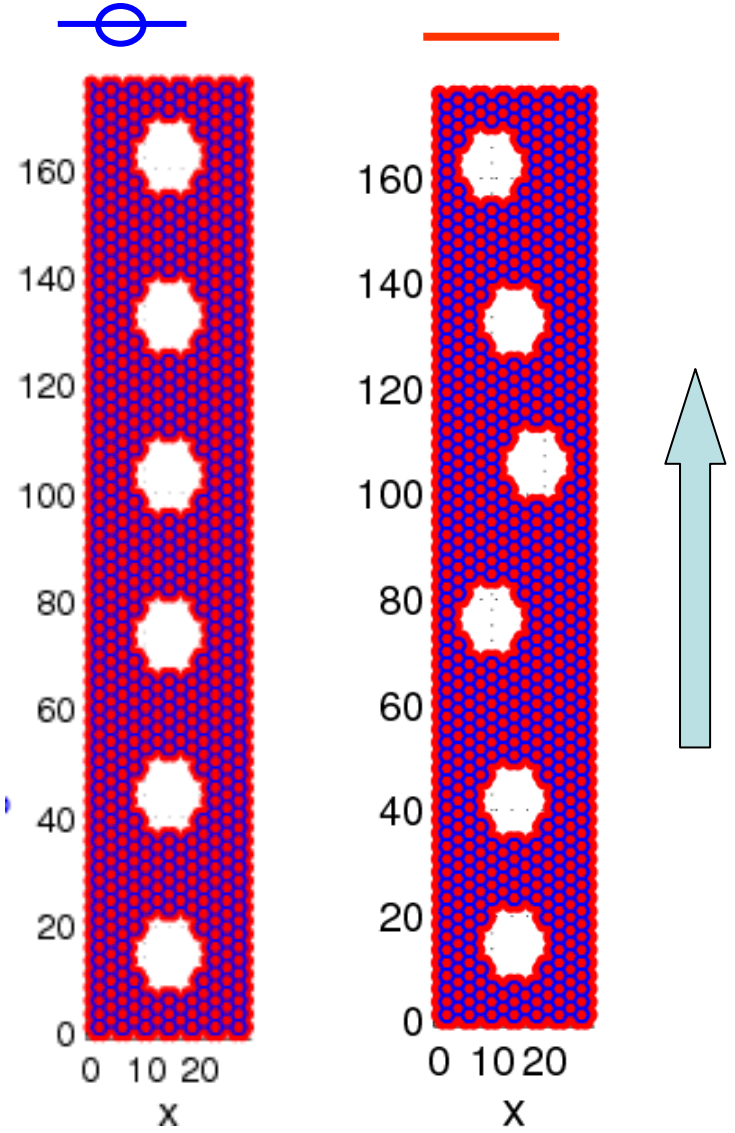

Bigger systems look more robust...

- Hole-hole distance: 38 Å
- Hole radius ~ 17 Å

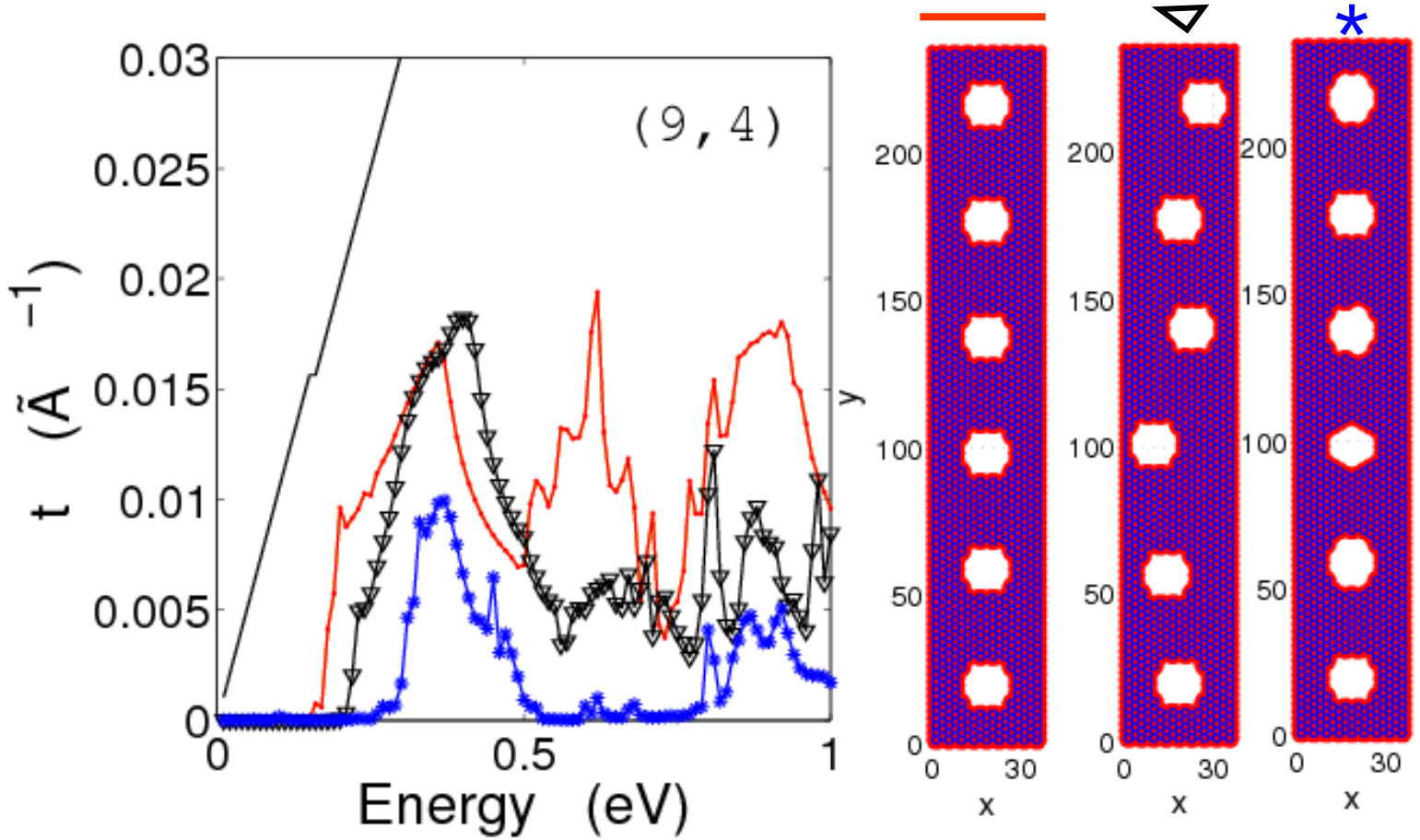

Technical University of Denmark DTU

Transistor: T vs Gate volt

- Hole-hole distance: 38 Å
- Hole radius ~ 17 Å
- E = 0.02 eV

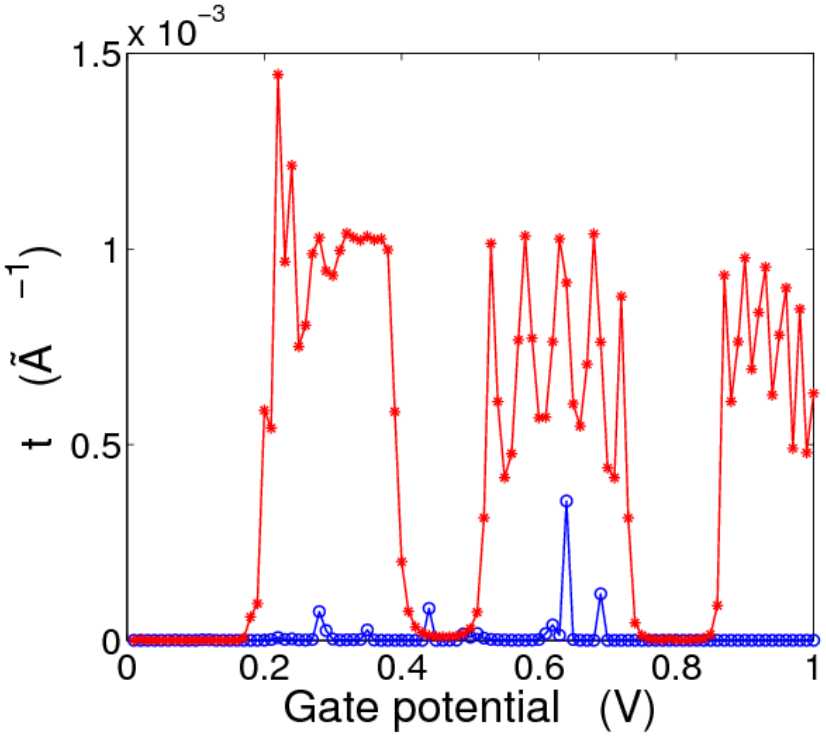

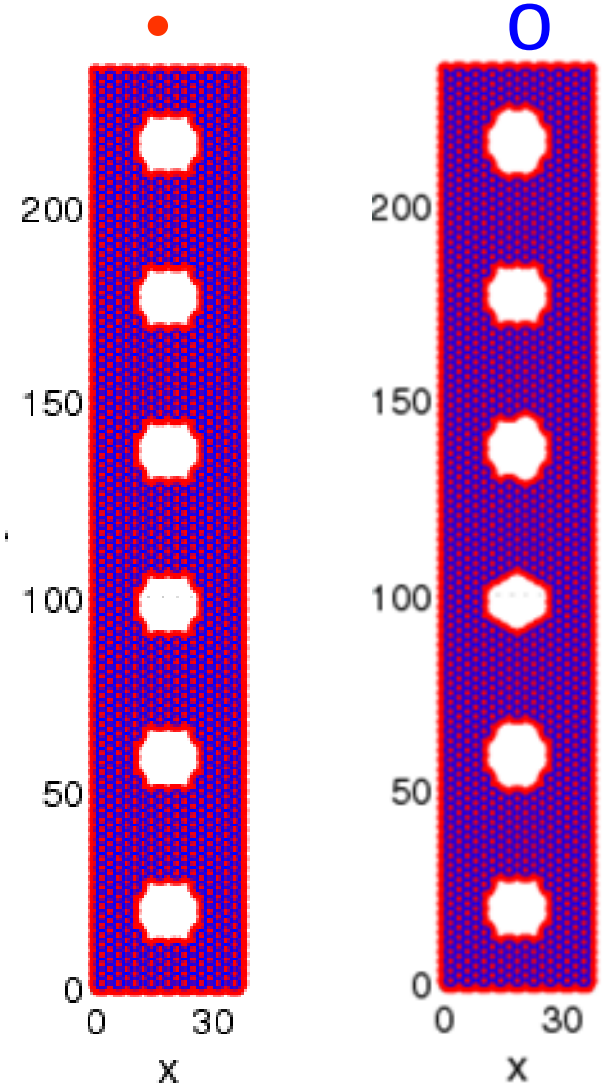

TKK

Technical University of Denmark DTU

Square antidot lattices – does symmetry matter?

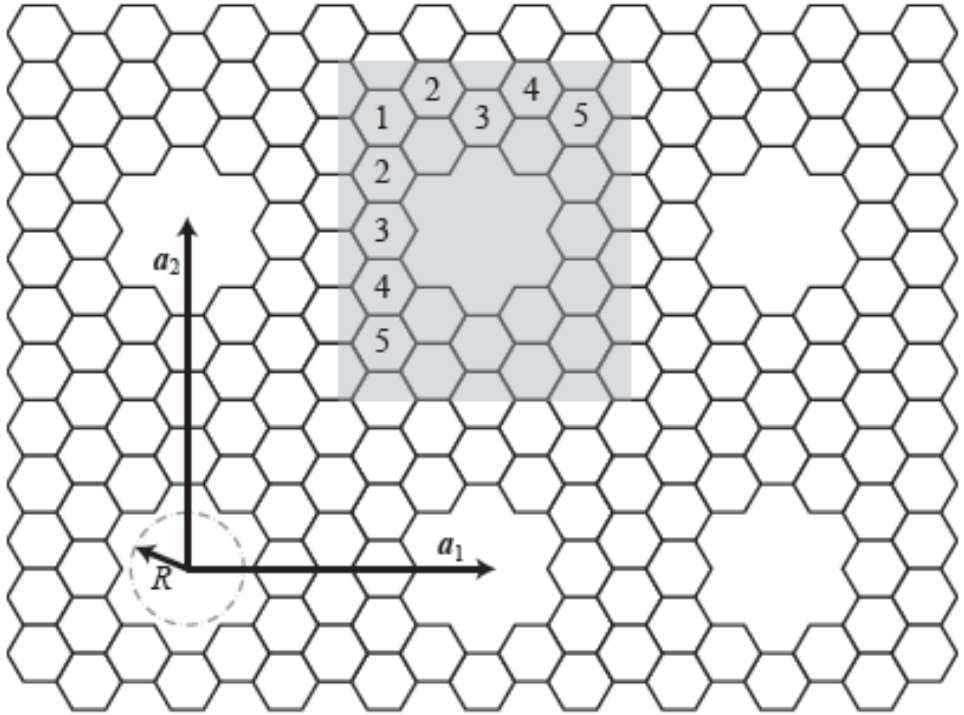

Structure	E_g[eV]	Pos b_1	Pos b_2	N_{Hx}	N_{Sx}
{5,5,1.0}*	0.742	0.000	0.000	29	11
{5,6,1.0}	0.002	0.000	0.375	35	11
{5,7,1.0}	0.000	0.000	0.409	41	14
{5,8,1.0}*	0.490	0.000	0.000	47	17
{5,9,1.0}	0.013	0.000	0.368	53	17
{5,10,1.0}	0.008	0.000	0.417	59	20
{5,11,1.0}*	0.366	0.000	0.000	65	23
{5,12,1.0}	0.001	0.000	0.375	71	23
{5,13,1.0}	0.010	0.000	0.400	77	26

Square antidot lattices – does symmetry matter?

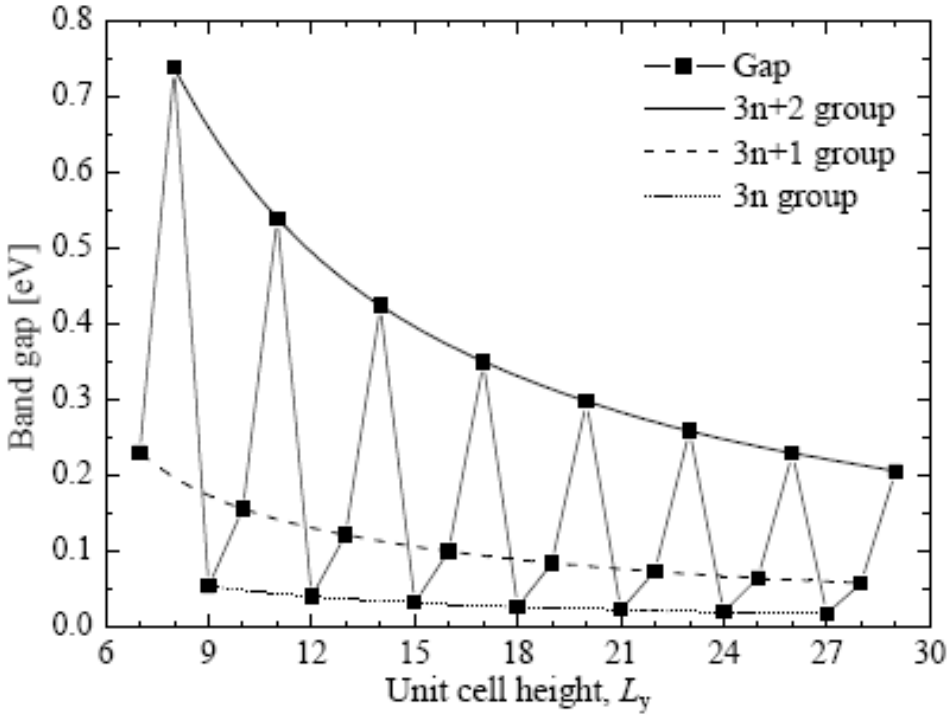

Square antidot lattices – does symmetry matter?

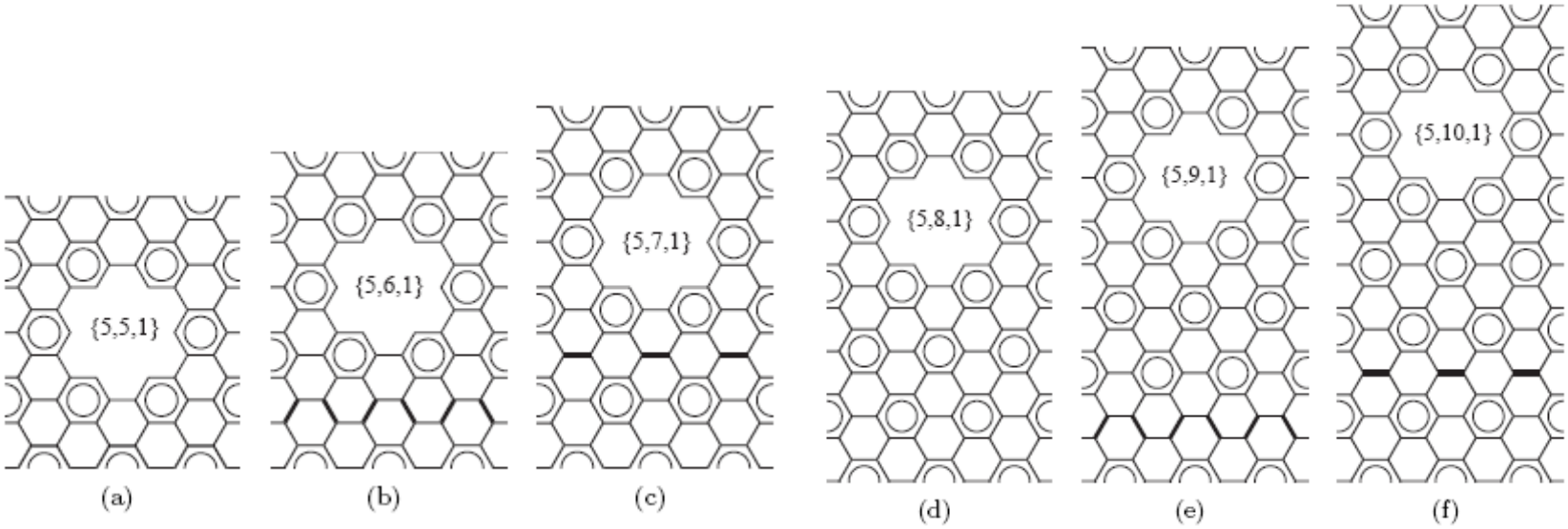

Empirical rule based on Clar sextets: If N(hexagon) < 1/3 N(sextet), the band gap is "large".

Take-home message: perhaps square lattices are not best candidates for devices, because 5/6 of them have small band gaps.

TKK

Technical University of Denmark DTU

Summary:

- Antidot lattices on graphene are very interesting (at least, theoretically)
- Feasible hole sizes are large -> computational challenge
- Relaxation, disorder, and magnetism are important
- Optical characterization and study of collective effects appear as primary first tasks
- (Magneto) Transport measurements would be highly intersting
- Possibility for new devices – but it ain't easy.

Thank you for your attention!

Derivation of the radiative thermal conductance formula

$$H_{L/R} = \sum_{j\in L/R} \hbar\omega_j(\hat{a}_j^\dagger \hat{a}_j + 1/2), \quad H_C = M\hat{I}(\hat{i}_L + \hat{i}_R), \quad \hat{i}_{L/R} = \sum_{j\in L/R} g_j(\hat{a}_j + \hat{a}_j^\dagger)$$

Note the inductive coupling between reservoirs and the central region, whose Hamiltonian is not yet needed. The energy flow is

$$J_{L/R}(t) = \langle \dot{H}_{L/R}\rangle = iM \sum_{j\in L/R} [g_j\omega_j\langle \hat{a}_j(t)\hat{I}(t)\rangle - \text{H.c.}] = -2M\text{Re}\sum_{j\in L/R} g_j\omega_j G_j^<(t,t),$$

Using the Keldysh approach, one can derive an e-o-m for the path-ordered nonequilibrium GF, and Langreth analytic continuation rules give

$$G_j^<(t,t') = \frac{Mg_j}{\hbar}\int dt_1[\langle \hat{I}(t)\hat{I}(t_1)\rangle^r D_j^<(t_1 - t') + \langle \hat{I}(t)\hat{I}(t_1)\rangle^< D_j^a(t_1 - t')]$$

where D's are free Bose correlators. The thermal current becomes

$$J_L = 2M^2\int_0^\infty \frac{d\omega\omega}{2\pi\hbar}\Big[-\text{Im}\langle \hat{I}\hat{I}\rangle^r(\omega)S_{i_L}(-\omega) + \text{Im}\langle \hat{I}\hat{I}\rangle^<(\omega)\ \frac{1}{2}[S_{i_L}(\omega) - S_{i_L}(-\omega)]\Big]$$

where the noise power for the reservoir L is

$$S_{i_L}(\omega) = \sum_{j\in L} g_j^2[n(\omega_j)2\pi\delta(\omega + \omega_j) + (n(\omega_j) + 1)2\pi\delta(\omega - \omega_j)]$$

Def. of noise power for operator A: $S_A(\omega) = \int_{-\infty}^{\infty} dt e^{i\omega(t-t')} \langle \hat{A}(t)\hat{A}(t') \rangle$

Thus:

$$-\mathrm{Im}\langle \hat{I}\,\hat{I} \rangle^r(\omega) = \tfrac{1}{2}[S_I(\omega) - S_I(-\omega)] \qquad \mathrm{Im}\langle \hat{I}\,\hat{I} \rangle^<(\omega) = -S_I(-\omega)$$

Plug these in:

$$J_L = M^2 \int_0^\infty \frac{d\omega\,\omega}{2\pi\hbar}[S_I(\omega)S_{i_L}(-\omega) - S_I(-\omega)S_{i_L}(\omega)].$$

Recall Fluctuation-Dissipation Theorem (for equilibrium reservoirs)

$$S_{i_{L/R}}(\omega) = \mathrm{Re}[Y_{L/R}(\omega)]\hbar\omega[\coth(\beta_{L/R}\hbar\omega/2) + 1]$$

Finally, assume proportionality of reservoir admittances $Y_L(\omega) = cY_R(\omega)$

$$J_L = \int_0^\infty \frac{d\omega\,\omega^2 M^2}{2\pi}\{2[S_I(\omega) - S_I(-\omega)]\mathrm{Re}[Y_L(\omega)]n_L(\omega) - S_I(-\omega)2\mathrm{Re}[Y_L(\omega)]\}.$$

which, after L/R symmetrization, gives the result stated two slides ago.

Application 1: Mesoscopic Photonic Heat Transistor (PRL 100, 155902)

Assume the central region consists of a single LC-resonator:

$$H_M = \hbar\omega_0(\hat{b}^\dagger\hat{b} + \tfrac{1}{2}) \qquad \hat{I} = I_0(\hat{b} + \hat{b}^\dagger) \qquad I_0 = \sqrt{\hbar\omega_0/2L} \qquad \omega_0 = 1/\sqrt{LC}$$

The required correlation functions are (note anomalous propagators!)

$$\langle \hat{I}\,\hat{I}\rangle^r(\omega) = I_0^2[\langle \hat{b}\hat{b}^\dagger\rangle^r(\omega) + \langle \hat{b}^\dagger\hat{b}\rangle^r(\omega) + \langle \hat{b}\,\hat{b}\rangle^r(\omega) + \langle \hat{b}^\dagger\hat{b}^\dagger\rangle^r(\omega)]$$

These satisfy

$$(\omega - \omega_0 + i\eta)\langle \hat{b}\hat{b}^\dagger\rangle^r = 1 + \Sigma^r(\omega)[\langle \hat{b}\hat{b}^\dagger\rangle^r + \langle \hat{b}^\dagger\hat{b}^\dagger\rangle^r]$$

$$(\omega + \omega_0 + i\eta)\langle \hat{b}^\dagger\hat{b}^\dagger\rangle^r = -\Sigma^r(\omega)[\langle \hat{b}\hat{b}^\dagger\rangle^r + \langle \hat{b}^\dagger\hat{b}^\dagger\rangle^r]$$

$$(\omega + \omega_0 + i\eta)\langle \hat{b}^\dagger\hat{b}\rangle^r = -1 - \Sigma^r(\omega)[\langle \hat{b}\,\hat{b}\rangle^r + \langle \hat{b}^\dagger\hat{b}\rangle^r]$$

$$(\omega - \omega_0 + i\eta)\langle \hat{b}\,\hat{b}\rangle^r = \Sigma^r(\omega)[\langle \hat{b}\,\hat{b}\rangle^r + \langle \hat{b}^\dagger\hat{b}\rangle^r]$$

$$\Sigma^r(\omega) = \frac{(MI_0)^2}{\hbar^2}\sum_{j\in L,R} g_j^2\left(\frac{1}{\omega - \omega_j + i\eta} - \frac{1}{\omega + \omega_j + i\eta}\right) = -\frac{iM^2I_0^2\omega}{\hbar}[Y_L(\omega) + Y_R(\omega)]$$

NB: this is a non-interacting problem and hence be solved exactly!